181 | 1967

SCHRIFTENREIHE SCHIFFBAU

K. Hasselmann

Weak-interaction theory of ocean waves

TUHH
Technische Universität Hamburg-Harburg

Weak-interaction theory of ocean waves

K. Hasselmann, University of Hamburg

Contents

Weak-interaction theory of ocean waves

K. Hasselmann

1. Introduction

Ocean wave research covers a broad range of topics including the theoretical analysis of the basic processes of wave growth and decay, semi-empirical methods of wave-forecasting and engineering problems related to the effects of waves on ships, structures and beaches. We shall be concerned here primarily with the state of the sea as such, rather than the secondary effects of waves.

The increased interest in ocean waves in the past two decades was originally stimulated by the wave prediction problem. Since dynamical wave theory was virtually nonexistent, wave forecasting evolved for many years as an essentially empirical art. However, the latest developments show promise of a stronger interaction with dynamical wave theory, which has made considerable advances in recent years. A general theoretical framework has emerged, enabling a rational discussion of both the prediction problem and the dynamical processes determining the local energy balance of the waves. An assessment of the present state of the field may be useful before proceeding to the more detailed measurements and computations which will be needed to place the theoretical framework on a sounder quantitative basis.

The first prediction methods by Svedrup and Munk (1943, unclassified 1947) and Suthons (1945) were based on a simplified parametric description of both wind and wave fields. Empirical relationships were established between the characteristic parameters of each field. The introduction of a wave spectrum in the prediction methods of Neumann (1953) and Pierson, Neumann and James (1955) represented an important conceptual advance. However, the reliability of these methods and the alternative prediction formulae suggested by Darbyshire (1955, 1959), Bretschneider (1959), Roll and Fischer (1956), Burling (1959) and others was

still basically limited by the parametric description of the wind fields, which was retained in the new methods, but was now no longer matched to the more sophisticated description of the wave field.

The present forecasting methods use a complete description of both the wind and wave fields and are based on the numerical integration of the radiative transfer equation. The approach was pioneered by Gelci and collaborators (cf. Gelci et al, 1956, Gelci and Cazalé, 1962, Fons, 1966) and has been developed independently by Baer (1962), Pierson et al, (1966) and Barnett (1966). The source functions used in these methods are still largely empirical. However, a closer interaction with dynamical wave theory may be expected in the future. The functional form of most terms in the source function can now be predicted theoretically, although extensive measurements and computations are still needed to fill in many details.

Dynamical wave theory is the statistical theory of the local interactions of the wave field with the atmosphere and ocean. The first significant contributions to this problem were Phillips' (1957) and Miles' (1957) theories of wave generation, which yielded rigorous transfer expressions for certain aspects of the wave-atmosphere interactions which had been discussed previously by Eckart (1953), Jeffreys (1925, 1926), Wuest (1949), Lock (1954) and others. A further contribution was the determination and computation of the energy transfer due to non-linear wave-wave interactions (Phillips, 1960, Hasselmann 1960, 1962, 1963 a,b).

We shall see in the following that these processes may be regarded as particular applications of a general theory of weak interactions, which yields the energy transfer for all expansible interactions between the wave field and the atmosphere and ocean.

The lowest-order set of transfer expressions for wave-atmosphere interactions consists of the Phillips and Miles processes, a non-linear correction to Miles' process, and wave-turbulence interactions. Present data suggests that the wave-turbulence interactions may be the most important of the four.

The interactions between waves and the ocean are formally very similar to wave-atmosphere interactions. The lowest-order processes consist of parametric damping by mean currents, scattering by large and medium-scale turbulence and parametric damping by small-scale turbulence. The last process may be interpreted as an eddy viscosity. A further application of the general interaction theory is the diffusion due to waves, but this will not be considered here.

The major part of this paper will be devoted to the development and application of the weak interaction theory. The theory yields the source functions for the radiative transfer problem, which will be discussed briefly in the first section. The interaction and transfer problems are complementary aspects of the complete problem of determining the state of the sea for a given wind field. Although we shall consider only ocean waves in detail, the basic concepts are applicable to all random wave fields. We shall accordingly present the theory first for an arbitrary set of interacting fields, following Hasselmann (1966, 1967 a). Since the emphasis is on developing a general approach, we cannot do adequate justice to many specific contributions to the subject; we refer in this respect to the more extensive expositions of Kinsman (1965) and Phillips (1966).

2. The radiation balance

2.1 Representation of the wave field

Ocean waves are a statistical phenomenon; it is meaningful to consider only average properties of the wave field. In practice, the mean values are determined either as time or spacial averages. For theoretical purposes, it is more convenient to consider the mean values as averages over a hypothetical ensemble of fields. Our averages will be defined in this latter sense. The two definitions are equivalent if the field is either statistically stationary or homogeneous, i.e. if all mean quantities are invariant under either time or (horizontal) spacial translations.

To a first approximation, an ocean wave field is both stationary and homogeneous. This implies that the dynamical processes changing the state of the field are weak, and the field may thus be regarded approximately as a superposition of free waves. The field can then be represented as a Fourier-Stielties integral (which we write in a more convenient sum notation)

$$\zeta(\underset{\sim}{x},t) = \sum_{\underset{\sim}{k}} \left\{ \eta_{\underset{\sim}{k}} e^{i(\underset{\sim}{k}\cdot\underset{\sim}{x}-\sigma t)} + \eta^{*}_{\underset{\sim}{k}} e^{-i(\underset{\sim}{k}\cdot\underset{\sim}{x}-\sigma t)} \right\} \qquad (2.1.1)$$

where ζ is the surface displacement (positive upwards)

$\underset{\sim}{x} = (x_1, x_2)$ is the horizontal coordinate vector

$\underset{\sim}{k} = (k_1, k_2)$ is the horizontal wave-number vector

$\sigma = (gk \tanh kH)^{1/2}$ is the frequency of a free surface gravity wave in water of depth H, which we take to be constant, and

$\eta_{\underset{\sim}{k}}$ is a random Fourier amplitude.

For a homogeneous, stationary wave field, the covariance matrix of the Fourier amplitudes is diagonal,

$$\langle \eta_{\underset{\sim}{k}_1} \eta_{\underset{\sim}{k}_2} \rangle = 0 ,$$

$$\langle \eta_{\underset{\sim}{k}_1} \eta_{\underset{\sim}{k}_2} \rangle = 0 \quad \text{for } \underset{\sim}{k}_1 \neq \underset{\sim}{k}_2$$

$$\langle \eta_{\underset{\sim}{k}} \eta^*_{\underset{\sim}{k}} \rangle = \frac{2}{\varrho g} F(\underset{\sim}{k}) \Delta \underset{\sim}{k}$$

where the cornered parentheses denote ensemble means,
ϱ is the density of water,
g is the acceleration of gravity,
$\Delta \underset{\sim}{k}$ is the wave-number increment of the Fourier sum and
$F(\underset{\sim}{k})$ is the (continuous) energy spectrum.

The total wave energy per unit surface area is then

$$E = \varrho g \langle \zeta^2 \rangle = 2 \int F(\underset{\sim}{k}) \, d\underset{\sim}{k}$$

The normalisation of F is that used in the general interaction theory; it differs from the more usual definition by a factor $2/\varrho g$.

It can be shown that a homogeneous field consisting only of dispersive, free-wave components rapidly attains a Gaussian state (Hasselmann, 1967 a). In this case the energy spectrum $F(\underset{\sim}{k})$ completely specifies the field statistically.

Since the wave components undergo weak interactions, the Gaussian property, the stationarity and the homogeneity of the wave field are only approximately valid. The field can still be described locally by a spectrum, but this must now be regarded as a slowly varying function of $\underset{\sim}{x}$ and t, where

$$\frac{1}{k} \frac{\partial F}{\partial x_i} \ll 1, \quad \frac{1}{\sigma} \frac{\partial F}{\partial t} \ll 1 .$$

2.2 The radiative transfer equation

The evolution of the spectrum $F(\underset{\sim}{k},\underset{\sim}{x},t)$ is determined by the energy balance, or radiative transfer, equation

$$\frac{DF}{Dt} \equiv \frac{\partial F}{\partial t} + \dot{x}_i \frac{\partial F}{\partial x_i} + \dot{k}_i \frac{\partial F}{\partial k_i} = S \qquad (2.2.1)$$

where

$$\dot{x}_i = \frac{\partial}{\partial k_i} \sigma(\underset{\sim}{x},\underset{\sim}{k}) \qquad (2.2.2)$$

$$\dot{k}_i = -\frac{\partial}{\partial x_i} \sigma(\underset{\sim}{x},\underset{\sim}{k}) \qquad (2.2.3)$$

The source function S represents the net transfer of energy to (or from) the spectrum at the wave number $\underset{\sim}{k}$ due to all interaction processes which affect the component $\underset{\sim}{k}$. $\frac{DF}{Dt}$ is the Lagrangian rate of change of the spectrum relative to a wave group $\underset{\sim}{k}$ moving along the path in $\underset{\sim}{x}$ - $\underset{\sim}{k}$ phase space determined by the Hamiltonian equations (2.2.2) and (2.2.3) (the dot denotes differentiation with respect to t.) It is assumed that the depth H is slowly varying, $\frac{1}{k}\frac{\partial H}{\partial x_i} \ll 1$, so that the geometrical refraction laws (2.2.2) and (2.2.3) are applicable . In deep water, the refraction term $\dot{k}_i \frac{\partial F}{\partial k_i}$ in (2.2.1) vanishes. Equations (2.2.1) - (2.2.3) apply for a plane ocean. The corresponding relations for wave propagation on a sphere are given in Groves and Melcer (1961) and Backus (1962).

Equation (2.2.1) can be derived from geometric ray theory by assuming that the wave-numbers and amplitudes in equation (2.1.1) are slowly varying functions of $\underset{\sim}{x}$ and t. It can best be understood by regarding $F(\underset{\sim}{k},\underset{\sim}{x})$ as the energy density in $\underset{\sim}{x}$-$\underset{\sim}{k}$ phase space of an ensemble of wave groups. In the case S = 0, the energy of each wave group remains constant, so that the energy density is proportional to the number density. Equation (2.2.1) can then be inter-

preted as the continuity equation for the number density of wave groups in phase space. The number density, and therefore F, remains constant along a wave-group trajectory, since the flow in phase space defined by equations (2.2.2) and (2.2.3) is incompressible (Longuet-Higgins, 1957. The analogy with the Liouville theorem was pointed out by Dorrestein, 1960). If the energy of a wave group changes along its propagation path, a source term appears on the right hand side of the equation.

The transfer equation may be expressed in the integral form

$$F(\underset{\sim}{k},\underset{\sim}{x},t) = F(\underset{\sim}{k}_o,\underset{\sim}{x}_o,t) + \int_{t_o}^{t} S(\underset{\sim}{k}',\underset{\sim}{x}',t')\,dt' \qquad (2.2.4)$$

where $\underset{\sim}{k}'$, $\underset{\sim}{x}'$ and t' vary along a wave group trajectory from an initial value $\underset{\sim}{k}_o$, $\underset{\sim}{x}_o$, t_o to the point $\underset{\sim}{k}$, $\underset{\sim}{x}$, t. Equation (2.2.4) does not, in general, represent a solution of the transfer problem, since the source function in the integral is a functional of the spectrum.

The major part of this paper will be devoted to determining the source function S. We shall show that S is of the general form

$$S(\underset{\sim}{k}) = S_1 + S_2 + S_3 + S_4 + S_1' + S_2' + S_3' + S_4' + S_5 + S_6 + S_7 + \ldots \qquad (2.2.5)$$

where

$S_1 = \alpha$

$S_2 = \beta F(\underset{\sim}{k})$

$S_3 = F(\underset{\sim}{k}) \int \gamma(\underset{\sim}{k},\underset{\sim}{k}') F(\underset{\sim}{k}')\,d\underset{\sim}{k}'$

$S_4 = -\delta F(\underset{\sim}{k}) + \int \varepsilon(\underset{\sim}{k},\underset{\sim}{k}') F(\underset{\sim}{k}')\,d\underset{\sim}{k}'$

S_1', S_2', S_3' and S_4' are of the same functional form as S_1, S_2, S_3 and S_4, respectively,

$S_5 = \int [T_1 F(\underset{\sim}{k}') F(\underset{\sim}{k}'') F(\underset{\sim}{k}-\underset{\sim}{k}'-\underset{\sim}{k}'') - T_2 F(\underset{\sim}{k}) F(\underset{\sim}{k}') F(\underset{\sim}{k}'')]\,d\underset{\sim}{k}'\,d\underset{\sim}{k}''$

$S_6 = -\nu_{ij}' k_i k_j F(\underset{\sim}{k})$

S_7 represents the as-yet-unknown dissipation due to wave breaking.

We have expressed only the dependence on the wave spectrum F explicitly. The coefficients α, β etc. depend in a known manner on the properties of the other interacting fields.

The source function S_1 represents the constant energy transfer to the wave field through turbulent atmospheric pressure fluctuations (Eckart, 1953, Phillips, 1957); S_2 corresponds to Miles' (1957) unstable coupling mechanism between the wave field and the mean boundary layer flow; S_3 is a non-linear correction of Miles' theory, and S_4 represents the energy transfer due to wave-turbulence interactions (Hasselmann, 1967 a).

The processes S_1 to S_4 represent the complete set of lowest order transfer expressions due to interactions with the atmosphere. With the possible exception of S_2, all are probably important in various frequency ranges and stages of development of a wind-generated sea.

The interaction of waves with mean currents and turbulence in the ocean are formally very similar to the interactions with the mean flow and turbulence in the atmosphere. The corresponding transfer expressions S_1' to S_4' are of the same functional form as the transfer expressions S_1 to S_4. However, S_1' and S_2' are normally negligible.

S_5 represents the energy transfer due to non-linear wave-wave interactions (Hasselmann, 1960, 1962). The energy transfer has been computed for typical wave spectra and was found to be not inconsistent with spectra observed to the lee of generating areas (Snodgrass et al, 1966).

S_6 represents the dissipation in shallow water due to turbulent bottom friction (Hasselmann and Collins, 1967). ν_{ij} is a known functional of the wave spectrum. The expression is based on a quadratic friction law. In contrast to the processes mentioned above, it cannot be derived from the weak-interaction theory, since the friction law is non-expansible.

Another example of a weak, but probably non-expansible process is the energy loss S_7 due to wave-breaking, which is still undetermined.

We note that with the exception of S_1, S_2 and S_1', S_2', all source functions depend on the entire wave spectrum, and not only on the component $\underset{\sim}{k}$. The source functions S_4, S_4', S_5, S_6 and S_7 are furthermore non-linear in F. The first property is common to many transfer problems (c.f. Chandresekhar, 1960, Kourganoff, 1963). It implies that all wave components of the field are coupled. It is not possible to determine the spectrum at any point P in the ocean by integrating the source function along only those wave trajectories which terminate in P; the spectrum must be determined simultaneously in the entire region of the ocean in which S is non-zero. The numerical integration of the transfer equation nontheless lies within the capacity of present-day digital computers, and several programs for predicting areal wave spectral distributions are already in operation.

2.3 Empirical source functions

The source functions adopted in present wave forecasting programs are largely empirical.

In the latest version of their method DSA (distribution spectro-angulaire) Gelci and Cazalé (1966) introduce a source function

$$S_{DSA} = \alpha - A\sigma^4 F(\underset{\sim}{k}) \int (B - C\cos\varphi) F(\underset{\sim}{k}') d\underset{\sim}{k}' \qquad (2.3.1)$$

where α is a function of $\underset{\sim}{k}$ and the wind velocity $\underset{\sim}{U}$, φ is the angle between $\underset{\sim}{k}$ and $\underset{\sim}{U}$ and A, B and C are constants. S_{DSA} is of the form $S_1 + S_3$. However, the non-linear term is introduced as the energy loss due to wave breaking, rather than a non-linear correction to Miles' theory. A linear term S_2 corresponding to Miles' theory is not included.

Pierson, Tick and Baer (1966) suggest a source function

$$S_{PTB} = \begin{cases} \left[\alpha(1-\gamma^2)^{1/2} + \beta E(k)\right](1-\gamma^2)\, s(k,\varphi) & \text{for } F < F_\infty,\ |\varphi| < \pi/2 \\ 0 & \text{for } F > F_\infty,\ |\varphi| < \pi/2 \\ \Phi & \text{for } |\varphi| > \pi/2 \end{cases} \qquad (2.3.2)$$

in which

α, β are functions of $\underset{\sim}{k}$ and $\underset{\sim}{U}$,

$E(k) = \int_{-\pi}^{+\pi} F(\underset{\sim}{k})\, k\, d\varphi$ is the one-dimensional spectrum,

$s(k,\varphi)$ is an empirical angular spreading factor, with

$$\int_{-\pi}^{+\pi} s(k,\varphi)\, d\varphi = 1$$

Φ is a dissipation function which acts only for waves travelling against the wind,

$\gamma = \dfrac{E(k)}{E_\infty(k)}$

and $F_\infty(\underset{\sim}{k},\underset{\sim}{U})$, $E_\infty(k,\underset{\sim}{U})$ are empirical fully developed spectra taken from Pierson and Moskowitz (1964). As a function of frequency, the one-dimensional Pierson-Moskowitz spectrum is given by

$$E_\infty(\sigma) = \alpha g^2 \sigma^{-5} \exp\{-\beta(\sigma_1/\sigma)^4\} \qquad (2.3.3)$$

where $\sigma_1 = g/U$, $\alpha = 0.0081$ and $\beta = 0.74$

The form of the source function (2.3.2) ensures that the waves tend to a fully-developed Pierson-Moskowitz spectrum in a uniform wind field. For small values of the spectrum, the growth of the one-dimensional spectrum E(k) (but not $F(\underset{\sim}{k})$) is in accordance with a combined Phillips-Miles mechanism, $S = S_1 + S_2$. The functions α and β were determined from the field measurements of Snyder and Cox (1966) (section 4.6).

Barnett (1966) introduces a source function

$$S_B = \alpha + \beta F(\underset{\sim}{k})(1 - \Phi) + S_5 \qquad (2.3.4)$$

in which α and β are functions of $\underset{\sim}{k}$ and $\underset{\sim}{U}$,

$\Phi = a \exp\{-b(R-F)/F\}$, with a,b constant, and

$R = \gamma k^{-4} s(\varphi)$ corresponds to Phillips' (1958) universal equilibrium spectrum (section 5.5), with γ = const, $s(\varphi) = \frac{\gamma}{3\pi}\cos^4\varphi$. For computational convenience, the wave-wave scattering integral S_5 was approximated by a parametrical expression. α and β were determined from the measurements of Snyder and Cox (1966).

The source function S_B is of the general form

$$S = S_1 + S_2 + S_5 + S_7$$

(with $S_7 = -(S_1 + S_2)\,\Phi$)
suggested by Hasselmann (1960) on the basis of then existing

theories of wave generation and wave-wave scattering.

A similar source function, with $S_5 = 0$, $S_7 = -(S_1 + S_2)\left(\frac{E}{E_\infty}\right)^2$ has been considered in the one-dimensional case by Inoue (1966).

The discrepancy between the various empirical source functions is considerable. It points to the difficulty of making sufficiently detailed, conclusive measurements of wave growth and decay in the ocean. A considerable gap exists still between our understanding of the basic dynamical processes, as indicated by the general form of the theoretical source function (2.2.5), and the application of this knowledge to the forecasting problem. The difficulty is that although theory can furnish the transfer expressions for wave interactions with other fields, the transfer rates depend on the detailed statistical properties of the interacting fields, which can be determined only experimentally. To determine the source functions reliably, measurements of wave growth and decay need to be combined with detailed measurements of the interacting fields. Although the present source functions will almost certainly be modified in the light of future experiments, the development of the radiative transfer method is nontheless an important first step towards a rational treatment of the wave prediction problem.

3. Theory of weak interactions in random fields

The principal goal of dynamical wave theory is the determination of the theoretical source functions summarized in equation (2.2.5). The problem may be divided into two:

(i) the determination of the coupling coefficients characterizing the interactions between the wave field and its physical environment, and

(ii) the evaluation of the energy transfer due to these interactions.

The first problem involves the detailed analysis of the non-linear equations of motion of the interacting fields. We shall consider this in later sections.

The second problem may be treated without specific reference to the type of interacting field. The theory applies to any system involving weak interactions between wave fields and other random fields, e.g. the generation of sound by turbulence, the scattering of light and sound in the atmosphere, interactions between Rossby waves and currents, plasma-wave interactions, etc.

In this section we shall develop the theory in a general form, considering later its specific application to ocean waves.

The theory is as a rather straightforward extension of the analysis of conservative wave-wave interactions, which was first considered in detail for the case of non-linear lattice vibrations in solids by Peierls (1929), and is well known in many branches of physics, particularly in quantum field scattering theory.

One of the main difficulties which arise is keeping track of the numerous terms occuring in the perturbation expansion of the fields and ordering the various transfer expressions associated with different term combinations. Here, diagram notations are useful. In the case of conservative wave-wave interactions, both the perturbation expansion and the transfer expressions can be summarized by a single set of diagrams, which may be interpreted

in a particle picture and correspond to Feynman diagrams in quantum field theory (Hasselmann, 1966). The general case of non-conservative interactions with non-wave fields is more complicated. Two types of diagrams are needed: interaction diagrams, to describe the perturbation expansion of the field amplitudes, and transfer diagrams, to summarize the energy-transfer expressions (Hasselmann, 1967 a).

3.1 The interacting fields

Consider a set of weakly interacting fields consisting of wave fields, denoted by indices ν, and non-wave (external) fields μ. We shall be concerned only with interactions which affect the wave fields. We can then distinguish between two types of interaction: wave-wave interactions, involving wave components only and external interactions, involving both wave components and external-field components. Interactions between external fields only have no effect on the wave fields.

The set of all wave fields will be termed the wave-field system. We assume that the wave-wave interactions conserve energy and momentum of the wave-field system. (Non-conservative wave-wave interactions can be treated formally as external interactions.)

The physical system is assumed to be homogeneous in $\underset{\sim}{x}$, where $\underset{\sim}{x}$ is either a two- or three-dimensional coordinate vector (in the case of the ocean, $\underset{\sim}{x} = (x_1, x_2)$ is the horizontal coordinate vector). We assume further that all fields are random and statistically homogeneous with respect to $\underset{\sim}{x}$.

In the linear approximation, let the wave-field system consist of a set of normal modes $\varphi^{\nu}_{\underset{\sim}{k}} \exp\{i(\underset{\sim}{k}\cdot\underset{\sim}{x} \pm \omega^{\nu}_{\underset{\sim}{k}} t)\}$ where $\varphi^{\nu}_{\underset{\sim}{k}}$ is an eigenfunction (for three-dimensional $\underset{\sim}{x}$, $\varphi^{\nu}_{\underset{\sim}{k}}$ may degenerate to an eigenvector or simply a constant) and $\omega^{\nu}_{\underset{\sim}{k}}$ is the eigenfrequency. We assume that the amplitudes $q^{\nu}_{\underset{\sim}{k}}$ of the eigenfunctions represent a complete set of coordinates for the wave-field system.

Let the evolution of the wave-field system, excluding the non-conservative external interactions, be specified by a Lagrangian

$$\mathcal{L}(q_{\underset{\sim}{k}}^{\nu}, \dot{q}_{\underset{\sim}{k}}^{\nu}) = \mathcal{L}_2 + \mathcal{L}_{int}$$

where

$$\mathcal{L}_2 = \sum_{\underset{\sim}{k},\nu} \tfrac{1}{2}\left(\dot{q}_{\underset{\sim}{k}}^{\nu}\,\dot{q}_{-\underset{\sim}{k}}^{\nu} - (\omega_{\underset{\sim}{k}}^{\nu})^2 q_{\underset{\sim}{k}}^{\nu}\, q_{-\underset{\sim}{k}}^{\nu}\right)$$

is the free-field Lagrangian of the linear system and L_{int} is the wave-wave interaction Lagrangian. The harmonic-oscillator form of L_2 is uniquely determined, except for an arbitrary normalisation factor, by the form of the normal modes (symmetrical propagation characteristics in the positive and negative $\underset{\sim}{k}$ direction) and the homogeneity condition.

It is convenient to transform to canonical variables $q_{\underset{\sim}{k}}^{\nu}$, $p_{\underset{\sim}{k}}^{\nu}$,

$$p_{\underset{\sim}{k}}^{\nu} = \frac{\partial \mathcal{L}}{\partial \dot{q}_{\underset{\sim}{k}}^{\nu}} \quad , \quad H(p_{\underset{\sim}{k}}^{\nu}, q_{\underset{\sim}{k}}^{\nu}) = \sum_{\underset{\sim}{k},\nu} p_{\underset{\sim}{k}}^{\nu}\dot{q}_{\underset{\sim}{k}}^{\nu} - \mathcal{L}$$

and then to standard wave variables $a_{\underset{\sim}{k}}^{\nu}$, $a_{\underset{\sim}{k}}^{-\nu}$ defined by

$$a_{\underset{\sim}{k}}^{\nu} = \frac{1}{\sqrt{2}}\left(p_{-\underset{\sim}{k}}^{\nu} - i\omega_{\underset{\sim}{k}}^{\nu} q_{\underset{\sim}{k}}^{\nu}\right)$$

$$a_{\underset{\sim}{k}}^{-\nu} = \frac{1}{\sqrt{2}}\left(p_{-\underset{\sim}{k}}^{\nu} + i\omega_{\underset{\sim}{k}}^{\nu} q_{\underset{\sim}{k}}^{\nu}\right) \qquad (3.1.1)$$

The equations of motion become in these variables

$$\dot{a}_{\underset{\sim}{k}}^{\nu} = -i\omega_{\underset{\sim}{k}}^{\nu} \frac{\partial H}{\partial a_{-\underset{\sim}{k}}^{-\nu}} \qquad (3.1.2)$$

where for negative indices the frequency is defined by

$$\omega_{\underset{\sim}{k}}^{-\nu} = -\omega_{\underset{\sim}{k}}^{\nu}$$

The free-field Hamiltonian is given by

$$H_2 = \sum_{\underset{\sim}{k},\nu\gtrless 0} \tfrac{1}{2} a_{\underset{\sim}{k}}^{\nu} a_{-\underset{\sim}{k}}^{-\nu}$$

The linear solution of equation (3.1.2) for $H = H_2$ is

$$a_{\underset{\sim}{k}}^{\nu} = \alpha_{\underset{\sim}{k}}^{\nu} e^{-i\omega_{\underset{\sim}{k}}^{\nu} t} \quad , \quad \alpha_{\underset{\sim}{k}}^{\nu} \text{ constant}, \ \nu \gtrless 0 \tag{3.1.3}$$

which represents a wave travelling in the positive $\underset{\sim}{k}$-direction.

We assume now that the interaction Hamiltonian can be regarded as a small perturbation of the complete Hamiltonian $H = H_2 + H_{int}$, $H_{int} \ll H_2$. We assume further that H_{int} can be expanded in a Taylor series,

$$H_{int} = H_3 + H_4 + \ldots \tag{3.1.4}$$

where

$$H_n = \sum_{\underset{\sim}{k}_j, \nu_j \gtrless 0} \mathcal{D}_{\underset{\sim}{k}_1 \cdots \underset{\sim}{k}_n}^{\nu_1 \cdots \nu_n} a_{\underset{\sim}{k}_1}^{\nu_1} \cdots a_{\underset{\sim}{k}_n}^{\nu_n} \tag{3.1.5}$$

and $\mathcal{D}_{\underset{\sim}{k}_1 \cdots \underset{\sim}{k}_n}^{\nu_1 \cdots \nu_n}$ is a constant coupling coefficient.

The condition $H_{int} \ll H_2$ is implicit in the definition of a wave field. If $H_{int} = O(H_2)$, it is no longer meaningful to speak of normal modes, dispersion relations, etc. The expansibility assumption is valid in most cases, but not always. (For example, white-capping interactions are probably non-expansible.)

The Hamiltonian represents the total energy of the wave-field system per unit $\underset{\sim}{x}$ and is therefore real. The reality of H_2 implies

$$a^{\nu}_{\underset{\sim}{k}} = \left(a^{-\nu}_{-\underset{\sim}{k}}\right)^{*} \tag{3.1.6}$$

The reality of H_n, together with the condition (3.1.6), yields the relations

$$D^{\nu_1 \cdots \nu_n}_{\underset{\sim}{k_1} \cdots \underset{\sim}{k_n}} = \left(D^{-\nu_1 \cdots -\nu_n}_{-\underset{\sim}{k_1}, \cdots -\underset{\sim}{k_n}}\right)^{*} \tag{3.1.7}$$

for the interaction coefficients. A second condition for the interaction coefficients follows from the invariance of the physical system under horizontal translations,

$$D^{\nu_1 \cdots \nu_n}_{\underset{\sim}{k_1} \cdots \underset{\sim}{k_n}} = 0 \quad \text{for} \quad \underset{\sim}{k_1} + \cdots + \underset{\sim}{k_n} \neq 0 \tag{3.1.8}$$

For under a translation $\tilde{\underset{\sim}{x}} = \underset{\sim}{x} + \underset{\sim}{\xi}$, the wave components transform to $\tilde{a}^{\nu}_{\underset{\sim}{k}} = a^{\nu}_{\underset{\sim}{k}} e^{-i\underset{\sim}{k}\cdot\underset{\sim}{\xi}}$. The coupling coefficients therefore transform to $\tilde{D}^{\nu_1 \cdots \nu_n}_{\underset{\sim}{k_1} \cdots \underset{\sim}{k_n}} = D^{\nu_1 \cdots \nu_n}_{\underset{\sim}{k_1} \cdots \underset{\sim}{k_n}} \exp\left\{i\left(\underset{\sim}{k_1} + \cdots + \underset{\sim}{k_n}\right)\underset{\sim}{\xi}\right\}$ which is invariant only under condition (3.1.8).

We note further that the coefficients $D^{\nu_1 \cdots \nu_n}_{\underset{\sim}{k_1} \cdots \underset{\sim}{k_n}}$ can be defined to be symmetrical with respect to the indices 1, ... n.

The equations of motion (3.1.2) for the Hamiltonian (3.1.4) become

$$\dot{a}^{\nu}_{\underset{\sim}{k}} + i\omega^{\nu}_{\underset{\sim}{k}} a^{\nu}_{\underset{\sim}{k}} = -3i\omega^{\nu}_{\underset{\sim}{k}} \sum D^{-\nu\,\nu_1\nu_2}_{-\underset{\sim}{k}\,\underset{\sim}{k_1}\underset{\sim}{k_2}} a^{\nu_1}_{\underset{\sim}{k_1}} a^{\nu_2}_{\underset{\sim}{k_2}} - \cdots \tag{3.1.9}$$

$$-i(p+1)\omega^{\nu}_{\underset{\sim}{k}} \sum D^{-\nu\,\nu_1 \cdots \nu_p}_{-\underset{\sim}{k}\,\underset{\sim}{k_1} \cdots \underset{\sim}{k_p}} a^{\nu_1}_{\underset{\sim}{k_1}} \cdots a^{\nu_p}_{\underset{\sim}{k_p}} - \cdots .$$

To include external interaction within the same framework as wave-wave interactions, we assume now that the external fields can be described by a set of variables

$$b_{\underset{\sim}{k}}^{\mu}(\lambda,t) = \beta_{\underset{\sim}{k}}^{\mu}(\lambda)\, e^{-i\omega_{\underset{\sim}{k}}^{\mu} t} \qquad (3.1.10)$$

in analogy with the representation (3.1.3) of the free wave fields.

The superscript μ is a combination of a discrete index specifying the external field and an additional variable which determines the frequency $\omega_{\underset{\sim}{k}}^{\mu}$. In the case of wave fields, the frequency $\pm\omega_{\underset{\sim}{k}}^{\nu}$ is uniquely determined by a discrete index ν which specifies the wave field and the appropriate dispersion curve. Since the frequencies of the external fields can vary continuously for fixed $\underset{\sim}{k}$, a further variable is needed to specify the frequency. To maintain the analogy with the wave-component notation, we choose μ such that $\omega_{\underset{\sim}{k}}^{\mu} > 0$ for $\mu > 0$ and

$$\omega_{\underset{\sim}{k}}^{-\mu} = -\omega_{\underset{\sim}{k}}^{\mu} \qquad (3.1.11)$$

The variable λ represents the set of all further parameters specifying the external field.

The reality condition corresponding to equation (3.1.6) is

$$b_{\underset{\sim}{k}}^{\mu}(\lambda) = \left(b_{-\underset{\sim}{k}}^{-\mu}(\lambda)\right)^{*} \qquad (3.1.12)$$

As example, consider the turbulence fields in the ocean (w) or the atmospheric boundary layer (a). We assume that the fields are statistically stationary and homogeneous with respect to the horizontal coordinate vector $\underset{\sim}{x} = (x_1, x_2)$. The fluctuating velocity fields $u_i^{\gamma}(\underset{\sim}{x}, z, t)$, where $\gamma = w$ or a, z = vertical coordinate, may then be expressed as Fourier sums (Fourier-Stieltjes integrals)

$$u_i^{\gamma}(\underset{\sim}{x}, z, t) = \sum_{\underset{\sim}{k}, \omega} u^{\gamma}_{i, \underset{\sim}{k}, \omega}(z) e^{i(\underset{\sim}{k}.\underset{\sim}{x} + \omega t)} \qquad (3.1.13)$$

If we define

$$b^{\mu}_{\underset{\sim}{k}}(\lambda, t) = \beta^{\mu}_{\underset{\sim}{k}}(\lambda) e^{-i\omega^{\mu}_{\underset{\sim}{k}} t} \equiv u^{\gamma}_{i, \underset{\sim}{k}, \omega}(z)$$

and use the notation

$$\mu \equiv (\gamma, -\omega), \quad \omega^{\mu}_{\underset{\sim}{k}} = -\omega, \quad \lambda \equiv (i, z)$$

this may be written

$$u_i^{\gamma}(\underset{\sim}{x}, z, t) = \sum b^{\mu}_{\underset{\sim}{k}}(\lambda, t) e^{i \underset{\sim}{k}.\underset{\sim}{x}}$$

Using this notation, we may include interactions with external fields in equation (3.1.9) simply by adding further terms to the right hand side,

$$\begin{aligned} \dot{a}^{\nu}_{\underset{\sim}{k}} + i\omega^{\nu}_{\underset{\sim}{k}} a^{\nu}_{\underset{\sim}{k}} = & -3i\omega^{\nu}_{\underset{\sim}{k}} \sum D^{-\nu\nu_1\nu_2}_{-\underset{\sim}{k}\,\underset{\sim}{k}_1\underset{\sim}{k}_2} a^{\nu_1}_{\underset{\sim}{k}_1} a^{\nu_2}_{\underset{\sim}{k}_2} - \cdots - i(p+1)\omega^{\nu}_{\underset{\sim}{k}} \sum D^{-\nu\nu_1\cdots\nu_p}_{-\underset{\sim}{k}\,\underset{\sim}{k}_1\cdots\underset{\sim}{k}_p} a^{\nu_1}_{\underset{\sim}{k}_1} \cdots a^{\nu_p}_{\underset{\sim}{k}_p} \\ & - \cdots\cdots \\ & - 2i\omega^{\nu}_{\underset{\sim}{k}} \left(\sum_{\nu_1} E^{-\nu\nu_1}_{-\underset{\sim}{k}\,\underset{\sim}{k}} a^{\nu_1}_{\underset{\sim}{k}_1} + \sum_{\mu} E^{-\nu\mu}_{-\underset{\sim}{k}\,\underset{\sim}{k}} b^{\mu}_{\underset{\sim}{k}} \right) - \cdots \\ & - i(p+1)\omega^{\nu}_{\underset{\sim}{k}} \sum E^{-\nu\nu_1\cdots\nu_q\mu_{q+1}\cdots\mu_p}_{-\underset{\sim}{k}\,\underset{\sim}{k}_1\cdots\underset{\sim}{k}_q\underset{\sim}{k}_{q+1}\cdots\underset{\sim}{k}_p} a^{\nu_1}_{\underset{\sim}{k}_1} \cdots a^{\nu_q}_{\underset{\sim}{k}_q} b^{\mu_{q+1}}_{\underset{\sim}{k}_{q+1}} \cdots b^{\mu_p}_{\underset{\sim}{k}_p} \end{aligned} \qquad (3.1.14)$$

The external coupling coefficients $E^{-\nu\nu_1\cdots\nu_q\mu_{q+1}\cdots\mu_p}_{\underset{\sim}{k}\underset{\sim}{k}_1\cdots\underset{\sim}{k}_q\underset{\sim}{k}_{q+1}\cdots\underset{\sim}{k}_p}$ satisfy the same reality and homogeneity conditions (3.1.7) and (3.1.8) as the internal coupling coefficients. However, since they are not derived from a Hamiltonian, they are *not symmetrical* with respect to all permutations of the indices. Besides the indices shown, the coefficients depend on the variables λ_j, which are also included in the summations in equation (3.1.14).

We note that the external interactions include non-conservative interactions between wave components, and that the lowest order-terms are linear.

Equations (3.1.14) represent the equations of motion for the wave fields only. The external fields are regarded as given. The back-interaction of the wave fields on the external fields is assumed to be either negligible or already included in the definition of the coupling coefficients E. In the latter case, the external field components $b^{\nu}_{\underset{\sim}{k}}$ refer to the undisturbed external fields.

3.2 Interaction diagrams

Since the interactions are weak, we can construct solutions of equation (3.1.14) by perturbation or iteration methods. For a general discussion, the iteration method is more convenient, as the perturbation parameters need not be specified.

Writing equation (3.1.14) symbolically in the form

$$L\left[a\right] = N\left[a, b\right]$$

the n'th iteration ${}_n a^{\nu}_{\underset{\sim}{k}}$ is given by

$${}_n a = L^{-1} N\left[{}_{n-1}a, b\right] \qquad (3.2.1)$$

The first order solution ${}_1a^{\nu}_{\underset{\sim}{k}}$ is the free field solution, equation (3.1.3).

Explicitly, equation (3.2.1) is given by

$$
{}_n a^{\nu}_{\underset{\sim}{k}}(t) = \alpha^{\nu}_{\underset{\sim}{k}} e^{-i\omega^{\nu}_{\underset{\sim}{k}} t} + \int_0^t dt' e^{-i\omega^{\nu}_{\underset{\sim}{k}}(t-t')} \times
$$

$$
\times \Big\{ \cdots - i(p+1) \sum \Big[E^{-\nu\nu_1\cdots\nu_q\mu_{q+1}\cdots\mu_p}_{-\underset{\sim}{k}\,\underset{\sim}{k}_1\cdots\underset{\sim}{k}_q\,\underset{\sim}{k}_{q+1}\cdots\underset{\sim}{k}_p} \, {}_{n-1}a^{\nu_1}_{\underset{\sim}{k}_1}(t') \cdots {}_{n-1}a^{\nu_q}_{\underset{\sim}{k}_q}(t') \cdot
$$

$$
\cdot b^{\mu_{q+1}}_{\underset{\sim}{k}_{q+1}}(t') \cdots b^{\mu_p}_{\underset{\sim}{k}_p}(t') \Big] \cdots \Big\} \qquad (3.2.2)
$$

where $\alpha^{\nu}_{\underset{\sim}{k}} = a^{\nu}_{\underset{\sim}{k}}(t=0)$.

The structure of the solutions rapidly becomes complicated as n increases and it is convenient to introduce a simpler notation in terms of <u>interaction diagrams</u>. To this end, let us represent the field components $a^{\nu}_{\underset{\sim}{k}}$, $b^{\mu}_{\underset{\sim}{k}}$ with $\nu, \mu > 0$ by arrows equal to the wave-number vectors $\underset{\sim}{k}$. Similarly, let the complex conjugate <u>anti-components</u> $a^{-\nu}_{-\underset{\sim}{k}}$, $b^{-\mu}_{-\underset{\sim}{k}}$, with negative indices $-\nu, -\mu$, be represented by cross-stroked arrows equal to $\underset{\sim}{k}$. The sign convention is chosen such that the arrows point in the propogation directions for both components ν, μ and anti-components $\bar{\nu}, \bar{\mu}$.

We may now represent the general term in the square parentheses in equation (3.2.2) by p arrows (q components ${}_{n-1}a^{\nu_j}_{\underset{\sim}{k}_j}$ and p-q components $b^{\mu_j}_{\underset{\sim}{k}_j}$) entering a vertex and a single arrow (the contribution of the term $[\ldots]$ to ${}_n a^{\nu}_{\underset{\sim}{k}}$) leaving the vertex. The linear term $\alpha^{\nu}_{\underset{\sim}{k}} e^{-i\omega^{\nu}_{\underset{\sim}{k}} t} = {}_1a^{\nu}_{\underset{\sim}{k}}$ is represented simply by an arrow. The complete expression (3.2.2) is then given by the linear diagram and the set of all possible diagrams with one vertex and one outgoing component.

The ingoing components ${}_{n-1}a^{\nu_j}_{\underset{\sim}{k}_j}$ in these diagrams can be reduced by further diagrams to components ${}_{n-2}a^{\nu}_{\underset{\sim}{k}}$, the components ${}_{n-2}a^{\nu}_{\underset{\sim}{k}}$ to ${}_{n-3}a^{\nu}_{\underset{\sim}{k}}$, and so forth to the components ${}_{1}a^{\nu}_{\underset{\sim}{k}}$, which are given by the initial conditions. One obtains in this manner branch diagrams contracting through a series of vertices from a number of input components ${}_{1}a^{\nu_j}_{\underset{\sim}{k}_j}$, $b^{\nu_j}_{\underset{\sim}{k}_j}$ to a single output component. The n'th order iteration ${}_{n}a^{\nu}_{\underset{\sim}{k}}$ is represented by the set of all interaction diagrams containing not more than n-1 vertices.

Each vertex of a digram is associated with a coupling coefficient and a number of field components. In applications, these are normally characterized by certain small parameters. The order of an interaction diagram with respect to these parameters is immediately apparent. The representation of the iteration solutions as a perturbation series involves only the ordering of diagrams with respect to the parameters chosen; the diagrams themselves are independent of the representation of the solution.

3.3 The resonant interaction

The forcing terms in equation (3.1.14) consist of products of exponentials $e^{\pm i\omega t}$. If the resultant sum frequency is equal to the eigenfrequency $\omega^{\nu}_{\underset{\sim}{k}}$, the response is non-stationary. An interaction diagram represents a resonant interaction if

$$\sum_{\gamma} s_\gamma \omega_\gamma = s_\nu \omega_\nu \qquad (3.3.1)$$

where $\omega_j > 0$, $s_j = \begin{cases} +1 & \text{for components} \\ -1 & \text{for anti-components} \end{cases}$

and the sum is taken over all ingoing components γ.

Further resonances occur if equation (3.3.1) holds for any subdiagram within an interaction diagram.

The homogeneity condition (3.1.8) yields an analogous relation for the wave numbers,

$$\sum_{\gamma} s_{\gamma} \underset{\sim}{k}_{\gamma} = s_{\nu} \underset{\sim}{k}_{\nu} \qquad (3.3.2)$$

which is valid for all diagrams.

We shall distinguish between resonant (free-wave) and forced (virtual) components in a diagram by full and dotted arrows, respectively.

Forced components represent small modifications of the free fields. They are normally of secondary physical interest. However, the analysis of higher order non Gaussian properties due to the forced components can yield important information about the coupling coefficients (cf. Hasselmann et al, 1963).

The resonant interactions lead to a continuous redistribution of energy between the interacting components. Our primary goal will be to determine the source functions characterizing this energy flux.

3.4 The energy transfer

Let us consider first the effect of the interactions on the statistical properties of the fields.

It can be shown that free, dispersive wave fields asymptotically become Gaussian, stationary and statistically independent (Hasselmann, 1967 a). These properties hold in the coarse-grained sense, assuming that all mean values can be determined only with an arbitrary large, but finite spectral resolution. In practice, this is always the case.

The fields are then completely determined statistically by the set of time-independent energy spectra

$$F_{\underset{\sim}{k}}^{\nu} = \tfrac{1}{2}\langle a_{\underset{\sim}{k}}^{\nu}\, a_{-\underset{\sim}{k}}^{-\nu}\rangle \qquad (3.4.1)$$

The total energy of the wave-field system is accordingly

$$H_2 = \sum_{\underset{\sim}{k},\nu\gtrless 0} F_{\underset{\sim}{k}}^{\nu} = \text{const}$$

We may expect the interactions to modify this simple picture in two respects: firstly, the non-linear distortion of the field due to the forced-interaction components will give rise to non-Gaussian statistical properties; secondly, the resonant interactions will destroy the stationarity of the system, producing , in particular, a continuous redistribution of energy within the spectrum. We are concerned here with the latter effect.

It is not immediately apparent that the energy transfer can be considered separately from the non-Gaussian distortion. For example, in the case of conservative wave-wave interactions, the total energy $H = H_2 + H_{int}$ consists of the total spectral energy H_2 and the energy H_{int} associated with the field distortions. It is an important result of weak-interaction theory that to lowest order the resonant interactions affect only the spectral distributions, and not the partition of energy between H_2 and H_{int}; thus the total spectral energy is conserved, $\frac{\partial H_2}{\partial t} = 0$. The statistical properties of the distortion field are given to lowest order as stationary functions of the spectral distributions. As the spectral distributions vary, there is therefore a secondary, lower order redistribution of energy between H_2 and H_{int}. The same situation applies if energy is introduced or withdrawn by external interactions; to first order, the energy transfer affects only the energy spectra associated with H_2.

The redistribution of energy can be determined by expanding $F_{\underset{\sim}{k}}$ in terms of the various diagram contributions to $a^{\nu}_{\underset{\sim}{k}}$ and $a^{-\nu}_{-\underset{\sim}{k}}$. The resonant diagrams yield secular spectral perturbations which grow linearly in t. The secular terms can then be rewritten as the rate of change of a slowly varying spectrum. The analysis is well known from various scattering problems in solid state and quantum field theory. A derivation in the present context is given in Hasselmann (1967 a). We indicate here only the structure of the analysis in terms of the interaction diagrams associated with typical transfer terms. Since $F^{\nu}_{\underset{\sim}{k}}$ is quadratic, each term involves two diagrams representing the relevant contributions to $a^{\nu}_{\underset{\sim}{k}}$ and $a^{-\nu}_{-\underset{\sim}{k}}$, respectively.

The net energy transfer, or source function S, consists of a number of contributions, which are listed below. We return to the continuous spectrum notation $F_{\nu}(\underset{\sim}{k}) = \frac{F^{\nu}_{\underset{\sim}{k}}}{\Delta \underset{\sim}{k}}$, where $\Delta \underset{\sim}{k}$ is the wave-number increment of the Fourier sum. The source functions represent the energy transfer to the normal mode ν, $S^{\nu}_{\cdots}(\underset{\sim}{k}) = \frac{D}{Dt} E(\underset{\sim}{k})$

The <u>linear interactions</u> yield the transfer expressions

$$S^{\nu}_{\nu}(\underset{\sim}{k}) = T^{\nu}_{\nu}(\underset{\sim}{k}) F_{\nu}(\underset{\sim}{k}) \qquad (3.4.2)$$

and

$$S^{\nu}_{(\mu\nu)}(\underset{\sim}{k}) = \int T^{\nu}_{\mu\to\nu}(\underset{\sim}{k}, \lambda, \lambda') F_{\mu}(\underset{\sim}{k}, \lambda, \lambda') \, \delta(\omega^{\nu}_{\underset{\sim}{k}} - \omega^{\mu}_{\underset{\sim}{k}}) \, d\lambda \, d\lambda' \qquad (3.4.3)$$

where

$$T^{\nu}_{\nu}(\underset{\sim}{k}) = 4 \omega^{\nu}_{\underset{\sim}{k}} \mathcal{I}_m \left(E^{-\nu\nu}_{-\underset{\sim}{k}\,\underset{\sim}{k}} \right) \qquad (3.4.4)$$

$$T^{\nu}_{\mu\to\nu}(\underset{\sim}{k},\lambda,\lambda') = 8\pi(\omega^{\nu}_{\underset{\sim}{k}})^2 E^{-\nu\mu}_{-\underset{\sim}{k}\,\underset{\sim}{k}}(\lambda)\left(E^{-\nu\mu}_{-\underset{\sim}{k}\,\underset{\sim}{k}}(\lambda')\right)^* \qquad (3.4.5)$$

and

$$F_{\mu}(\underset{\sim}{k},\lambda,\lambda') = \frac{\langle b^{\mu}_{\underset{\sim}{k}}(\lambda)\, b^{-\mu}_{-\underset{\sim}{k}}(\lambda')\rangle}{\Delta\underset{\sim}{k}} \qquad (3.4.6)$$

is the external field spectrum.

The index notation for source functions S and transfer functions T refer to the transfer diagrams introduced in the next section. The relevant interaction diagram pairs are shown in figure 1. We note that although both processes are linear, the transfer rates (3.4.2) and (3.4.3) are of different order with respect to the coupling coefficients.

The non-linear interactions yield transfer integrals involving quadratic and higher products or spectra. We give here only the quadratic expressions.

The wave-wave interactions lead to four transfer expressions which in the general, non-conservative case are given by

$$S^{\bar{\nu}}_{(\nu_1\nu_2\bar{\nu})} = \int\Big(T^{\nu}_{\nu_1\nu_2\to\nu} F_{\nu_1} F_{\nu_2} - T^{\nu}_{\nu\bar{\nu}_1\to\nu_2} F_{\nu} F_{\nu_1} - T^{\nu}_{\nu\bar{\nu}_2\to\nu_1} F_{\nu} F_{\nu_2}\Big) \cdot \delta(\underset{\sim}{k}_1+\underset{\sim}{k}_2-\underset{\sim}{k})\,\delta(\omega^{\nu_1}_{\underset{\sim}{k}_1}+\omega^{\nu_2}_{\underset{\sim}{k}_2}-\omega^{\nu}_{\underset{\sim}{k}})\,d\underset{\sim}{k}_1\,d\underset{\sim}{k}_2 \qquad (3.4.7)$$

$$S^{\bar{\nu}}_{(\nu_1\bar{\nu}_2\nu)} = \int\Big(T^{\nu}_{\nu_1\bar{\nu}_2\to\nu} F_{\nu_1} F_{\nu_2} + T^{\bar{\nu}}_{\bar{\nu}\nu_1\to\nu_2} F_{\nu} F_{\nu_1} - T^{\nu}_{\nu\nu_2\to\nu_1} F_{\nu} F_{\nu_2}\Big) \cdot \delta(\underset{\sim}{k}_1-\underset{\sim}{k}_2-\underset{\sim}{k})\,\delta(\omega^{\nu_1}_{\underset{\sim}{k}_1}-\omega^{\nu_2}_{\underset{\sim}{k}_2}-\omega^{\nu}_{\underset{\sim}{k}})\,d\underset{\sim}{k}_1\,d\underset{\sim}{k}_2 \qquad (3.4.8)$$

$S^{\bar{\nu}}_{(\nu_2 \bar{\nu}_1 \bar{\nu})}$ = equation (3.4.8) with indices 1 und 2 interchanged, and

$$S^{\nu}_{\nu\nu_1} = -\int T^{\nu}_{\nu\nu_1} F_\nu F_{\nu_1} d\underset{\sim}{k}_1 \tag{3.4.9}$$

where $F_\nu = F_\nu(\underset{\sim}{k})$, $F_{\nu_j} = F_{\nu_j}(\underset{\sim}{k}_j)$, $\nu_j > 0$ is any wave index, including ν, and

$$T^{\nu}_{\nu_1\nu_2 \to \nu} = 72\pi \left(\omega^{\nu}_{\underset{\sim}{k}}\right)^2 \left| E^{-\nu\nu_1\nu_2}_{-\underset{\sim}{k}\,\underset{\sim}{k}_1\,\underset{\sim}{k}_2} \right|^2 \tag{3.4.10}$$

$$T^{\nu}_{\nu\bar{\nu}_1 \to \nu_2} = 72\pi\, \omega^{\nu}_{\underset{\sim}{k}}\, \omega^{\nu_2}_{\underset{\sim}{k}_2}\, (Re)\, \Lambda(1,2) \tag{3.4.11}$$

$$T^{\nu}_{\nu\bar{\nu}_2 \to \nu_1} = 72\pi\, \omega^{\nu}_{\underset{\sim}{k}}\, \omega^{\nu_1}_{\underset{\sim}{k}_1}\, (Re)\, \Lambda(2,1) \tag{3.4.12}$$

$$T^{\nu}_{\nu\nu_1} = -96\, \omega^{\nu}_{\underset{\sim}{k}}\, (\mathcal{J}_m)\, E^{-\nu\nu-\nu_1\nu_1}_{-\underset{\sim}{k}\,\underset{\sim}{k}\,-\underset{\sim}{k}_1\,\underset{\sim}{k}_1} + 144\, \omega^{\nu}_{\underset{\sim}{k}}\, (P\mathcal{J}_m) \cdot \sum_{\nu_2 > 0} \omega^{\nu_2}_{\underset{\sim}{k}_2} \left\{ \tilde{\Lambda}(1,2) + \tilde{\Lambda}(-1,2) - \tilde{\Lambda}(1,-2) - \tilde{\Lambda}(-1,-2) \right\} \tag{3.4.13}$$

with

$$\Lambda(\pm 1, \pm 2) = E^{-\nu\,\pm\nu_2\,\pm\nu_1}_{-\underset{\sim}{k}\,\pm\underset{\sim}{k}_2\,\pm\underset{\sim}{k}_1} E^{\mp\nu_2\,\nu\,\mp\nu_1}_{\mp\underset{\sim}{k}_2\,\underset{\sim}{k}\,\mp\underset{\sim}{k}_1} \tag{3.4.14}$$

$$\tilde{\Lambda}(\pm 1, \pm 2) = \frac{\Lambda(\pm 1, \pm 2)}{\left(-\omega^{\nu}_{\underset{\sim}{k}} \pm \omega^{\nu_1}_{\underset{\sim}{k}_1} \pm \omega^{\nu_2}_{\underset{\sim}{k}_2}\right)} \qquad (3.4.15)$$

The transfer functions of equation (3.4.8) follow from equations (3.4.10) - (3.4.12) by changing the signs of the indices ν_j and $\underset{\sim}{k}_j$ in the coupling coefficients wherever components ν_j and anti-components $\bar{\nu}_j$ are interchanged in the transfer functions. Operators in parentheses apply to all later expressions in the transfer integrals. P denotes the Chauchy principal value.

The interaction diagrams associated with the various terms of the source function $S^{\bar{\nu}}_{(\nu_1\nu_2\bar{\nu})}$, equation (3.4.7), are shown in figure 2. The source function $S^{\bar{\nu}}_{(\nu_2\bar{\nu}_1\bar{\nu})}$ is identical with $S^{\bar{\nu}}_{(\nu_1\bar{\nu}_2\bar{\nu})}$ except for a notational interchange of the indices 1 and 2. It has been listed as a distinct source function, however, since the net energy transfer is obtained by adding all source function seperately.

In the case of conservative wave-wave interactions, the coupling coefficients E are replaced by the symmetrical coefficients D. The three transfer functions (3.4.10), (3.4.11) and (3.4.12) then become identical except for a frequency factor, and the source functions $S^{\bar{\nu}}_{(\nu_1\nu_2\bar{\nu})}$, $S^{\bar{\nu}}_{(\nu_1\bar{\nu}_2\bar{\nu})}$ and $S^{\bar{\nu}}_{(\nu_2\bar{\nu}_1\bar{\nu})}$ can each be characterized by a single transfer function. The fourth source function $S^{\nu}_{\nu\nu_1}$ vanishes, since the expressions in the parentheses $\{\cdots\}$ become real (section 3.6).

The <u>interactions with external fields</u> yield the seven transfer expressions

$$S^{\bar{\nu}}_{(\nu_1\mu_2\bar{\nu})} = \int \left(T^{\nu}_{\nu_1\mu_2\to\nu} F_{\nu_1} F_{\mu_2} - T^{\nu}_{\nu\mu_2\to\nu_1} F_{\nu} F_{\mu_2} \right) \cdot \qquad (3.4.16)$$

$$\cdot\, \delta(\underset{\sim}{k}_1 + \underset{\sim}{k}_2 - \underset{\sim}{k})\, \delta(\omega^{\nu_1}_{\underset{\sim}{k}_1} + \omega^{\mu_2}_{\underset{\sim}{k}_2} - \omega^{\nu}_{\underset{\sim}{k}})\, d\underset{\sim}{k}_1 d\underset{\sim}{k}_2$$

$$S^{\bar{\nu}}_{(\nu_1\bar{\mu}_2\bar{\nu})} = \int \left(T^{\nu}_{\nu_1\bar{\mu}_2\to\nu} F_{\bar{\nu}_1} F_{\bar{\mu}_2} - T^{\nu}_{\nu\bar{\mu}_2\to\nu_1} F_{\bar{\nu}} F_{\bar{\mu}_2} \right) \cdot \delta(\underset{\sim}{k}_1 - \underset{\sim}{k}_2 - \underset{\sim}{k}) \, \delta(\omega^{\nu_1}_{\underset{\sim}{k}_1} - \omega^{\mu_2}_{\underset{\sim}{k}_2} - \omega^{\nu}_{\underset{\sim}{k}}) \, d\underset{\sim}{k}_1 \, d\underset{\sim}{k}_2 \tag{3.4.17}$$

$$S^{\bar{\nu}}_{(\bar{\nu}_1\mu_2\bar{\nu})} = \int \left(T^{\nu}_{\bar{\nu}_1\mu_2\to\nu} F_{\bar{\nu}_1} F_{\mu_2} + T^{\bar{\nu}}_{\bar{\nu}\mu_2\to\nu_1} F_{\bar{\nu}} F_{\mu_2} \right) \cdot \delta(\underset{\sim}{k}_2 - \underset{\sim}{k}_1 - \underset{\sim}{k}) \, \delta(\omega^{\mu_2}_{\underset{\sim}{k}_2} - \omega^{\nu_1}_{\underset{\sim}{k}_1} - \omega^{\nu}_{\underset{\sim}{k}}) \, d\underset{\sim}{k}_1 \, d\underset{\sim}{k}_2 \tag{3.4.18}$$

$$S^{\bar{\nu}}_{(\mu_1\mu_2\bar{\nu})} = \int T^{\nu}_{\mu_1\mu_2\to\nu} F_{\mu_1} F_{\mu_2} \, \delta(\underset{\sim}{k}_1 + \underset{\sim}{k}_2 - \underset{\sim}{k}) \, \delta(\omega^{\mu_1}_{\underset{\sim}{k}_1} + \omega^{\mu_2}_{\underset{\sim}{k}_2} - \omega^{\nu}_{\underset{\sim}{k}}) \, d\underset{\sim}{k}_1 d\underset{\sim}{k}_2 \tag{3.4.19}$$

$$S^{\bar{\nu}}_{(\mu_1\bar{\mu}_2\bar{\nu})} = \int T^{\nu}_{\mu_1\bar{\mu}_2\to\nu} F_{\mu_1} F_{\mu_2} \, \delta(\underset{\sim}{k}_1 - \underset{\sim}{k}_2 - \underset{\sim}{k}) \, \delta(\omega^{\mu_1}_{\underset{\sim}{k}_1} - \omega^{\mu_2}_{\underset{\sim}{k}_2} - \omega^{\nu}_{\underset{\sim}{k}}) \, d\underset{\sim}{k}_1 d\underset{\sim}{k}_2 \tag{3.4.20}$$

$S^{\bar{\nu}}_{(\mu_2\bar{\mu}_1\bar{\nu})}$ = equation (3.4.20) with indices 1 and 2 interchanged, and

$$S^{\nu}_{\nu\mu_1} = - \int T^{\nu}_{\nu\mu_1} F_{\mu_1}(\underset{\sim}{k}_1) F_{\nu}(\underset{\sim}{k}) \, d\underset{\sim}{k}_1 \tag{3.4.21}$$

with $F_{\mu_j} = F_{\mu_j}(\underset{\sim}{k}_j, \lambda, \lambda')$,

$\mu_j > 0$ and

$$T^{\nu}_{\nu_1\mu_2\to\nu} = 36 (\omega^{\nu}_{\underset{\sim}{k}})^2 (Re) \, E^{-\nu\nu_1\nu_2}_{-\underset{\sim}{k}\,\underset{\sim}{k}_1\,\underset{\sim}{k}_2}(\lambda) \left(E^{-\nu\nu_1\mu_2}_{-\underset{\sim}{k}\,\underset{\sim}{k}_1\,\underset{\sim}{k}_2}(\lambda') \right)^* \tag{3.4.22}$$

$$T^{\nu}_{\nu\mu_2\to\nu_1} = 36\pi\,\omega^{\nu}_{\underset{\sim}{k}}\,\omega^{\nu_1}_{\underset{\sim}{k}_1}\,(Re)\,\Lambda(2,1) \tag{3.4.23}$$

$$T^{\nu}_{\mu_1\mu_2\to\nu} = 72\pi\left(\omega^{\nu}_{\underset{\sim}{k}}\right)^2(Re)\,E^{-\nu\mu_1\mu_2}_{-\underset{\sim}{k}\,\underset{\sim}{k}_1\underset{\sim}{k}_2}(\lambda_1,\lambda_2)\left(E^{-\nu\mu_1\mu_2}_{-\underset{\sim}{k}\,\underset{\sim}{k}_1\underset{\sim}{k}_2}(\lambda_1',\lambda_2')\right)^* \tag{3.4.24}$$

$$T^{\nu}_{\nu\mu_1} = -32\,\omega^{\nu}_{\underset{\sim}{k}}\,(\gamma_{fm})\,E^{-\nu\nu\,-\mu_1\mu_1}_{-\underset{\sim}{k}\,\underset{\sim}{k}\,-\underset{\sim}{k}_1\,\underset{\sim}{k}_1} + 32\,\omega^{\nu}_{\underset{\sim}{k}}\cdot$$

$$\cdot\sum_{\nu_2>0}\omega^{\nu_2}_{\underset{\sim}{k}_2}\,(P\gamma_{fm})\left\{\tilde{\Lambda}(1,2)+\tilde{\Lambda}(-1,2)-\tilde{\Lambda}(1,-2)-\tilde{\Lambda}(-1,-2)\right\} \tag{3.4.25}$$

where Λ and $\tilde{\Lambda}$ are defined as in equations (3.4.14), (3.4.15), the indices ν_j being replaced where appropriate by μ_j. The first coefficient E in the expressions for Λ, $\tilde{\Lambda}$ depends on λ_j, the second on λ_j'.

The transfer functions of equations (3.4.17), (3.4.18) and (3.4.20) are obtained from equations (3.4.20) - (3.4.22) as before by changing the signs of indices.

The source functions (3.4.16) - (3.4.20) are similar in structure to the source functions (3.4.7) and (3.4.8) for wave-wave interactions. They are associated with the interaction-diagram combinations shown in fig. 2. The source function $S^{\nu}_{\nu\mu_1}$ is analogous to the function $S^{\nu}_{\nu\nu_1}$ and is characterized by the interaction diagram of fig. 3. (The numerical factors in the transfer functions differ from the corresponding factors for wave-wave interactions. This is due to a difference in the admissable permutations of the indices of the coupling coefficients. For external interactions, the permutations are restricted by the side condition that wave indices precede external indices.)

The total source function S is given by the sum over all individual source functions, including all combinations of indices $\nu_j > 0$, $\mu_j > 0$.

The derivation of closed transfer expressions in terms of the field spectra is based on certain statistical assumptions. In transfer expressions involving mixed spectral products of more than one field, the interacting fields are assumed to be statistically independent. In the case of interactions involving several components of the same field, the components are treated as statistically independent, i.e. the field is regarded as Gaussian. The corresponding transfer expressions are characterized by quadratic or higher-order products of the spectrum of a single field. The linear transfer expressions involve no statistical assumptions.

The validity of these assumptions has been demonstrated for the case of weakly interacting wave fields by Prigogine (1962). The proof is rather complicated, but can be understood physically by interpreting the energy transfer in terms of interacting wave packets. The assumptions are then seen to be very similar to the Boltzmann hypothesis of statistical independence of interacting particles in a dilute gas (cf. Hasselmann, 1966). The physical argument can be similarly applied to support the hypothesis of statistical independence between wave fields and external fields. On the other hand, the external fields themselves are in general neither statistically independent nor Gaussian. In this sense, the transfer expressions (3.4.19) and (3.4.20) are only approximate, the complete transfer expressions including further integrals over cross spectra and third and fourth cumulants. However, we shall not require these in our applications. The expressions (3.4.19) - (3.4.20) can be a useful approximation in cases in which the cumulants are not well known, for example, in the problem of aerodynamically generated sound (cf. Lighthill, 1963).

3.5 Transfer diagrams

The formal analysis of a weakly interacting system of wave fields and external fields has lead to thirteen distinct source functions at lowest order, most of which involve several transfer terms. Thus even in rather simple systems we may expect a wide variety of transfer processes (as we shall indeed find). To discuss these, some form of systematic nomenclature is clearly needed. It is again convenient to base this on a diagram notation.

We shall refer in the present context to transfer diagrams, as distinct from the interaction diagrams introduced in section 3.5.

Each transfer term in a source function may be associated with a particular component of a transfer diagram. The superscript of the transfer functions in section 3.4 refers to the component, the group of subscripts to the diagram. We shall distinguish between two types of diagrams:

a) Scattering diagrams consist of a number of components or anti-components entering a vertex and a single wave component leaving the vertex. The frequencies and wave-numbers of the components satisfy the relations (3.3.1) and (3.3.2) for a resonant interaction diagram.

b) Parametric diagrams consist only of a number of components entering a vertex. The diagram contains no anti-components and no outgoing components. There is no restriction on the wave-numbers and frequencies.

We shall denote scattering diagrams by the symbols $\nu_1\nu_2 \to \nu_3$, $\nu_1\bar{\mu}_2 \to \nu_3$, etc., parametric diagrams by $\nu\nu_1$, $\nu\mu_1$, etc.

Scattering diagrams can represent both conservative and non-conservative processes. There is always a net transfer of energy from the ingoing components to the outgoing component. In the case of conservative wave-wave interactions, the energy transfer of each component is proportional to the frequency of the component. The scattering diagrams can then be interpreted as collision diagrams in a particle picture (section 3.6). The wave-particle analogy is not applicable for non-conservative interactions.

The diagram resonance conditions correspond to δ-functions in the transfer integrals.

Parametric diagrams apply only to non-conservative interactions. They represent processes analogous to the parametric amplification of signals in non-linear electronic circuits. The rate of growth of a component is proportional to the power present in other components. In the simplest case, the diagrams contain only two components (excluding the degenerate linear case); there is no energy scattered into a third component. The diagrams are associated with transfer expressions which contain no δ-function resonance terms (the energy transfer is nontheless due to resonant interaction diagrams, cf. fig. 3). The distinction between components and anti-components is therefore lost, as this is based - for transfer diagrams - on the sign combinations occuring in the resonance conditions.

The transfer expressions of any interacting system can be derived from the transfer diagrams with the aid of a single transfer rule: the rate of change of the spectrum of any wave component or anti-wave component in a diagram is proportional to the product of the spectra of the ingoing components.

The lowest-order transfer expressions of section (4.4), (for example,) are obtained by applying the transfer rule to the components ν and $\bar{\nu}$ in the set of all transfer diagrams containing not more than two ingoing components. The transfer expressions (3.4.3), (3.4.7), (3.4.8) and (3.4.16) - (3.4.20) correspond to scattering diagrams, the expressions (3.4.2), (3.4.9) and (3.4.21) to parametric diagrams. Typical transfer diagrams are shown in figure 4. (The degenerate linear transfer expression (3.4.2) may be characterized by either a scattering or parametric diagram. In Hasselmann (1967 a) a scattering diagram is used. A parametric diagram is in some respects preferable, cf. section 4.6). We could distinguish further between 'generating' processes, in which all ingoing components of a scattering diagram are external components, and 'scattering processes proper' in which at least one ingoing component is a wave component. However, we shall not do this in the following.

Scattering transfer expressions containing the same δ-function resonance factors have been grouped into a single source function. The associated scattering diagrams define a diagram set. Members of a diagram set are obtained by interchanging ingoing and outgoing components of a scattering diagram, the interchanged components changing sign (if this leads to an outgoing anti-wave component instead of a wave component, all components of the diagram change sign). For example, the diagrams $\nu_1 \nu_2 \rightarrow \nu$, $\bar{\nu}_1 \nu \rightarrow \nu$ and $\bar{\nu}_2 \nu \rightarrow \nu_1$ represent a diagram set. We denote the set by the symmetrical symbol $(\nu_1 \nu_2 \bar{\nu})$, which lists all interacting components on the same side of the resonance equation. The source functions $S^{\vec{\nu}}_{(\nu_1 \nu_2 \bar{\nu})}$ represents the net energy transfer of the wave component ν or $\bar{\nu}$ for all diagrams of the set $(\nu_1 \nu_2 \bar{\nu})$ (figure 4).

We have introduced transfer diagrams primarily as a notational convenience. They reflect the structure of the transfer expressions, but yield no information about the transfer functions themselves. These can be determined only from the detailed interaction analysis as characterized by the interaction diagrams. Comparison of figures 1-3 with figure 4 indicate that the interaction and transfer diagrams of a given transfer expression are generally not very closely related.

However, in the case of conservative wave-wave interactions an interrelationship exists on account of the symmetry of the coupling coefficients. Both the interaction analysis and the transfer expressions can be characterized in this case by a single set of diagrams. The transfer rules become particularly simple if expressed in a particle picture. They are closely related to the transition rules of quantum field scattering theory, and the diagrams themselves may be regarded as modified Feynman diagrams.

3.6 Conservative wave-wave interactions

The lowest-order energy transfer due to conservative wave-wave interactions is given by

$$S^{\bar{\nu}}_{(\nu_1\nu_2\bar{\nu})} = \omega^{\nu}_{\underset{\sim}{k}} \int T_{(\nu_1\nu_2\bar{\nu})} \left(n_1 n_2 - n_1 n - n_2 n\right) \delta(\underset{\sim}{k}_1 + \underset{\sim}{k}_2 - \underset{\sim}{k}) \cdot \delta(\omega^{\nu_1}_{\underset{\sim}{k}_1} + \omega^{\nu_2}_{\underset{\sim}{k}_2} - \omega^{\nu}_{\underset{\sim}{k}}) \, d\underset{\sim}{k}_1 d\underset{\sim}{k}_2 \qquad (3.6.1)$$

$$S^{\bar{\nu}}_{(\nu_1\bar{\nu}_2\bar{\nu})} = \omega^{\nu}_{\underset{\sim}{k}} \int T_{(\nu_1\bar{\nu}_2\bar{\nu})} \left(n_1 n_2 + n_1 n - n_2 n\right) \delta(\underset{\sim}{k}_1 - \underset{\sim}{k}_2 - \underset{\sim}{k}) \cdot \delta(\omega^{\nu_1}_{\underset{\sim}{k}_1} - \omega^{\nu_2}_{\underset{\sim}{k}_2} - \omega^{\nu}_{\underset{\sim}{k}}) \, d\underset{\sim}{k}_1 d\underset{\sim}{k}_2 \qquad (3.6.2)$$

and

$S^{\bar{\nu}}_{(\nu_2\bar{\nu}_1\bar{\nu})}$ = equation (3.6.2) with indices 1 and 2 interchanged,

where $n = \dfrac{F_\nu(\underset{\sim}{k})}{\omega^{\nu}_{\underset{\sim}{k}}}$, $n_j = \dfrac{F_{\nu_j}(\underset{\sim}{k}_j)}{\omega^{\nu_j}_{\underset{\sim}{k}_j}}$

and

$$T_{(\nu_1\nu_2\bar{\nu})} = 72\pi \, \omega^{\nu_1}_{\underset{\sim}{k}_1} \omega^{\nu_2}_{\underset{\sim}{k}_2} \omega^{\nu}_{\underset{\sim}{k}} \left| D^{-\nu\nu_1\nu_2}_{-\underset{\sim}{k}\,\underset{\sim}{k}_1\,\underset{\sim}{k}_2} \right|^2 \qquad (3.6.3)$$

$$T_{(\nu_1\bar{\nu}_2\bar{\nu})} = 72\pi \, \omega^{\nu_1}_{\underset{\sim}{k}_1} \omega^{\nu_2}_{\underset{\sim}{k}_2} \omega^{\nu}_{\underset{\sim}{k}} \left| D^{-\nu\nu_1\,-\nu_2}_{-\underset{\sim}{k}\,\underset{\sim}{k}_1\,-\underset{\sim}{k}_2} \right|^2 \qquad (3.6.4)$$

Equations (3.6.1) - (3.6.4) follow from the general transfer expressions (3.4.7) - (3.4.12) in the case of symmetrical coupling coefficients. They were first derived by Peierls (1929) for non-linear interactions between crystal lattice vibrations.

We shall be interested primarily in wave-wave interactions within a gravity wave spectrum. On account of the negative curvature of the dispersion curve, it is not possible in this case to satisfy the resonance conditions with only three wave components (Phillips, 1960). The lowest order energy transfer involves scattering from three components to a fourth,

$$S^{\bar{g}}_{(g_1 g_2 \bar{g}_3 \bar{g})} = \omega^g_{\underset{\sim}{k}} \frac{Dn}{Dt} = \omega^g_{\underset{\sim}{k}} \int T_{(g_1 g_2 \bar{g}_3 \bar{g})} (n_1 n_2 + n_3 n - n n_1 - n n_2) \cdot \quad (3.6.5)$$

$$\cdot \delta(\underset{\sim}{k}_1 + \underset{\sim}{k}_2 - \underset{\sim}{k}_3 - \underset{\sim}{k}) \delta(\omega^{g_1}_{\underset{\sim}{k}_1} + \omega^{g}_{\underset{\sim}{k}_2} - \omega^{g}_{\underset{\sim}{k}_3} - \omega^{g}_{\underset{\sim}{k}}) d\underset{\sim}{k}_1 d\underset{\sim}{k}_2 d\underset{\sim}{k}_3$$

where

$$T_{(g_1 g_2 \bar{g}_3 \bar{g})} = 192\pi \omega^{g}_{\underset{\sim}{k}_1} \omega^{g}_{\underset{\sim}{k}_2} \omega^{g}_{\underset{\sim}{k}_3} \omega^{g}_{\underset{\sim}{k}} \left| 2 D^{g\,g\,-g\,-g}_{\underset{\sim}{k}_1 \underset{\sim}{k}_2 - \underset{\sim}{k}_3 - \underset{\sim}{k}} \right. \quad (3.6.6)$$

$$\left. - 9 \sum_{s'=\pm} \sum_{\substack{\text{cycl.} \\ \text{perm.} \\ 1,2,3}} \frac{s' \omega^{g}_{\underset{\sim}{k}'} D^{g\,g\,-s'g}_{\underset{\sim}{k}_1 \underset{\sim}{k}_2 - \underset{\sim}{k}'} D^{s'g\,g\,-g}_{\underset{\sim}{k}' \underset{\sim}{k}_3 - \underset{\sim}{k}}}{(\omega^{g}_{\underset{\sim}{k}_1} + \omega^{g}_{\underset{\sim}{k}_2} - s' \omega^{g}_{\underset{\sim}{k}'})} \right|^2$$

with $\omega^{g}_{\underset{\sim}{k}}, \omega^{g}_{\underset{\sim}{k}_j}, \omega^{g}_{\underset{\sim}{k}'} > 0$ and $\underset{\sim}{k}' = \underset{\sim}{k}_1 + \underset{\sim}{k}_2$.

The coupling coefficients and transfer fuctions are given in Hasselmann (1962, 1963 a). The general features of the computed transfer rates agree with observations made by Snodgrass et al (1966), cf section (5.6).

The transfer expressions (3.6.1), (3.6.2) and (3.6.5) have the general form of Boltzmann collision integrals for an ensemble of interacting particles, the spectra $n_\nu = F_\nu/\omega$ corresponding to the number densities in $\underset{\sim}{x}$ - $\underset{\sim}{k}$ phase space of particles of momentum $\underset{\sim}{k}$ and energy ω . The resonance conditions represent the conservation of energy and momentum, and the transfer functions correspond to interaction cross sections.

The wave-particle analogy is understandable if one regards the interacting wave-system formally as the classical limit of a set of quantised fields. The transfer expressions follow in this limit from the interaction rates of an ensemble of bosons (cf. Peierls, 1955).

An alternative particle picture which is not related to the rules of second quantisation may be defined in terms of an ensemble of both particles and anti-particles, anti-particles being characterized by negative energies, momenta and number densities. Although not realisable physically, the particle picture leads to simpler interaction rules and is more convenient for geophysical applications. The scattering diagrams may be interpreted in this picture as collision processes in which particles and anti-particles are created or annihilated. The expressions for the transfer functions may be summarized by a few rules involving the coupling coefficients of interaction diagrams with the same inputs and output as the associated scattering diagram (fig. 5). In the case of the lowest-order processes, only one coupling coefficient occurs, and the expressions become particularly simple, equations (3.6.3), (3.6.4). We refer to Hasselmann (1966) for a summary of the interaction rules and their application to geophysical scattering problems. An advantage of the particle analogy is that it determines the ratios of the energy and momentum transfer rates of all components of a scattering process. However, we shall be concerned here primarily with non-conservative processes, which can be characterized only by the general transfer rule stated in the previous section.

Once the general form of the transfer expressions has been established, the analysis of the wave energy balance of an interacting system is reduced to the determination of coupling coefficients. In the following, we consider the various coupling coefficients occuring in ocean wave interactions.

4. Interactions between gravity waves and the atmosphere

4.1 The lowest order processes

We consider in this section the interactions between a gravity-wave field and a turbulent atmospheric boundary-layer. We shall assume that the boundary-layer flow consists of a mean horizontal velocity field $\underset{\sim}{U} = (U_1(z), U_2(z), 0)$ and a superimposed fluctuating field $\underset{\sim}{u}\ (\underset{\sim}{x}, \underset{\sim}{z}, t)$ which is statistically stationary and homogenous with respect to $\underset{\sim}{x}$.

The fluctuating field is characterized by the spectrum

$$F_{ij}(\underset{\sim}{k}, \omega, z, z') = \frac{u_{i,\underset{\sim}{k},\omega}(z)\left[u_{j,\underset{\sim}{k},\omega}(z')\right]^*}{\Delta\underset{\sim}{k}\,\Delta\omega} \qquad (4.1.1)$$

where $u_{i,\underset{\sim}{k},\omega}$ is the Fourier component of the fluctuating velocity field, equation (3.1.13) (the index (a) refering to the atmosphere may be discarded in this section).

We shall find that the wave-atmosphere interactions can be expanded in the form (3.1.14) with respect to the gravity-wave components g and the turbulence Fourier components t ; the mean flow enters only implicitly in the coupling coefficients. We are thus concerned formally with a two-component system.

The complete set of lowest-order transfer diagrams for this system are shown in figure 6. All combinations involving not more than three components occur, with the exception of the diagram set ($g_1 g_2 \bar{g}_3$), which cannot satisfy the resonance conditions. Interactions between gravity waves and oceanic turbulence or currents are characterized by the same diagrams, cf. section 5.

Diagram (i) corresponds to Miles' linear interaction between the wave field and the mean boundary layer flow. A non-linear correction to Miles' theory is represented by diagram (ii).

The three diagrams (iii) correspond to the Eckart-Phillips theory of wave generation by random turbulent pressure fluctuations. They may be replaced more simply by the linear diagram $p^t \rightarrow g$, where p^{*t} is the turbulent pressure at the surface. The remaining transfer diagrams (iv) and (v) represent wave-turbulence interactions (Hasselmann, 1967 a). The net source function due to these processes is given by the first four terms of equation (2.2.5).

4.2 The generation of waves by turbulent pressure fluctuations

Let

$$\zeta(\underset{\sim}{x},t) = \sum_{\underset{\sim}{k}} \zeta_{\underset{\sim}{k}}(t) e^{i\underset{\sim}{k}\cdot\underset{\sim}{x}} \qquad (4.2.1)$$

and

$$p(\underset{\sim}{x},t) = \sum_{\underset{\sim}{k}} p_{\underset{\sim}{k}}(t) e^{i\underset{\sim}{k}\cdot\underset{\sim}{x}} \qquad (4.2.2)$$

be the Fourier representations of the surface elevation ζ and surface pressure p.

For an ideal fluid, the response of the wave components $\zeta_{\underset{\sim}{k}}$ to the forcing pressure components $p_{\underset{\sim}{k}}$ is determined in the linear approximation by the harmonic oscillator equation

$$\ddot{\zeta}_{\underset{\sim}{k}} + \sigma^2 \zeta_{\underset{\sim}{k}} = -\frac{\sigma^2}{\rho g} p_{\underset{\sim}{k}} \qquad (4.2.3)$$

$$\left(\sigma \equiv \omega^g_{\underset{\sim}{k}} = (gk \tanh kH)^{1/2}\right).$$

Introducing standard wave variables, which in this case are given by

$$a_{\underset{\sim}{k}}^{g} = \sqrt{\frac{\rho g}{2}}\left(\frac{\dot{\zeta}_{\underset{\sim}{k}}}{\sigma} - i\zeta_{\underset{\sim}{k}}\right)$$

$$a_{\underset{\sim}{k}}^{-g} = \sqrt{\frac{\rho g}{2}}\left(\frac{\dot{\zeta}_{\underset{\sim}{k}}}{\sigma} + i\zeta_{\underset{\sim}{k}}\right) \qquad (4.2.4)$$

equation (4.2.3) becomes

$$\dot{a}_{\underset{\sim}{k}}^{g} + i\sigma a_{\underset{\sim}{k}}^{g} = -\frac{\sigma}{\sqrt{2\rho g}} p_{\underset{\sim}{k}} \qquad (4.2.5)$$

For $p_{\underset{\sim}{k}} = 0$, the free-wave solutions $a_{\underset{\sim}{k}}^{\pm g} = \alpha_{\underset{\sim}{k}}^{\pm g} e^{\mp i\sigma t}$ lead to the representation (2.1.1), with $\alpha_{\underset{\sim}{k}}^{g} = -i\sqrt{\frac{\rho g}{2}}\eta_{\underset{\sim}{k}}$, $\alpha_{\underset{\sim}{k}}^{-g} = i\sqrt{\frac{\rho g}{2}}\eta_{\underset{\sim}{k}}^{*}$

The determination of the wave-atmosphere coupling coefficients reduces to the determination of the coupling field $p_{\underset{\sim}{k}}$ as a function of the interacting fields. (We shall neglect the effect of surface shear stresses. In the linear approximation, shear stresses are not coupled to waves, but to rotational eddy motions and currents. We shall consider the interactions of waves with these motions in section 5. The local transfer of wind energy to waves via shear stresses would require a three-fold coupling between waves, rotational flow in the ocean, and air flow, which is probably negligible.)

To determine all the coupling coefficients, we shall expand the surface pressure later in powers of the wave components and the turbulent velocity components. As first step, we consider here the interactions which involve turbulence components only. The lowest order energy transfer due to these processes is represented by the three diagrams of figure 6 (iii). However, since the pressure field in this case is simply the turbulent pressure p^{t} in the absence of waves, it is more convenient to regard the surface pressure as the given external

field instead of the velocity field. The transfer diagrams then reduce to the linear diagram $p^t \longrightarrow g$.

Introducing the Fourier representation

$$p^t(\underset{\sim}{x},t) = \sum_{\underset{\sim}{k},\omega} P^t_{\underset{\sim}{k},\omega}\, e^{i(\underset{\sim}{k}.\underset{\sim}{x}+\omega t)}$$

and the three-dimensional pressure spectrum

$$F_{p^t}(\underset{\sim}{k},\omega) = \frac{P^t_{\underset{\sim}{k},\omega}\left(P^t_{\underset{\sim}{k},\omega}\right)^*}{\Delta \underset{\sim}{k}\,\Delta\omega}$$

equations (4.2.5) and (3.4.3) yield the energy transfer

$$\frac{DF(\underset{\sim}{k})}{Dt} = S^{\bar{j}}_{(p\bar{j})} = \frac{\pi\sigma^2}{2\varrho g} F_{p^t}(\underset{\sim}{k},-\sigma) \qquad (4.2.7)$$

We shall discuss the pressure spectrum in more detail in section (4.6).

4.3 The linear interaction with the mean boundary-layer flow

As next step in the expansion of the pressure field we consider terms which are linear in the wave components but independent of the turbulence field. This requires investigating the velocity field $\delta\underset{\sim}{u}$ induced in the boundary layer by the waves. The problem has been considered in detail by Miles (1957,1959).

The velocity field $\delta\underset{\sim}{u}$ may be represented as a superposition of two-dimensional flows characterized by stream-functions $\psi_{\underset{\sim}{k}}$ and horizontal shear flows $\varphi_{\underset{\sim}{k}}$.

$$\delta u_j = \sum_{\underset{\sim}{k}} \left\{ -\frac{k_j}{k}\frac{\partial \psi_{\underset{\sim}{k}}}{\partial z} + \eta_j \varphi_{\underset{\sim}{k}} \right\} e^{i\underset{\sim}{k}.\underset{\sim}{x}} \quad (j=1,2) \qquad (4.3.1)$$

$$\delta u_3 = \sum_{\underset{\sim}{k}} ik\eta_{\underset{\sim}{k}} e^{i\underset{\sim}{k}\cdot\underset{\sim}{x}} \qquad (4.3.2)$$

where $\underset{\sim}{\chi}$ is the horizontal unit vector perpendicular to $\underset{\sim}{k}$ and $\eta_{\underset{\sim}{k}}$, $\varphi_{\underset{\sim}{k}}$ are functions of z. The representation (4.3.1), (4.3.2) is valid for any incompressible flow.

Since in the present approximation the flow is linear in the wave components and the interactions involve only the mean flow, we may write

$$\eta_{\underset{\sim}{k}} = i(2gq)^{-1/2}\left(w_{\underset{\sim}{k}}^{\sigma} a_{\underset{\sim}{k}}^{q} + w_{\underset{\sim}{k}}^{-\sigma} a_{\underset{\sim}{k}}^{-q}\right) \qquad (4.3.3)$$

$$\varphi_{\underset{\sim}{k}} = i(2gq)^{-1/2}\left(v_{\underset{\sim}{k}}^{\sigma} a_{\underset{\sim}{k}}^{q} + v_{\underset{\sim}{k}}^{-\sigma} a_{\underset{\sim}{k}}^{-q}\right) \qquad (4.3.4)$$

where $w_{\underset{\sim}{k}}^{\pm\omega}$, $v_{\underset{\sim}{k}}^{\pm\omega}$ represent the response of the boundary layer to a periodic, unit-amplitude surface displacement of (arbitrary) phase velocity $\pm\omega/k$. We need consider only positive frequencies, since $w_{\underset{\sim}{k}}^{\omega} = \left(w_{-\underset{\sim}{k}}^{-\omega}\right)^*$, $\varphi_{\underset{\sim}{k}}^{\omega} = \left(\varphi_{-\underset{\sim}{k}}^{-\omega}\right)^*$ on account of the reality of the fields.

Neglecting variations of the Reynolds'stresses, the perturbed equations of mean motion yield

$$v_{\underset{\sim}{k}}^{\sigma} = -\frac{\frac{d\bar{u}}{dz}}{\bar{u}-c} w_{\underset{\sim}{k}}^{\sigma} \qquad (4.3.5)$$

and the inviscid Orr-Sommerfeld equation

$$L[w_{\underset{\sim}{k}}^{\sigma}] = \left\{(\bar{u}-c)\left(\frac{d^2}{dz^2} - k^2\right) - \frac{d^2\bar{u}}{dz^2}\right\} w_{\underset{\sim}{k}}^{\sigma} = 0 \qquad (4.3.6)$$

where $\bar{u} = \frac{\underset{\sim}{k}.\underset{\sim}{u}}{k}$, $\hat{u} = \underset{\sim}{\eta}.\underset{\sim}{u}$ and $c = \sigma/k$

The neglect of the viscous terms in equations (4.3.5), (4.3.6) has been justified in greater detail by Benjamin (1959). The appropriate boundary conditions are

$$w_{\underset{\sim}{k}}^{\sigma} = (\bar{u}-c) \quad \text{at} \quad z = 0 \qquad (4.3.7)$$

and

$$w_{\underset{\sim}{k}}^{\sigma} = 0 \quad \text{at} \quad z = \infty \qquad (4.3.8)$$

Equation (4.3.7) follows from equations (4.2.4), (4.3.2), (4.3.3) and the kinematic boundary condition

$$\frac{D}{Dt}(\zeta - z) = \frac{\partial \zeta}{\partial t} + u_i \frac{\partial \zeta}{\partial x_i} - \delta u_3 \quad \text{at} \quad z = 0$$

where $\frac{D}{Dt}$ denotes the substantial derivative.

After solution of equations (4.3.6) - (4.3.8), the pressure field at the surface follows from the horizontal equations of motion,

$$p_{\underset{\sim}{k}} - p^{t}_{\underset{\sim}{k}} = \sum_{s=\pm} \frac{i\varrho_a}{\sqrt{2}sg} \left\{ (\bar{U}_o - sc) \frac{d w^{s\sigma}_{\underset{\sim}{k}}(o)}{dz} a^{sg}_{\underset{\sim}{k}} - w^{s\sigma}_{\underset{\sim}{k}} a^{s\sigma}_{\underset{\sim}{k}} \frac{d\bar{U}_o}{dz} \right\} \qquad (4.3.9)$$

where $\bar{U}_o = \bar{U}(o)$ and ϱ_a = density of air.

The linear coupling coefficient is obtained from equations (3.1.14) and (4.2.5),

$$E^{-g\,g}_{-\underset{\sim}{k}\,\underset{\sim}{k}} = \frac{\sigma}{4g} \frac{\varrho_a}{\varrho} \left\{ (\bar{U}_o - c) \frac{d w^{\sigma}_{\underset{\sim}{k}}}{dz} - w^{\sigma}_{\underset{\sim}{k}} \frac{d\bar{U}_o}{dz} \right\} \qquad (4.3.10)$$

The energy transfer is then given by equation (3.4.2).

The solution $w^{\sigma}_{\underset{\sim}{k}}$ of the Orr-Sommerfeld equation can normally be determined only numerically. However, the energy transfer can be expressed in an alternative form which is easier to estimate and illustrates more clearly the physical nature of the pressure feedback.

According to equation (3.4.4), the energy transfer depends only on the imaginary part of the coupling coefficient, i.e. on the imaginary part of $\frac{d}{dz} w^{\sigma}_{\underset{\sim}{k}}(o)$. If we multiply equation (4.3.6) by $(w^{\sigma}_{\underset{\sim}{k}})^{*}/(\bar{U}-c)$, subtract the complex conjugate expression and integrate from z = 0 to $\hat{z}$, we obtain

$$\gamma_{Im} \left[\frac{dw^{\sigma}_{\underset{\sim}{k}}}{dz} (w^{\sigma}_{\underset{\sim}{k}})^{*} \right]_0^{\hat{z}} = \gamma_{Im} \int_0^{\hat{z}} \frac{d^2\bar{U}}{dz^2} \frac{|w^{\sigma}_{\underset{\sim}{k}}|^2}{(\bar{U}-c)} dz \qquad (4.3.11)$$

Taking $\hat{z} = \infty$ and applying the boundary conditions (4.3.7) and (4.3.8), this becomes

$$\mathcal{I}_m\left(\frac{d\underset{\sim}{w}_k^{\sigma}(0)}{dz}\right) = \frac{1}{\bar{U}_0 - c}\,\mathcal{I}_m \int_0^{\infty} \frac{d^2\bar{U}}{dz^2}\,\frac{|\underset{\sim}{w}_k^{\sigma}|^2}{(\bar{U}-c)}\,dz$$

The integral is indeterminate. The singularity at the critical layer $\bar{U}-c = o$ arises from the singularity of the inviscid Orr-Sommerfeld equation and can be removed either by inclusion of the viscous terms or by treating the resonant response at the critical layer as a non-stationary initial-value problem. The correct value of the integral is then found by indenting the integration path *below* the singularity (cf. Lin, 1955). Hence

$$\mathcal{I}_m\left(\frac{d\underset{\sim}{w}_k^{\sigma}(0)}{dz}\right) = \frac{\pi}{\bar{U}_0 - c}\left(\frac{d^2\bar{U}_c}{dz^2}\Big/\frac{d\bar{U}_c}{dz}\right)|\underset{\sim}{w}_k^{\sigma}|^2 \qquad (4.3.12)$$

where the subscript c refers to values at the critical layer. The energy transfer follows then from equations (3.4.2), (4.3.10) and (4.3.12),

$$\frac{DF(\underset{\sim}{k})}{Dt} = S_g^g = -\frac{\pi\sigma^2\rho_a}{2\rho g}\left(\frac{d^2\bar{U}_c}{dz^2}\Big/\frac{d\bar{U}_c}{dz}\right)|\underset{\sim}{w}_k^{\sigma}|^2 F(\underset{\sim}{k}) \qquad (4.3.13)$$

The essential feature of expressions (4.3.12) is the proportionality to the curvature-slope ratio of the velocity profile at the critical layer. The energy transfer is positive for normal profiles with negative curvature and positive wave slope. For a logarithmic profile, the energy transfer increases with decreasing height of the critical layer. Thus the Miles mechanism is particularly effective for waves with phase velocities appreciably lower than the wind velocity. For phase velocities greater than the maximal wind velocity or at angles greater than 90° to the wind, the waves are neither damped nor enhanced.

The energy and momentum is transfered to the waves entirely from the critical layer. This follows from equation (4.3.11) by noting that $\mathcal{I}m\left[\frac{d w_{\underset{\sim}{k}}^{(s)}}{dz}(w_{\underset{\sim}{k}}^{(s)})^*\right] = -2\frac{\tau_{\underset{\sim}{k}}}{\rho_a k}$, where $\tau_{\underset{\sim}{k}}$ is the shear stress $\rho_a \overline{\delta u_3 \delta u_j} \frac{k_j}{k}$ for a unit amplitude wave (the bar denotes the time mean). The shear stress is zero above the critical layer and constant between the critical layer and the surface. A physical explanation (of the energy transfer) in terms of the vortex forces acting on fluid particles near the critical layer has been given by Lighthill (1962).

We shall discuss measurements in connection with Miles' theory in section (4.7).

4.4 Wave-turbulence interactions

We consider now the terms in the pressure expansion which are linear in the wave-field but contain arbitrary powers of the turbulence components. These arise from the wave-turbulence interactions in the equations for the wave-induced velocity field $\delta \underset{\sim}{u}$. We linearise as before with respect to $\delta \underset{\sim}{u}$. The viscous terms can again be neglected.

Including the cross interactions between the wave-induced field and the turbulence field, equations (4.3.5) and (4.3.6) become

$$\tilde{L}[\psi_{\underset{\sim}{k}}] = \sum_{\substack{\underset{\sim}{k}'+\underset{\sim}{k}''=\underset{\sim}{k} \\ \omega'', j}} \left\{ A^{(1)} \psi_{\underset{\sim}{k}'} u_{j\underset{\sim}{k}''\omega''} + A^{(2)} \varphi_{\underset{\sim}{k}'} u_{j\underset{\sim}{k}''\omega''} \right\} e^{i\omega'' t} \qquad (4.4.1)$$

$$\left(\bar{U} - \frac{i}{k}\frac{\partial}{\partial t}\right)\varphi_{\underset{\sim}{k}} = -\frac{d\hat{U}}{dz}\psi_{\underset{\sim}{k}} + \sum_{\substack{\underset{\sim}{k}'+\underset{\sim}{k}''=\underset{\sim}{k} \\ \omega'', j}} \left\{ A^{(3)} \psi_{\underset{\sim}{k}'} u_{j\underset{\sim}{k}''\omega''} + A^{(4)} \varphi_{\underset{\sim}{k}'} u_{j\underset{\sim}{k}''\omega''} \right\} e^{i\omega'' t} \qquad (4.4.2)$$

where

$$\tilde{L} = \left(\bar{U} - \frac{i}{k}\frac{\partial}{\partial t}\right)\left(\frac{\partial^2}{\partial z^2} - k^2\right) - \frac{\partial^2 \bar{U}}{\partial z^2} \qquad (4.4.3)$$

(we can now no longer apply the normalisation (4.3.3), (4.3.4')).

The coupling coefficients $A^{(n)} = A^{(n)}(\underset{\sim}{k}; \underset{\sim}{k}'', \omega'', j)$ are listed in the appendix.

The boundary conditions become

$$\psi_{\underset{\sim}{k}} = \frac{i}{\sqrt{2sg}} \sum_{s=\pm} s(\bar{U} - sc) a_{\underset{\sim}{k}}^{sg} + \sum_{\substack{\underset{\sim}{k}'+\underset{\sim}{k}''=\underset{\sim}{k} \\ s', \omega'', j}} B^{(1)} a_{\underset{\sim}{k}'}^{s'g} u_{j\underset{\sim}{k}''\omega''} e^{i\omega'' t} \quad \text{at } z=0 \qquad (4.4.4)$$

and

$$\psi_{\underset{\sim}{k}} \to 0 \quad \text{for } z \to \infty \qquad (4.4.5)$$

where $B^{(1)}$ is given in the appendix.

In the inviscid approximation, the boundary condition (4.4.4) must be applied at the edge of the laminar sublayer. The turbulent velocity field at "z = 0" is horizontal, but non zero. Although the mean profiles and turbulent intensities vary rapidly in this region, the final results are insensitive to the precise definition of the sublayer thickness. They involve only the pressure field, which is effectively constant across the sublayer. (Similarly, in Miles' theory the boundary condition (4.3.7) is sensitive to the definition of z = 0, but not the final transfer expression (4.3.12)).

The pressure at the surface is again given by the horizontal component of the equations of motion,

$$p_{\underline{k}} - p^{t}_{\underline{k}} = \rho_a \left(\bar{U} - \frac{i}{k}\frac{\partial}{\partial t}\right)\frac{\partial \eta_{\underline{k}}}{\partial z} - \rho_a \eta_{\underline{k}} \frac{\partial \bar{U}}{\partial z} \qquad (4.4.6)$$

$$+ \sum_{\substack{\underline{k}'+\underline{k}''=\underline{k} \\ \omega'+\omega''=\omega}} \left\{ C^{(1)} \eta_{\underline{k}'} u_{j\underline{k}''\omega''} + C^{(2)} \varphi_{\underline{k}'} u_{j\underline{k}''\omega''} \right\} e^{i\omega'' t}$$

The coupling coefficients $C^{(1)}$ and $C^{(2)}$ are listed in the appendix.

We attempt now to construct a solution to equations (4.4.1) - (4.4.4) by expanding $\eta_{\underline{k}}$ and $\varphi_{\underline{k}}$ in powers of the turbulence components,

$$\eta_{\underline{k}} = \eta^{(0)}_{\underline{k}} + \eta^{(1)}_{\underline{k}} + \eta^{(2)}_{\underline{k}} + \cdots$$

$$\varphi_{\underline{k}} = \varphi^{(0)}_{\underline{k}} + \varphi^{(1)}_{\underline{k}} + \varphi^{(2)}_{\underline{k}} + \cdots$$

The leading term is the Miles' solution $\eta^{(0)}_{\underline{k}}$, $\varphi^{(0)}_{\underline{k}}$, which we assume to be a good first-order approximation. Observations by Longuet-Higgins et al (1961) indicate that this is indeed the case (cf. section 4.7).

We note that this does not necessarily imply that the energy transfer due to wave-turbulence interactions is small as compared with the Miles transfer. Miles' (1959) calculations indicate that the surface pressure is almost 180° out of phase with the surface elevation over the greater part of the wave spectrum (as one would expect from a simple constant-velocity model). The energy transfer is due to the pressure component which is 90° out of phase with the surface elevation, which is only a small fraction of the total pressure. Thus the Miles feed-back represents a small term in the first order theory; the higher-order pressure corrections can well be of the same order or larger.

The n'th order terms of the expansion are obtained by solving inhomogeneous Orr-Sommerfeld equations in which the (n-1)-order terms appear as forcing terms in the bilinear expressions. Substituting the expansions in equations (4.4.1) - (4.4.4) we obtain, using symbolic notation,

$$\tilde{L}[\psi^{(n)}] = A^{(1)}\psi^{(n-1)}_{\underset{\sim}{u}} + A^{(2)}\varphi^{(n-1)}_{\underset{\sim}{u}} \qquad (4.4.7)$$

$$\left(\bar{U} - \frac{i}{k}\frac{\partial}{\partial t}\right)\varphi^{(n)} = -\frac{d\hat{U}}{dz}\psi^{(n)} + A^{(3)}\psi^{(n-1)}_{\underset{\sim}{u}} + A^{(4)}\varphi^{(n-1)}_{\underset{\sim}{u}} \qquad (4.4.8)$$

with boundary conditions

$$\psi^{(1)} = B^{(1)}\psi^{(0)}a$$
$$\psi^{(n)} = 0, \quad n \geq 2 \qquad \text{at } z = 0 \qquad (4.4.9)$$

$$\psi^{(n)} \longrightarrow 0 \qquad \text{for } z \longrightarrow \infty \qquad (4.4.10)$$

It can be shown that for the lowest-order (transfer) expressions the time dependence of $a^{\pm q}_{\underset{\sim}{k}}$ in equation (4.4.9) can be taken as the free-wave time dependence $e^{\mp i\sigma t}$. The solutions can then be expressed in terms of the response functions $G^{\omega}_{\underset{\sim}{k}}(z,z')$ and $w^{\omega}_{\underset{\sim}{k}}(z)$, where

$$L\left[G^{\omega}_{\underset{\sim}{k}}(z,z')\right] = \delta(z-z') \qquad (z,z' > 0)$$

$$G^{\omega}_{\underset{\sim}{k}}(0,z') = G^{\omega}_{\underset{\sim}{k}}(\infty,z') = 0$$

and $w_{\underset{\sim}{k}}^{\omega}$ is defined by equations (4.3.6) - (4.3.8),

$$L[w_{\underset{\sim}{k}}^{\omega}] = 0 \qquad (z > 0)$$

$$w_{\underset{\sim}{k}}^{\omega} = (\bar{U}_0 - \omega/k) \text{ at } z = 0$$

$$w_{\underset{\sim}{k}}^{\omega} \to 0 \quad \text{for} \quad z \to \infty$$

The surface pressure is then obtained in the form

$$\rho_{\underset{\sim}{k}} - \rho_{\underset{\sim}{k}}^{t} = \rho_{\underset{\sim}{k}}^{(0)} + \rho_{\underset{\sim}{k}}^{(1)} + \rho_{\underset{\sim}{k}}^{(2)} + \cdots .$$

where $P_{\underset{\sim}{k}}^{(0)}$ is the Miles term and

$$\rho_{\underset{\sim}{k}}^{(1)} = \int \sum_{\substack{\underset{\sim}{k}'+\underset{\sim}{k}''=\underset{\sim}{k} \\ s',\omega''}} T^{(1)}(z')\, a_{\underset{\sim}{k}'}^{s'g}\, u_{j\,\underset{\sim}{k}''\omega''}(z')\, dz' \tag{4.4.11}$$

$$\rho_{\underset{\sim}{k}}^{(2)} = \iint \sum_{\substack{\underset{\sim}{k}'+\underset{\sim}{k}''+\underset{\sim}{k}'''=\underset{\sim}{k} \\ s',\omega'',\omega'''}} T^{(2)}(z',z'')\, a_{\underset{\sim}{k}'}^{s'g}\, u_{j\,\underset{\sim}{k}''\omega''}(z')\, u_{\ell\,\underset{\sim}{k}'''\omega'''}(z'')\, dz'dz'' \tag{4.4.12}$$

The coupling coefficients $T^{(1)}$, $T^{(2)}$ depend on the response functions and the coupling coefficients $A^{(1)}$ - $A^{(4)}$, $B^{(1)}$, $C^{(1)}$ and $C^{(2)}$. They are given in the appendix.

The coupling coefficients E of equation (3.1.15) follow from equations (4.2.5), (4.4.11) and (4.4.12). The energy transfer, finally, is given by equations (3.4.14) - (3.4.16) and (3.4.19). It may be written in the form

$$\frac{DF(\underset{\sim}{k})}{Dt} = \sum_{s=\pm} \int \left\{ T_{ij}^{s}(\underset{\sim}{k},\underset{\sim}{k}',z,z')F(\underset{\sim}{k}') - \hat{T}_{ij}^{s}(\underset{\sim}{k},\underset{\sim}{k}',z,z')F(\underset{\sim}{k}) \right\} \cdot F_{ij}(\underset{\sim}{k}+s\underset{\sim}{k}', \sigma+s\sigma', z, z')\, d\underset{\sim}{k}'\, dz\, dz'$$

$$- F(\underset{\sim}{k}) \int \tilde{T}_{ij}(\underset{\sim}{k},\underset{\sim}{k}',\omega',z,z') F_{ij}(\underset{\sim}{k}',\omega',z,z')\, d\underset{\sim}{k}'\, d\omega'\, dz\, dz' \qquad (4.4.13)$$

where the transfer functions T_{ij}^{s}, $\hat{T}_{ij}^{s}$ and $\tilde{T}_{ij}^{s}$ are determined by equations (3.4.22), (3.4.23) and (3.4.25).

The first integral of equation (4.4.13) represents the contributions from the three scattering diagrams, fig. 6 (iv). The second integral corresponds to the parametric process, fig. 6 (v). The scattering transfer expressions (3.4.16) and (3.4.17) have been reordered with respect to components rather than diagrams. The first term of the first integral represents the net energy gained by the three outgoing components of the diagrams. The second term represents the energy lost by the three ingoing components. The three sign combinations have been reduced to two by using the symmetry relation

$$F_{ij}(\underset{\sim}{k}, \omega, z, z') = F_{ji}(-\underset{\sim}{k}, -\omega, z', z)$$

and including both positive and negative frequencies in the transfer expression.

The first transfer function T_{ij}^{s} is always positive; the remaining two may be of either sign.

The transfer functions depend on the response functions, which for an arbitrary profile can be determined only numerically. However, for idealised models such as a constant-velocity or line-segment profile, the functions become rather simple analytic expressions. In contrast to the laminar interaction problem,

these models may yield acceptable approximations in the present case. In the laminar interaction problem, the constant-velocity model predicts the absolute value and phase of the surface pressure quite well for a fairly broad of range of phase velocities of the order of the wind velocity. However, since the energy transfer is zero to this approximation, the small phase shifts due to the critical layer are nevertheless essential. In the case of wave-turbulence interactions, the phase shifts can be treated as higher-order effects, since an energy transfer occurs already in the first approximation of a constant-velocity profile.

4.5 Non-linear wave-atmosphere interactions

We consider finally the complete expansion of the surface pressure in which we include both the wave-turbulence interactions and the non-linear wave-wave-mean flow interactions.

In symbolic notation, the complete equations of the wave-induced field are

$$\tilde{L}[\eta] = A^{(1)}\eta\underset{\sim}{u} + A^{(2)}\varphi\underset{\sim}{u} + A^{(5)}\eta\eta + A^{(6)}\eta\varphi + A^{(7)}\varphi\varphi \tag{4.5.1}$$

$$\left(\bar{u} - \frac{i}{k}\frac{\partial}{\partial t}\right)\varphi = \frac{d\hat{u}}{dz}\eta + A^{(3)}\eta\underset{\sim}{u} + A^{(4)}\varphi\underset{\sim}{u} + A^{(8)}\eta\eta + A^{(9)}\eta\varphi + A^{(10)}\varphi\varphi \tag{4.5.2}$$

with boundary conditions

$$\eta = \frac{i}{\sqrt{2g}}\sum_s s(\bar{u}-sc)a_{\underset{\sim}{k}}^{sg} + B^{(1)}a\underset{\sim}{u} + B^{(2)}a\eta + B^{(3)}a\varphi + B^{(4)}aa + \cdots \tag{4.5.3}$$

at $z = 0$

and

$$\eta \to 0 \quad \text{for} \quad z \to \infty \tag{4.5.4}$$

where $A^{(5)} - A^{(10)}$ and $B^{(2)}, B^{(3)}, \ldots$ are further coupling coefficients.

Similarly, the surface pressure is now

$$p - p^t = \rho_a\left(\bar{U} - \frac{i}{k}\frac{\partial}{\partial t}\right)\frac{\partial \eta}{\partial z} - \rho_a \frac{d\bar{U}}{dz}\eta + C^{(1)}\eta\underset{\sim}{u} + C^{(2)}\varphi\underset{\sim}{u} \qquad (4.5.5)$$
$$+ C^{(3)}\eta\eta + C^{(4)}\eta\varphi + C^{(5)}\varphi\varphi + C^{(6)}\eta a + C^{(7)}\varphi a + \ldots$$

with additional coupling coefficients $C^{(3)}$, $C^{(4)}$, ...

The solutions can be constructed as before by expanding about the Miles solution with respect to both wave components and turbulence components. We shall not go into details.

To lowest order, the only transfer expression not already included in the previous analysis is the parametric process, diagram 6 (ii),

$$\frac{DF(\underset{\sim}{k})}{Dt} = S^{j}_{gg'} = -F(\underset{\sim}{k})\int T^{j}_{gg'}(\underset{\sim}{k},\underset{\sim}{k}')F(\underset{\sim}{k}')\,d\underset{\sim}{k}' \qquad (4.5.6)$$

The process gg' is probably less important than the wave-turbulence interactions, for the coupling coefficients are similar in both cases, but the wave-induced velocity fluctuations are normally weaker than the turbulent fluctuations.

4.6 The pressure spectra

The relationship between the various transfer processes becomes clearer physically if one considers the surface-pressure distributions.

The turbulent surface pressure p^t of the unmodified boundary layer is characterized by a three-dimensional spectrum $F_{p^t}(\underset{\sim}{k},\omega)$ (,) (section 4.2). The power spectrum of the free-wave

field ζ , on the other hand, is a two-dimensional distribution.

$$F_\zeta(\underset{\sim}{k},\omega) = \frac{1}{8g}\left\{F(\underset{\sim}{k})\delta(\omega+\sigma) + F(-\underset{\sim}{k})\delta(\omega-\sigma)\right\}$$

confined to the positive and negative sheets of the dispersion surface $\omega = \pm\sigma(\underset{\sim}{k})$. Interactions between the wave field and turbulent boundary layer lead to mixed two- and three-dimensional distributions for both pressure and wave fields. For example, the linear interactions between the wave field and the mean flow yields a two-dimensional pressure distribution on the dispersion surface. Conversely, the turbulent pressure fluctuations generate a three-dimensional continuum of forced waves.

The energy transfered to the waves is equal to the work done by the pressure against the surface. This is proportional to the quadrature spectrum of the surface pressure and wave height, which is zero everywhere except on the dispersion surface. Thus the energy transfer is due entirely to the pressure components in resonance with free waves, and we need consider only the pressure distributions on the dispersion surface.

The three-dimensional pressure continuum yields an energy transfer proportional to the three-dimensional pressure spectrum at the resonance frequency (see, for example, equation (4.2.7)).

The two-dimensional pressure distribution yields an energy transfer proportional to the wave spectrum (see, for example, equation (4.3.13)).

Three-dimensional pressure spectra are associated with scattering processes, two-dimensional distributions with parametric processes.

The distributions of the lowest-order transfer processes are indicated schematically in figure 7.

The general form of the turbulent-pressure distribution follows from Taylor's hypothesis, which states that the frequency and wave-number spectra of a turbulent field are approximately related as though the turbulence were a "frozen" spacial pattern convected downstream with the mean velocity of the flow. In our case, this implies that the turbulent pressure spectrum is concentrated about the surface $\omega + k_1 U_m = 0$, where U_m is a "mean" boundary-layer velocity. Since the velocity profile is curved, the effective mean velocity depends on the eddy scale $2\pi/k$. It is not precisely defined. The indeterminacy is generally of the same order as the spread of the pressure distribution about the surface $\omega + k_1 U_m = 0$. For simplicity, U_m has been taken as constant in figure 7.

Atmospheric turbulence spectra are normally peaked at considerably lower frequencies then wave spectra. Hence, in the range of wind-wave frequencies the turbulent pressure spectrum decreases with increasing frequency along the surface $\omega + k_1 U_m = 0$.

An appreciable energy transfer occurs only where the surface $\omega + k_1 U_m = 0$ intercepts the dispersion surface $\omega + \sigma(\underset{\sim}{k}) = 0$, i.e. along the resonance curve $\sigma = k U_m \cos\varphi_r$, where φ_r is the angle between the direction of wave propagation and the wind. The longest waves are generated in the wind direction with a phase velocity equal to the wind speed. Shorter waves are generated at the angles φ_r for which the phase velocity $c/\cos\varphi_r$ in wind direction equals the wind speed. (An alternative explanation of the resonance angle φ_r in terms of the auto-correlation time scales of the pressure fluctuation is given in Phillips (1957).)

Linear interactions with the mean flow yield a two-dimensional pressure distribution on the dispersion surface. The component in quadrature with the wave height is proportional to the curvature/slope ratio of the wind profile at the critical layer. If we identify U_m with the "anemometer wind speed", the energy transfer per unit wave height is effectively zero to the left

of the resonance curve for a logarithmic profile and increases monotonically with frequency for $\sigma > k U_m \cos\varphi_r$.

Wave-turbulence interactions yield both two- and three-dimensional pressure distributions.

The scattering processes $g't \rightarrow g$, $g'\bar{t} \rightarrow g$ and $\bar{g}t \rightarrow g$ (diagrams (iv), fig.6) are characterized by three-dimensional pressure spectra. The pressure fluctuations arise from quadratic interactions between turbulence and wave-induced velocity fluctuations. Since the most energetic turbulence components are at low frequencies, the sum and difference frequencies of the resultant pressure components lie close to the frequencies of the wave-induced components. The same holds for the wave-numbers. Hence the pressure distribution is concentrated about the dispersion surface, the maximum lying close to the maximum of the wave spectrum. (We have ignored weighting effects due to the coupling coefficients. A more detailed analysis shows that these do not affect the conclusion.)

The parametric process gt (diagram (v), fig. 6) corresponds to a two-dimensional pressure distribution. The pressure field arises from a cubic interaction between a wave-induced component and two turbulence components of opposite wave-number and frequency (cf. figure 3).

The parametric process gg' (diagram (ii), fig. 6) is similarly associated with a two-dimensional pressure distribution. In this case, the turbulence components of the process gt are replaced by a conjugate pair of wave-induced components.

Estimates of the transfer rates are difficult to make without actually computing the transfer integrals.

Transfer rates of parametric processes are proportional to the air-water density ratio ϱ_a/ϱ , whereas scattering processes yield an energy transfer proportional to $(\varrho_a/\varrho)^2$. This suggests

that parametric processes generally dominate over scattering processes. However, it should be noted that parametric processes depend critically on phase relationships, which can reduce the energy transfer considerably.

Similarly, turbulent velocity fluctuations are generally greater than wave-induced velocities, so that the turbulent processes $tt' \rightarrow g$, ... may be expected to dominate over the wave-turbulence scattering processes $gt \rightarrow g$, ..However, this is offset by the more favorable spectral distribution of the wave-turbulence pressure fluctuations.

A reliable evaluation of the various transfer processes requires numerical calculations of the transfer expressions for typical boundary-layer models and comparison with observed wave growth and boundary layers. Some progress in this direction has been made, but our picture is still far from complete.

4.7 Comparison with observations

Our analysis of wave-atmosphere interactions was based on the assumption that the wave-induced perturbations could be described to first order by the linear interactions with the mean air flow. The hypothesis is supported by simultaneous measurements of wave height and surface pressure made by Longuet-Higgins et al. (1961) with a buoy. High coherency (0.8) between the wave and pressure records implied a two-dimensional pressure spectrum, and over 90 % of the coherent pressure was 180° out-of-phase with the wave height, as would be expected for a mean-flow interaction. The observed pressure spectra agreed well with theoretical calculations of the 180°-out-of-phase component for a logarithmic profile. The resolution was inadequate to determine the energy transfer due to the small quadrature component of the pressure or to estimate the spectral density of the residual turbulent pressure.

Wave growth has been measured by Snyder and Cox (1966). The development of a single spectral component was determined by towing a four-buoy array seewards from a lee shore at the group velocity of the wave component. The energy of the component was obtained from the array records by appropriate directional and frequency filtering. Only the 17 m wave-length component was analysed; 29 runs were made under varying wind conditions.

The first parts of the growth curves were fitted to a Miles-Phillips source function $S = \alpha + \beta F$. Initially, the α -term dominated, and the wave growth was linear. As F increased, the second term became more important and the waves grew exponentically The major part of the wave energy was generated in the exponential phase.

The emperical value of α was found to be reasonably consistent with Phillips' transfer expression, assuming that three-dimensional pressure spectra measured by Priestley (1965) over land were typical also of the ocean.

The β -term was found to be larger than predicted by Miles by a factor of 6 to 8 (figure 8). The theoretical values were based on a logarithmic wind profile. Although wind profiles were not measured, the experiments were performed under neutral conditions, for which logarithmic profiles are typical.

Barnett (1966) has measured wave growth at higher wind speeds (40 knots) using as wave sensor an air-borne radar altimeter. The method yields the wave growth over a broad frequency band, but the directional resolution was smaller than in Snyder and Cox's experiment. Only one case was analysed. The growth curves were again fitted to a source function $S = \alpha + \beta F$. The values of α and β , although more scattered, were consistent with Snyder and Cox's results, provided the turbulent pressure spectrum was scaled as the sixth power of the wind (Snyder and Cox assumed a more plausible fourth-power relationship). The exponential growth rate was again considerably larger than predicted by Miles.

The experiments indicate that neither Miles' nor Phillips' theory are capable of explaining the major part of the observed wave growth. This suggests that the remaining lowest-order processes, i.e. the wave turbulence interactions (or, conceivably, non-linear interactions with the mean flow) are the principal source of wave energy. However, the conclusion should be treated with caution, since the interaction theory is limited to expansible interactions. Large, local disturbances, such as flow separation at the wave crests, are excluded. (In the case of flow separation, however, one would expect Jeffreys' (1926) sheltering theory to apply, which is similarly unable to explain the observed wave growth, cf. figure 8). The mechanism of wave generation in the ocean is still an open question.

It is of interest that Miles' mechanism has been verified in the laboratory for sinusoidal water waves (Shemdin and Hsu, 1966) and artifical waves simulated by a moving sinusoidal belt (Zagustin et al., 1966). The phase shift of the wave-induced perturbations across the critical layer was particulary clear in the latter experiment.

The natural turbulence spectrum in laboratory experiments is normally of too high frequency to study wave-turbulence interactions. However, laboratory investigations of this interaction mechanism by low-frequency modulation of the mean air flow are feasible and would be of interest.

5. Interactions within the ocean

5.1 The lowest-order processes

An incompressible velocity field in an infinite, non-rotating ocean may be decomposed into surface gravity waves g, a mean current $\underset{\sim}{U}$ and a residual turbulent field t. If the fluid is stably stratified, the turbulence field can be decomposed further into internal gravity-wave modes i_1, i_2, ... and a horizontal turbulence field h. The decomposition is meaningful if the cross interactions between i_n and h are small compared with the linear restoring forces of the internal modes. This is normally the case for small wave-numbers.

We consider first the decomposition g, $\underset{\sim}{U}$ and t. As in the case of wave-atmosphere interactions, the equations of motion of the wave field g can be expanded in powers of the components g and t, the mean flow entering only implicitly in the expressions for the coupling coefficients. Formally, we are concerned with a two-component system g, t, and the lowest-order transfer processes are identical with the diagrams of figure 6.

Diagram (i) represents the energy transfer due to linear interactions with mean currents. It vanishes in the weak-interaction approximation, $|\underset{\sim}{U}| \ll c$.

Diagram (ii) represents the parametric energy transfer gg' due to non-linear interactions with mean currents. The corresponding interaction diagrams are shown in figure 3 (the coupling coefficients depend on the current profile). For $|\underset{\sim}{U}| \ll c$, the transfer is non zero only for $|\underset{\sim}{k}| \approx |\underset{\sim}{k}'|$.

Diagram (iii) represents the generation of waves by oceanic turbulence, which is probably unimportant.

Diagrams (iv) and (v) correspond, respectively, to scattering and parametric damping of waves by turbulence. The transfer rate of the parametric process is proportional to the wave spectrum, in accordance with the heuristic concept of a turbulent "eddy viscosity". The eddy viscosity can be expressed as a linear functional of the turbulence spectrum.

If the turbulence field is decomposed further into internal modes i_n and a horizontal turbulence field h, additional scattering processes into internal modes occur. However, these are normally unimportant for the energy balance of surface waves. (The process $g\bar{g}' \rightarrow i_n$ and several internal-wave scattering processes have been investigated by Kenyon, 1966).

Scattering by a random ocean bottom can also be included in the weak-interaction theory, but will not be treated here (cf. Hasselmann, 1966).

5.2 The interaction equations

Consider the interactions between a mean current $\underset{\sim}{U} = (U_1(z), U_2(z), o)$, a turbulence field $\underset{\sim}{u}(\underset{\sim}{x}, z, t)$ and a wave field $\underset{\sim}{u}^w$.

We assume that the turbulence and wave field are statistically homogeneous in $\underset{\sim}{x}$ and that the density is constant through-out the fluid.

Let the superposition of the mean flow and the turbulence field represent a stationary turbulent shear flow which satisfies the equations of motion and the boundary condition at the bottom. At the surface, we assume $\zeta = 0$, and therefore $u_3 = 0$; the condition of constant surface pressure is not satisfied. (The fulfillment of both surface boundary conditions for the complete flow is treated as part of the wave-turbulence interaction.) We regard the turbulent shear flow as given.

We define the wave field as the potential flow

$$u_j^w = \sum_{\underset{\sim}{k}} r_{\underset{\sim}{k}}(t) e^{i\underset{\sim}{k}\cdot\underset{\sim}{x}} \begin{cases} ik_j \dfrac{\cosh k(z+H)}{\cosh kH} & (j = 1,2) \\ k \dfrac{\sinh k(z+H)}{\cosh kH} & (j = 3) \end{cases} \qquad (5.2.1)$$

which satisfies the kinematic boundary conditions

$$\left(\frac{D}{Dt}\right)_w (\zeta - z) \equiv \frac{\partial \zeta}{\partial t} + u_1^w \frac{\partial \zeta}{\partial x_1} + u_2^w \frac{\partial \zeta}{\partial x_2} - u_3^w = 0 \qquad (5.2.2)$$

$$\text{at } z = \zeta$$

and

$$u_3 = 0 \qquad \text{at } z = -H$$

The wave field is uniquely determined by $\zeta(\underset{\sim}{x},t)$ (except for a constant horizontal velocity, which we assume to be zero). In terms of the standard wave variables defined by equations (4.2.4),

$$r_{\underset{\sim}{k}} = \frac{1}{\sigma}\sqrt{\frac{g}{2\varsigma}}\left(a_{\underset{\sim}{k}}^{g} + a_{\underset{\sim}{k}}^{-g}\right) + \tilde{A}^{(1)} aa + \tilde{A}^{(2)} aaa + \ldots . \qquad (5.2.3)$$

where $A^{(1)}$, $A^{(2)}$, ... are coupling coefficients determined by the non-linear terms in equation (5.2.2).

The complete flow consists of the turbulent shear flow, the wave field and an interaction field $\delta\underset{\sim}{u}$, which describes the coupling between the wave field and the turbulence flow.

The conditions for weak coupling depend in detail on the type of interaction and must be investigated individually for each transfer process. Generally, the turbulent shear flow can be treated as a perturbation of the wave field if both turbulent and mean velocities are small compared with the wave phase velocities. Conversely, the wave field represents a perturbation of the turbulent flow if the energy transfered from the waves to the turbulent flow is small compared with the total turbulent dissipation.

We describe the interaction field by the representation (4.3.1), (4.3.2). The equations for the components $\psi_{\underline{k}}$, $\varphi_{\underline{k}}$ are obtained by subtracting the equations of motion of the turbulent shear flow from the equations of motion of the complete field,

$$\tilde{L}[\psi] = \frac{d^2\bar{u}}{dz^2}\hat{\psi} + A^{(1)}(\psi+\hat{\psi})\underset{\sim}{u} + A^{(2)}\varphi\underset{\sim}{u} + A^{(5)}(\psi\psi + \psi\hat{\psi} + \hat{\psi}\psi) + A^{(6)}(\psi+\hat{\psi})\varphi + A^{(7)}\varphi\varphi \tag{5.2.4}$$

$$\left(\bar{u} - \frac{i}{k}\frac{\partial}{\partial t}\right)\varphi = -\frac{d\hat{u}}{dz}(\psi+\hat{\psi}) + A^{(3)}(\psi+\hat{\psi})\underset{\sim}{u} + A^{(4)}\varphi\underset{\sim}{u} + A^{(8)}(\psi\psi + \psi\hat{\psi} + \hat{\psi}\psi) + A^{(9)}(\psi+\hat{\psi})\varphi + A^{(10)}\varphi\varphi \tag{5.2.5}$$

Equations (5.2.3), (5.2.4) are identical with equations (4.5.1), (4.5.2) except for additional terms involving the wave-field stream function

$$\hat{\psi}_{\underset{\sim}{k}} = -i\tau_{\underset{\sim}{k}}\frac{\sinh k(z+H)}{\cosh kH} \tag{5.2.6}$$

The kinematic boundary condition at the surface,

$$\frac{D}{Dt}(\zeta - z) = 0 \qquad \text{at } z = \zeta$$

yields, on account of (5.2.2),

$$\psi_{\underset{\sim}{k}} = \bar{u}\zeta_{\underset{\sim}{k}} + \tilde{B}^{(1)}\zeta_{\underset{\sim}{u}} + \tilde{B}^{(2)}\zeta(\psi+\hat{\psi}) + \cdots \qquad (5.2.7)$$

$$\text{at } z = 0$$

Similarly,

$$\psi_{\underset{\sim}{k}} = 0 \quad \text{at } z = -H \qquad (5.2.8)$$

The condition of constant surface pressure yields

$$\frac{\partial^2}{\partial z \partial t}(\psi_{\underset{\sim}{k}} + \hat{\psi}_{\underset{\sim}{k}}) - gik\zeta_{\underset{\sim}{k}} = -ik\bar{u}\frac{\partial}{\partial z}(\psi_{\underset{\sim}{k}} + \hat{\psi}_{\underset{\sim}{k}}) + ik\frac{d\bar{u}}{dz}(\psi_{\underset{\sim}{k}} + \hat{\psi}_{\underset{\sim}{k}})$$
$$+ \tilde{C}^{(1)}(\psi+\hat{\psi})_{\underset{\sim}{u}} + \tilde{C}^{(2)}\varphi_{\underset{\sim}{u}} + \cdots \qquad (5.2.9)$$

$$\text{at } z = 0$$

Equation (5.2.9) follows by Taylor expansion of the conditior $\frac{d}{ds}$ (Phydrostatic + Pdynamic)$_{z=\zeta}$ = 0, where $\frac{d}{ds}$ is the surface tangential derivative parallel to $\underset{\sim}{k}$ and $\frac{d}{ds}$(Pdynamic) is expressed in terms of the velocities by means of the equations of motion.

Introducing standard wave variables in $\hat{\psi}_{\underset{\sim}{k}}$ and $\zeta_{\underset{\sim}{k}}$, and invoking equation (5.2.7), we obtain the wave equation

$$\dot{a}^{g}_{\underset{\sim}{k}} + i\sigma a^{g}_{\underset{\sim}{k}} = \sigma\sqrt{\frac{\rho}{2g}}\left(\bar{u} - \frac{i}{k}\frac{\partial}{\partial t}\right)\frac{\partial \psi_{\underset{\sim}{k}}}{\partial z} + \frac{i}{2}\left(\frac{\sigma^2}{gk}\frac{d\bar{u}}{dz} - k\bar{u}\right)\left(a^{g}_{\underset{\sim}{k}} + a^{-g}_{\underset{\sim}{k}}\right)$$
$$- \frac{i}{2}\frac{\sigma}{g}\bar{u}\frac{d\bar{u}}{dz}\left(a^{g}_{\underset{\sim}{k}} - a^{-g}_{\underset{\sim}{k}}\right) + \hat{C}^{(1)}\psi_{\underset{\sim}{u}} + \hat{C}^{(2)}\varphi_{\underset{\sim}{u}} + \cdots \qquad (5.2.10)$$

To determine the coupling coefficients, we need to express the forcing terms on the right hand side of the equation in terms of the basic fields g, t and $\underset{\sim}{U}$. This involves solving equations (5.2.4) - (5.2.8) for the interaction fields $\psi_{\underset{\sim}{k}}$ and $\varphi_{\underset{\sim}{k}}$.

5.3. Interactions with mean currents

Interactions between waves and currents can be treated as perturbations if $|\underset{\sim}{U}| \ll c$, where c is the phase velocity of the waves. In this case, the linear coupling coefficient $E^{-gg}_{-\underset{\sim}{k}\,\underset{\sim}{k}}$ is found to be real, and the energy transfer (3.4.2) vanishes. Linear interactions modify only the frequency and velocity distribution of the wave field. This is true generally for $\bar{U} < c$. As in Miles' problem, an energy transfer from the mean flow to the waves arises only through the phase shifts produced at a critical layer. In the present case, this would represent a strong interaction (since the coupling is not reduced by the factor g^a/g).

However, a weak energy transfer can occur at next order. Since second-order scattering processes are excluded by the negative curvature of the gravity-wave dispersion curve (section 3.6), we need consider only the parametric process gg'.

The relevant interaction diagram is shown in figure 9. The difference interaction at the first vertex yields a forced component g" with a phase velocity $c'' = (\omega - \omega')/|\underset{\sim}{k} - \underset{\sim}{k}'|$. If $c'' > \bar{U}$, the coupling coefficients at both vertices are imaginary; the net coefficient $E^{-g\,g'-g'\,g}_{-\underset{\sim}{k}\,\underset{\sim}{k}'-\underset{\sim}{k}'\,\underset{\sim}{k}}$ of the diagram is therefore real and yields no contribution to the energy transfer (3.4.13). However, if $c'' - \bar{U}$ passes through zero, a phase shift occurs in the first coupling coefficient, and an energy transfer results.

For $\bar{U} \ll c$, a critical layer exists only for difference interactions between components of approximately the same frequency. The net energy transfer is then of the form

$$\frac{DF(\underset{\sim}{k})}{Dt} \equiv S^{g}_{gg'} = - F(\underset{\sim}{k}) \int K(k,\varphi') F(\underset{\sim}{k}') \, d\varphi' \qquad (5.3.1)$$

where $k' = k$, $\cos\varphi' = \frac{\underset{\sim}{k}.\underset{\sim}{k}'}{kk'}$

The kernel K is a function of the mean current profile and can be expressed in terms of the response functions $w^{\omega}_{\underset{\sim}{k}}$ and $G^{\omega}_{\underset{\sim}{k}}$ of section (4.4). The details of the analysis are similar to the case of wave-turbulence interactions and need not be repeated.

5.4 Wave-turbulence interactions

Interactions between waves and turbulence in the ocean yield the transfer processes shown in diagrams (iv), (v), figure 6. The scattering processes (iv) involve interactions with turbulence scales of the same order or larger than a gravity wave length, whereas the parametric process (v) depends primarily on the small-scale turbulence structure.

Wave-turbulence scattering

The turbulence frequency ω_t can normally be neglected in the scattering condition $\pm\omega' \pm \omega_t = \omega$. It follows that a gravity-wave component g' of frequency ω' is scattered into a component g of practically the same frequency but different propagation direction. For a given component g', the wave-number of the scattering turbulence component $\underset{\sim}{k}_t = \pm \underset{\sim}{k}' \pm \underset{\sim}{k}$ is therefore confined to the interval $0 < k_t < 2k'$; turbulence components of scale smaller than a half wave length do not participate in scattering.

In the approximation $\omega_t \ll \omega$, the energy of the gravity-wave field is conserved by the scattering processes (Hasselmann, 1966). The transfer expression follows from the form (3.6.1) for conservative wave-wave interactions in the limit of a zero-frequency field ν_2,

$$\frac{DF(\underset{\sim}{k})}{Dt} \equiv S_{(g't\bar{g})}^{\bar{g}} + S_{(g'\bar{t}\bar{g})}^{\bar{g}} = \int K(\underset{\sim}{k},\underset{\sim}{k}')\left\{F(\underset{\sim}{k}') - F(\underset{\sim}{k})\right\} d\varphi' \qquad (5.4.1)$$

where $k' = k$, $\cos\varphi' = \frac{\underset{\sim}{k}\cdot\underset{\sim}{k}'}{kk'}$

(The source function $S_{(\bar{g}'t\bar{g})}^{\bar{g}}$ does not contribute, as the process $\bar{g}'t \rightarrow g$ is not compatible with the scattering condition for $\omega_t \ll \omega, \omega'$). The kernel K is symmetrical in $\underset{\sim}{k}$ and $\underset{\sim}{k}'$ and is a linear functional of the turbulence spectrum

$$\tilde{F}_{ij}(\underset{\sim}{k}'', z, z') = \int F_{ij}(\underset{\sim}{k}'', \omega'', z, z')\, d\omega''$$

where $\underset{\sim}{k}'' = \underset{\sim}{k} - \underset{\sim}{k}'$. F_{ij} is defined in equation (4.1.1).

The mean current $\underset{\sim}{U}$ represents a small correction in the present problem and can be neglected. The response function of the interaction equations then reduce to exponentials and the transfer function occuring in K becomes a straightforward combination of the coupling coefficients of equations (5.2.4) - (5.2.10). We shall not give K explicitly, however, as it is difficult to go further without more information about the turbulence spectrum F_{ij}.

Phillips (1959) has estimated the decay of a single wave beam due to scattering , i.e. equation (5.4.1) with $F(\underset{\sim}{k}') = o$, assuming an isotropic Kolmogoroff spectrum. The estimate is probably not very reliable, as the turbulence scales lie in the range in which the spectrum is strongly anisotropic, and the kernel K depends on both the scattering angle and the detailed tensor properties of F_{ij}. For the turbulence scales

in question, it may be more appropriate to allow for the density stratification of the ocean and regard the three-dimensional "turbulence" as a superposition of internal waves and a horizontal turbulence field. Formal expressions for scattering by internal waves and horizontal turbulence are given in Hasselmann (1966), but numerical estimates were not made. Kenyon (1966) has computed several cases of scattering between gravity-wave modes, but the processes considered were more relevant for the energy balance of internal waves than surface waves.

Parametric damping ("eddy viscosity")

The parametric process gt is determined by the interactions shown in figure 10. The contribution from a third diagram in which the components g' and g'' of the second diagram are interchanged turns out to be negligible. A detailed analysis shows that the principal interactions involve small-scale turbulence components in the inertial subrange of the equilibrium spectrum.

The interactions can be determined, as before, by expanding the interaction fields in powers of wave components $a^g_{\underset{\sim}{k}}$ and turbulence components $u_{j\underset{\sim}{k}\omega}$. For the gt process we need retain only terms which are linear in $a^g_{\underset{\sim}{k}}$ and may therefore write

$$\eta_{\underset{\sim}{k}} = \eta^{(0)}_{\underset{\sim}{k}} + \eta^{(1)}_{\underset{\sim}{k}} + \eta^{(2)}_{\underset{\sim}{k}} + \cdots$$

$$\varphi_{\underset{\sim}{k}} = \varphi^{(0)}_{\underset{\sim}{k}} + \varphi^{(1)}_{\underset{\sim}{k}} + \varphi^{(2)}_{\underset{\sim}{k}} + \cdots$$

where the superscript refers to the power of the turbulence components.

For $\underline{U} = 0$, the zero'th-order terms vanish, since the undisturbed wave solution is excluded in the definition of the interaction field.

The first-order solution is determined by the equations

$$\tilde{L}\left[\psi^{(1)}\right] = A^{(1)}\hat{\psi}\underset{\sim}{u} \tag{5.4.2}$$

$$-\frac{i}{k}\frac{\partial}{\partial t}\varphi^{(1)} = A^{(3)}\hat{\psi}\underset{\sim}{u} \tag{5.4.3}$$

with the boundary conditions

$$\psi^{(1)} = \tilde{B}^{(1)}\zeta\underset{\sim}{u} \quad \text{at} \quad z = 0 \tag{5.4.4}$$

$$\psi^{(1)} = 0 \qquad \text{at} \quad z = -H \tag{5.4.5}$$

Higher-order solutions are determined by solving the equations (4.4.7) - (4.4.10).

For $\underline{U} = o$, the inviscid Orr-Sommerfeld operator reduces to the Laplacian form

$$\tilde{L} = -\frac{i}{k}\frac{\partial}{\partial t}\left(\frac{\partial^2}{\partial z^2} - k^2\right) \tag{5.4.6}$$

which enables the analysis to be carried through explicitly. We need not give the complete solution, however, since the major contribution arises from interactions with turbulence components of scale small compared with a gravity wave length,

which simplifies the analysis considerably.

In the first-order equations (5.4.2) - (5.4.5), let $\underset{\sim}{k}$, $\underset{\sim}{k}'$ and $\underset{\sim}{k}''$ be the respective wave-numbers of the components $\hat{\psi}$ (wave-field), $\underset{\sim}{u}$ (turbulence) and $\psi^{(1)}$, $\varphi^{(1)}$ (first-order interaction field). We assume that $k' \ll k$. Then $\underset{\sim}{k}'' \approx \underset{\sim}{k}'$, since $\underset{\sim}{k}'' = \underset{\sim}{k}' + \underset{\sim}{k}$.

The interaction field $\psi^{(1)}$, $\varphi^{(1)}$ may be represented as a superposition of two fields $\psi_v^{(1)}$, $\varphi_v^{(1)}$ and $\psi_s^{(1)}$, $\varphi_s^{(1)}$, where $\psi_v^{(1)}$, $\varphi_v^{(1)}$ satisfies the inhomogeneous field equations (5.4.2), (5.4.3) with homogeneous boundary conditions and $\psi_s^{(1)}$, $\varphi_s^{(1)}$ is the solution of the homogeneous field equations with the inhomogeneous boundary conditions (5.4.4) - (5.4.5).

Since the Green function $G(z,z')$ of the Laplace operator (5.4.6) falls off as $e^{-k''|z-z'|}$, the component $\psi_v^{(1)}(z)$ is determined, for large k', by the local values of the forcing function $A^{(1)}\hat{\psi}\underset{\sim}{u}$ in a thin layer of thickness $\delta = 1/k$. The component $\psi_s^{(1)}$ is similarly limited to a surface layer of the thickness δ. ($\varphi_v^{(1)}$ is rigorously local, and $\varphi_s^{(1)}$ vanishes).

The second-order fields $\psi^{(2)}$, $\varphi^{(2)}$ are determined by similar equations (5.4.7) - (5.4.10) in which the products $\psi^{(1)}\underset{\sim}{u}$, $\varphi^{(1)}\underset{\sim}{u}$ occur as forcing terms. The wave-number of the $\underset{\sim}{u}$-component in this case is $-\underset{\sim}{k}'$, so that the second-order excitation appears at the wave-number $\underset{\sim}{k}'' - \underset{\sim}{k}' = \underset{\sim}{k}$ of the gravity-wave component. The net excitation involves a gravity-wave component and two turbulence components of opposite wave-number (figure 10).

The forcing functions consist of surface terms and volume terms, both depending on small-scale turbulence components in a layer of thickness δ. We assume that for these scales the turbulence can be regarded as locally isotropic. The integration over the layer can then be carried out and expressed in terms of the local scalar turbulence spectrum $E(k,\omega)$, where (cf. Batchelor, 1963)

$$F_{ij}(K,\omega) = \frac{\langle u_{i\underset{\sim}{K}\omega}(u_{j\underset{\sim}{K}\omega})^{*}\rangle}{\Delta\underset{\sim}{K}\,\Delta\omega} = \frac{E(K,\omega)}{4\pi}\left(\delta_{ij} - \frac{K_iK_j}{K^2}\right) \qquad (.4.7)$$

and we have introduced the Fourier representation

$$u_j(\underset{\sim}{x},z,t) = \sum_{\underset{\sim}{K},\omega} u_{j\underset{\sim}{K}\omega}\, e^{i(\underset{\sim}{k}\cdot\underset{\sim}{x} + k_3 z + \omega t)}$$

with respect to the three-dimensional wave-number $\underset{\sim}{K} = (\underset{\sim}{k}, k_3)$.

The wave equation (.2.10) involves the derivative $\frac{\partial q^{(2)}}{\partial z}$ at the surface. This is proportional to the surface forcing function plus an integral over the depth of the volume forcing function multiplied by e^{kz} (for the present discussion, we take the depth as infinite, which eliminates the negative exponential e^{-kz} in the Green function). Noting that the forcing functions are proportional to $\hat{q} \sim e^{kz}(a^{q}_{\underset{\sim}{k}} + a^{-q}_{\underset{\sim}{k}})$, the wave equation finally reduces to the form

$$\dot{a}^{q}_{\underset{\sim}{k}} + i\sigma a^{q}_{\underset{\sim}{k}} = -\gamma\left(a^{q}_{\underset{\sim}{k}} + a^{-q}_{\underset{\sim}{k}}\right) \qquad (.4.8)$$

$$\gamma \equiv \gamma_v + \gamma_s = \int T(\underset{\sim}{k},K,\omega)E(K,\omega)e^{2kz}\,dK\,d\omega\,dz + \gamma_s, \qquad (.4.9)$$

γ_s depending on the turbulence spectrum at the surface. The wave damping is given by the real part of γ,

$$\frac{D}{Dt}F(\underset{\sim}{k}) \equiv S^{q}_{qt} = -2Re(\gamma)F(\underset{\sim}{k}) \qquad (.4.10)$$

The coefficients γ_r and γ_s involve interactions in surface layers of the thickness of a gravity wave length and a turbulence scale, respectively. It may be expected that the energy transfer is not critically dependent on the turbulence characteristics in a thin surface layer of the order of a turbulence scale, and that therefore $\gamma_s \ll \gamma_r$. However, an inspection of the interactions in terms of the velocity components indicates that this is not the case.

Let $\underset{\sim}{v} = \underset{\sim}{u}^W + \delta\underset{\sim}{u}$ be the velocity of the combined wave and interaction fields. Subtracting the equations of motion of the turbulent field $\underset{\sim}{u}$ from the equations of motion of the total field $\underset{\sim}{u} + \underset{\sim}{v}$, we obtain

$$\frac{\partial v_i}{\partial t} = -\frac{1}{\rho}\frac{\partial \tilde{\omega}}{\partial x_i} - \frac{\partial}{\partial x_j}(v_i v_j) - \frac{\partial}{\partial x_j}(v_i u_j + v_j u_i) \qquad (5.4.11)$$

where $\tilde{\omega}$ is the pressure difference between the fields $\underset{\sim}{u} + \underset{\sim}{v}$ and $\underset{\sim}{u}$. The viscous terms are found later to be negligible and have been discarded. Equation (5.4.11) is equivalent to equations (5.2.4), (5.2.5).

The boundary conditions are

$$\frac{\partial \zeta}{\partial t} - v_3 + \sum_{j=1}^{2} \frac{\partial}{\partial x_j}(\zeta u_j) = 0 \quad \text{at } z = 0 \qquad (5.4.12)$$

$$\tilde{\omega} - g\zeta + \zeta\frac{\partial \tilde{\omega}}{\partial x_3} + \zeta\frac{\partial p}{\partial x_3} = 0 \quad \text{at } z = 0 \qquad (5.4.13)$$

and

$$v_3 \to 0 \quad \text{for } z \to -\infty \qquad (5.4.14)$$

If the field $\underset{\sim}{v}$ is expanded, as before, in powers of the turbulence components,

$$\underset{\sim}{v} = \underset{\sim}{v}^{(0)} + \underset{\sim}{v}^{(1)} + \underset{\sim}{v}^{(2)} + \dots$$

we obtain for the second-order equation, following the analysis outlined above,

$$\frac{\partial v_i}{\partial t} = -\frac{1}{\rho}\frac{\partial \tilde{\omega}}{\partial x_i} + \frac{\partial}{\partial x_j} T_{ij}^{(2)} \quad \text{for} \quad z < 0 \qquad (5.4.15)$$

$$\frac{\partial \zeta^{(2)}}{\partial t} - v_3^{(2)} = R^{(2)} \quad \text{at} \quad z = 0 \qquad (5.4.16)$$

$$\tilde{\omega}^{(2)} - g\zeta^{(2)} = 0 \quad \text{at} \quad z = 0 \qquad (5.4.17)$$

$$v_3^{(2)} \to 0 \quad \text{for} \quad z \to -\infty \qquad (5.4.18)$$

where the forcing terms $T_{ij}^{(2)}$ and $R^{(2)}$ are proportional to the zero'th order wave-height and the local turbulence spectrum.

The damping of the wave field can be deduced from energy considerations. If the energy spectrum

$$\tilde{F}(\underset{\sim}{k}) = \frac{\rho}{2\Delta \underset{\sim}{k}} \left\{ g\langle \zeta_{\underset{\sim}{k}} \zeta_{-\underset{\sim}{k}} \rangle + \int_{-\infty}^{0} \langle v_{i\underset{\sim}{k}} v_{i-\underset{\sim}{k}} \rangle dz \right\}$$

is expanded in powers of the turbulence components, $\tilde{F} = \tilde{F}^{(0)} + \tilde{F}^{(1)} + \tilde{F}^{(2)} + \ldots$ one finds readily that to lowest order

$$\frac{\partial \tilde{F}}{\partial t} = \frac{\partial \tilde{F}^{(2)}}{\partial t} = \frac{1}{\Delta \underset{\sim}{k}} Re \left\{ g \Sigma_{\underset{\sim}{k}}^{(0)} R_{\underset{\sim}{k}}^{(2)} + \int_{-\infty}^{0} \frac{\partial T_{ij\underset{\sim}{k}}^{(2)}}{\partial x_j} v_{i-\underset{\sim}{k}}^{(0)} dz \right\} \qquad (3.4.19)$$

where the subscripts $\underset{\sim}{k}$ refer to Fourier components with respect to horizontal wave number, and

$$\frac{\partial}{\partial x_j} \equiv \begin{cases} ik_j & (j = 1,2) \\ \frac{\partial}{\partial z} & (j = 3) \end{cases}$$

The energy loss represents the work done against a surface pressure proportional to $R_{\underset{\sim}{k}}^{(2)}$ and the volume stress-force $\frac{\partial T_{ij\underset{\sim}{k}}^{(2)}}{\partial x_j}$.

The essential feature of equation (3.4.19) is that the work per volume is associated with a stress force. The total energy loss can therefore not be uniquely divided into volume and surface contributions. This may be seen by rewriting the stress term in equation (3.4.19) as the difference between the work done by the surface stress and the dissipation $\Phi_{\underset{\sim}{k}}$,

$$Re \int_{-\infty}^{0} \frac{\partial T_{ij\underset{\sim}{k}}^{(2)}}{\partial x_j} v_{i-\underset{\sim}{k}}^{(0)} dz = Re \left\{ T_{i3\underset{\sim}{k}}^{(2)} v_{i-\underset{\sim}{k}}^{(0)} \right\}_{z=0} - \Phi_{\underset{\sim}{k}}$$

where

$$\Phi_{\underset{\sim}{k}} = Re \int_{-\infty}^{0} T_{ij\underset{\sim}{k}}^{(2)} \frac{\partial v_{i-\underset{\sim}{k}}^{(0)}}{\partial x_j} dz$$

The surface-stress term and the dissipation are comparable if the turbulence at the surface and within the fluid are of the same order.

A quantitative estimate of the surface contributions is difficult, since the turbulence in a surface layer of the dimension of a turbulence scale is not isotropic. However, the dissipation $\Phi_{\underset{\sim}{k}}$ is insensitive to the turbulence properties in the thin surface layer and can be evaluated assuming local isotropy throughout.

One finds, after some analysis (Hasselmann, 1967b)

$$\frac{DF}{Dt} = -\beta_\phi F \qquad (5.4.20)$$

$$\beta_\phi = \frac{16\pi k^2}{15} \int_{-\infty}^{0} \left\{ \int_{0}^{\infty} E(K',\sigma) dK' \right\} e^{2kz} 2k dz \qquad (5.4.21)$$

Equations (5.4.20) - (5.4.21) are exact if the turbulence does not extend to the surface (e.g. turbulence caused by breaking internal waves or internal shear layers).

In the inertial subrange, the scalar turbulence spectrum is given by (cf. Batchelor, 1963)

$$E(K,\omega) = \varepsilon^{2/3} K^{-5/3} \omega_0^{-1} f(\omega/\omega_0)$$

where $\rho\varepsilon$ is the turbulent energy dissipation per unit volume,

$$\omega_0 = \varepsilon^{1/3} K^{2/3}$$

and f(x) is a universal function. Turbulence measurements in a tidal channel by Grant et al. (1962) indicate that $\int_{-\infty}^{+\infty} f(x)dx \approx 1.5$.

If the wave damping is due primarily to interactions in the inertial subrange, equation (5.4.21) becomes

$$\beta_\phi = \frac{\bar{\varepsilon} k \delta}{g} \qquad (5.4.22)$$

where $\bar{\varepsilon} = \int_{-\infty}^{0} \varepsilon(z) 2k e^{2kz} dz$ is the weighted mean dissipation over the depth and $\delta = \frac{8\pi}{5} \int_{0}^{\infty} x f(x) dx$ is a constant. (For finite depth, $\bar{\varepsilon} = \int_{-H}^{0} \varepsilon \frac{\sinh^2 k(z+H)}{\sinh 2kH} 4k\, dz$). Equation (5.4.22) corresponds to a "turbulent viscosity" $\nu_t = \frac{\bar{\varepsilon}\delta}{4gk}$.

It is readily verified that the contributions to β_ϕ from interactions outside the inertial subrange are negligible.

At low wave-numbers, $E(K', \sigma) \to 0$, since $\sigma/\omega_0 \to \infty$: the wave frequency becomes large compared with the turbulence frequencies as the turbulence scales approach a wave-length. The contribution from anisotropic turbulence of scales comparable with are larger than a wave-length is negligible provided the integral $\int_0^\infty x f(x) dx$ converges at infinity. (This is ensured if the acceleration spectrum exists).

At high wave-numbers, the contribution from the dissipation range of the turbulence spectrum is negligible if $\sigma \ll \omega_0(K_s) = \varepsilon^{1/3} K_s^{2/3}$, where $K_s = \varepsilon^{1/4} \nu^{-3/4}$ is the upper limit of the inertial subrange at which the viscous and inertial forces become comparable (ν = viscosity). The condition yields $\varepsilon \gg \nu\sigma^2$ or, on account of equation (5.4.22), $\beta_\phi \gg \nu k^2 \delta$. The viscous decay factor for deep-water waves is $\beta_\nu = 4\nu k^2$; the expression (5.4.22) is therefore valid provided the parametric damping is large compared with the laminar viscous damping. This is, in fact, the only case of interest, since the viscous damping is always negligible for ocean waves.

It remains to be verified that the interactions are weak from the point of view of the turbulence field. This is presumably the case if the energy gained by the turbulence through interactions with waves is small compared with the energy transfer due to internal turbulence interactions. The wave-turbulence energy transfer per unit volume at depth z is $\frac{2\varepsilon\delta}{g} \int F(\underline{k}) k^2 e^{2kz} dz$.

This is clearly small compared with ε if the mean square wave slope is small, which we have assumed throughout.

Measurements of ε in the open ocean have not been made, but lower bounds can be infered from the known tidal dissipation of the oceans. A uniform dissipation over all oceans corresponds to $\varepsilon \approx 10^{-5}$ ergs cm^{-3} sec^{-1}, which yields entirely negligible damping. However, it is believed that the tidal energy is dissipated mainly in shallow seas of rather limited area. In these regions, the values of ε may range from about 0.1 to maximally 10 ergs cm^{-3} sec^{-1} (cf. Munk and MacDonald, 1960). This corresponds to a damping factor for a 60 m wave of $\beta_\phi = 10^{-7}$ to 10^{-5} secs, or a decay time of 100 days to 1 day. It appears that the parametric damping due to tidal turbulence is weak even in regions of high tidal dissipation. (We have assumed a fairly uniform distribution of turbulence. Localised wave-turbulence interactions in a boundary layer at the ocean bottom are more important, cf. section 5.5).

Another source of turbulence is white-capping. In this case ε is given by the energy lost by the waves through wave-breaking. Since we have seen that the energy loss due to wave-turbulence interactions is small compared with ε if the mean-square wave slope is small, the parametric wave damping is negligible also in this case (in a fully-developed sea, the mean square wave slope is of the order of 0.02).

By the same reasoning, the "turbulent viscosity" will always be negligible unless a source of turbulence energy exists which is large compared with the energy lost by the waves. It is difficult to find such a source in the open ocean. The energy transfer from the atmosphere is almost certainly too small. Excluding extreme situations such as very strong currents in shallow water, it appears that the turbulent viscosity, although often considered in wave-prediction methods, is not an important parameter in the energy balance of ocean waves.

5.5 Strong interactions

Our applications of the general interaction formalism have been limited to interaction which are weak and expansible. For ocean waves, all interactions are clearly weak in the mean, since the observed wave growth and decay times are large compared with a wave period. However, the interactions may be relatively strong in highly localized regions and can then no longer be expanded. Formally, the theory breaks down if abnormally large values of the skewness, kurtosis, etc. associated with highly intermittent fields outweigh the expansion parameter in the moment expansions.

The transfer expressions can then no longer be truncated at the lowest-order moments (the spectra). As examples of such interactions we discuss briefly white capping and the damping of finite-depth waves by bottom friction.

White capping

Quantitative measurements and an adequate theory of white capping are both lacking, but it is generally believed that white capping is the principal dissipative mechanism balancing the generating processes in a "fully developed" equilibrium spectrum.

Phillips (1958) has suggested that for dimensional reasons white capping leads to an equilibrium frequency spectrum proportional to ω^{-5}. The power law has been confirmed by several measurements, the observed exponent varying between -4.5 and -5.5. However, the dimensional argument is difficult to support.

An ω^{-5} frequency spectrum corresponds to a two-dimensional wave-number spectrum

$$F(\underline{k}) = C_g k^{-4} S(\varphi, k) \qquad (5.5.1)$$

where φ is the propagation direction, $s(\varphi,k)$ is the "spreading factor", normalized such that $\int_{-\pi}^{+\pi} s(\varphi,k)\, d\varphi = 1$, and C is a constant. Phillips deduced the spectrum (5.5.1) essentially by assuming that the equilibrium spectrum was determined entirely by the white capping process and that this could be completely characterized locally by the three parameters g, $\underset{\sim}{k}$ and $F(\underset{\sim}{k})$. However, this yields an isotropic spectrum, since the parameters do not define a reference direction. The observed spectrum is a strongly anisotropic distribution ($s(\varphi) \sim \cos^4\varphi$) with the mean propagation parallel to the wind. This implies that the wind velocity is also an essential parameter of the problem, and the dimensional argument leading to the ω^{-5} law is not applicable.[+)]

It is, indeed, difficult to imagine an equilibrium spectrum which is independent of the energy input, unless the dissipative mechanism is envisaged as a strong, on-off process which is effective only after the spectrum has exceeded a fixed, locally defined threshhold. But it is improbable that white capping is local in $\underset{\sim}{k}$-space. The visual impression suggests locality in $\underset{\sim}{x}$, and both properties are normally mutually exclusive. This is also indicated by the form of the spectrum (5.5.1). The instability conditions for white-capping are not known precisely, but it is generally believed that instability occurs when the local downward acceleration of the surface exceeds the gravitational acceleration g. Thus the root mean square acceleration of the surface is presumably one of the principal parameters characterizing white capping. For equation (5.5.1), this quantity diverges at both ends of the spectrum. Thus the probability of white capping is determined not only by the equilibrium range, but depends also on the cut-off frequencies of the range.

[+)] Phillips actually applied the dimensional argument only to the one-dimensional spectrum, which does not lead to a direct contradiction. However, in this case it must be assumed that the dependence on the wind velocity disappears after averaging our all propagation directions, which is difficult to justify physically.

The effect of white capping on the equilibrium spectrum is not yet understood; it appears that dimensional arguments are inadequate and that the wave-breaking process itself needs investigating.

Bottom friction

The damping of finite-depth waves by bottom friction involves strongly non-linear, localized interactions in a non-stationary turbulent boundary layer. A rigorous treatment appears at present impossible. We present here an approximate analysis (Hasselmann and Collins, 1967b) based on the empirical friction law

$$\underset{\sim}{\tau} = -\rho c_f \underset{\sim}{u}|\underset{\sim}{u}| \qquad (5.5.2)$$

where $\underset{\sim}{\tau}$ is the shear stress at the wall, $\underset{\sim}{u}$ is the flow velocity at the edge of the boundary layer and c_f is a "constant" friction coefficient. Equation (5.5.2) is known to be a fair approximation for a wide range of turbulent flows. It has been tested for periodic waves by Savage (1953), Iwagaki etal. (1965) and Jonsson (1965), among others, and has been used in semi-empirical wave prediction methods by Putnam and Johnson (1949) and Bretschneider and Reid (1954). The friction coefficient is, in fact, a slowly varying function of the flow parameters, but for the present first-order approach we shall regard c_f as a constant.

We assume that the flow consists of a wave field $\underset{\sim}{u}^w$ and a mean current $\underset{\sim}{u}^c$. We ignore interactions between the wave field and the mean current except in the turbulent boundary layer at the bottom. The complete flow in the $\underset{\sim}{w} = \underset{\sim}{u}^w + \underset{\sim}{u}^c + \underset{\sim}{u}^t$, where $\underset{\sim}{u}^t$ is the turbulent velocity field in the bottom boundary layer. We regard $\underset{\sim}{u}^t$ as zero outside a thin boundary layer of thickness $\delta \ll H$. (The wave velocity field is defined as the potential flow, equation (5.2.1), associated with the surface displacement ζ. We define $\underset{\sim}{u}^c$ arbitrarily as constant in the boundary layer. The turbulent velocity is then given as the difference between the complete flow $\underset{\sim}{w}$ and the velocity field $\underset{\sim}{u}^w + \underset{\sim}{u}^c$).

The surface displacement may be represented as

$$\zeta = \sum_{\underset{\sim}{k}} Z_{\underset{\sim}{k}}$$

where to first order $Z_{\underset{\sim}{k}}$ are statistically orthogonal, free-wave components,

$$Z_{\underset{\sim}{k}} = \hat{Z}_{\underset{\sim}{k}} \cos (\underset{\sim}{k}\cdot\underset{\sim}{x} - \sigma t + \vartheta_{\underset{\sim}{k}})$$

with

$$\langle Z_{\underset{\sim}{k}} \rangle = 0, \qquad (5.5.3)$$

$$\langle Z_{\underset{\sim}{k}} Z_{\underset{\sim}{k}'} \rangle = \frac{\langle \hat{Z}_{\underset{\sim}{k}} \hat{Z}_{\underset{\sim}{k}'} \rangle}{2} = \frac{2 \Delta_{\underset{\sim}{k}} F(\underset{\sim}{k})}{\varrho g} \delta_{\underset{\sim}{k}\underset{\sim}{k}'} \qquad (5.5.4)$$

The wave velocity field is accordingly

$$\underset{\sim}{u}^{w} = \sum \underset{\sim}{U}_{\underset{\sim}{k}}$$

where the components $\underset{\sim}{U}_{\underset{\sim}{k}}$ depend linearly on $Z_{\underset{\sim}{k}}$. In particular,

$$\underset{\sim}{U}_{\underset{\sim}{k}} = \frac{g\underset{\sim}{k}}{\sigma \cosh kH} Z_{\underset{\sim}{k}} \quad at \quad z = -H \qquad (5.5.5)$$

On account of the boundary-layer interactions, the amplitudes $Z_{\underset{\sim}{k}}$ and phases $\chi_{\underset{\sim}{k}}$ are not exactly constant, but vary slowly with time. To first order, the damping of the amplitudes can be determined from the free-wave field by calculating the work done by the bottom stress against the free-wave velocity.

If we multiply the equations of motion of the complete flow

$$\rho \frac{\partial w_i}{\partial t} = - \frac{\partial p}{\partial x_i} - \rho \frac{\partial}{\partial x_j}(w_i w_j) + \nu \rho \nabla^2 w_i$$

by $U_{i\underset{\sim}{k}}$, take expectation values and then integrate over the depth from -H to ζ we obtain, applying the usual boundary conditions and the orthogonality property (5.5.4),

$$2\Delta\underset{\sim}{k} \frac{\partial F(\underset{\sim}{k})}{\partial t} = \left\langle \tau_i U_{i\underset{\sim}{k}} \right\rangle_{z=-H} - \int_{-H}^{-H+\delta} \left\langle T_{ij} \frac{\partial U_{i\underset{\sim}{k}}}{\partial x_j} \right\rangle dz - \frac{\partial}{\partial t} \int_{-H}^{-H+\delta} \left\langle (u_i^t + u_i^c) U_{i\underset{\sim}{k}} \right\rangle dz$$

where $T_{ij} = - \rho \frac{\partial}{\partial x_j}(w_i w_j) + \rho \nu \nabla^2 w_i$ is the total stress tensor and $\tau_i = T_{3i}$

For $\delta \ll H$, the last two terms can be neglected, so that

$$2\Delta\underset{\sim}{k} \frac{\partial F(\underset{\sim}{k})}{\partial t} = \left\langle \tau_i U_{i\underset{\sim}{k}} \right\rangle_{z=-H} \qquad (5.5.6)$$

(the factor 2 arises from the normalisation of $F(\underset{\sim}{k})$ in section (2.1), $\int F(\underset{\sim}{k})\, d\underset{\sim}{k} = \frac{E}{2}$).

In deriving (5.5.6) we invoked only the orthogonality of the Fourier components. However, if the interactions are weak in the mean, we may now substitute the free-wave velocities in the expression on the right hand side of the equation . For $\delta \ll H$, we may further replace the velocity $\underset{\sim}{u} = \underset{\sim}{u}^w + \underset{\sim}{u}^c$ at the edge of the boundary layer by the velocity at the wall in equation (5.5.2) for $\underset{\sim}{\tau}$. In the following, all velocities refer to the values at the wall.

It is convenient to introduce, for fixed $\underset{\sim}{k}$, the variables

$$\underset{\sim}{u}' = \underset{\sim}{u} - \underset{\sim}{U}_k$$

which are orthogonal to $\underset{\sim}{U}_k$,

$$\langle u_i' U_{j\underset{\sim}{k}} \rangle = 0$$

(equations (5.5.3) - (5.5.5))

Since $\underset{\sim}{u}'$ differs from $\underset{\sim}{u}$ by an infinitesmal quantity, we may express $\underset{\sim}{\tau}$ in terms of $\underset{\sim}{u}'$, $\underset{\sim}{U}_k$ and then expand with respect to $\underset{\sim}{U}_k$:

$$\underset{\sim}{\tau} = -\varrho c_f \, u' (\underset{\sim}{u}' + \underset{\sim}{U}_k)\left(1 + \frac{\underset{\sim}{u}' \cdot \underset{\sim}{U}_k}{u'} + \cdots\right)$$

so that

$$\langle \tau_{i\underset{\sim}{k}} U_{i\underset{\sim}{k}} \rangle = -\varrho c_f \left\langle u' \left(u_i' U_{i\underset{\sim}{k}} + U_{i\underset{\sim}{k}} U_{i\underset{\sim}{k}} + \frac{u_i' u_j' U_{i\underset{\sim}{k}} U_{j\underset{\sim}{k}}}{u'} + \cdots \right) \right\rangle \quad (5.5.7)$$

Now, a linear field of dispersive free waves is always Gaussian (except for a short transition period after an initial, non-Gaussian state, cf. Hasselmann, 1967 a). Since $\underset{\sim}{u}'$ and $\underset{\sim}{U}_k$ depend linearly on the wave field, they are jointly Gaussian. Moreover, they are statistically orthogonal, and one component, $\underset{\sim}{U}_k$, has

zero mean. It follows that $\underset{\sim}{u}'$ and $\underset{\sim}{U}_k$ are, in fact, statistically independent. The mean product of equation (5.5.7) can therefore be divided into two factors,

$$\langle \tau_i U_{ik} \rangle = -\rho c_f \left\{ \langle U_{ik} U_{ik} \rangle \langle u' \rangle + \langle u_{ik} u_{jk} \rangle \left\langle \frac{u_i' u_j'}{u'} \right\rangle \right\}$$

We may now replace $\underset{\sim}{u}'$ again by $\underset{\sim}{u}$ and obtain, substituting in equation (5.5.6) and allowing for equations (5.5.4), (5.5.5.),

$$\frac{\partial F(\underset{\sim}{k})}{\partial t} = -\nu_{ij} k_i k_j F(\underset{\sim}{k}) \qquad (5.5.8)$$

where the anisotropic viscosity tensor

$$\nu_{ij} = \frac{g c_f}{\sigma^2 \cosh^2 kH} \left\{ \delta_{ij} \langle u \rangle + \left\langle \frac{u_i u_j}{u} \right\rangle \right\} \qquad (5.5.9)$$

The quantities $\langle u \rangle$, $\left\langle \frac{u_i u_j}{u} \right\rangle$ are determined by the Gaussian probability distribution of the variables u_i . The mean of the distribution is equal to $\underset{\sim}{u}^c$; the covariance matrix is determined by the spectrum,

$$\mu_{ij} = \langle (u_i - u_i^c)(u_j - u_j^c) \rangle = \frac{2g}{\rho} \int \frac{k_i k_j}{\sigma^2 \cosh^2 kH} F(\underset{\sim}{k}) \, d\underset{\sim}{k}$$

In the zero-current case, the mean quantities of equation (5.5.9) can be expressed in terms of complete elliptic integrals,

$$\langle u \rangle = \sqrt{\frac{2\mu_{11}}{\pi}} \, \underline{E}$$

$$\left\langle \frac{u_1^2}{u} \right\rangle = \sqrt{\frac{2\mu_{11}}{\pi}} \left(\frac{\underline{E}}{x^2} - \frac{\underline{K}}{x^2} (1 - x^2) \right)$$

$$\left\langle \frac{u_2^2}{u} \right\rangle = \sqrt{\frac{2\mu_{11}}{\pi}} \left(\frac{1 - x^2}{x^2} \right) (\underline{K} - \underline{E})$$

where $\varkappa = \sqrt{1 - \frac{\mu_{22}}{\mu_{11}}}$, $K(\varkappa)$ and $E(\varkappa)$ are complete elliptic integrals of the first and second kind, respectively, and the coordinate system has been chosen such that $\mu_{12} = 0, \mu_{22} < \mu_{11}$. The damping is a maximum in the mean propagation direction.

Figures 11 and 12 show two examples of the spectral decay computed for the case of a zero mean current and a mean current of 0.7 m/sec at 45° to the initial mean wave direction. The (constant) water depth of 100 m is representative of the North Sea. The initial energy distribution corresponds to a 40-knot Pierson-Moskowitz spectrum, equation (? 3.3), with a $\cos^4\varphi$ spreading factor. The friction factor $c_f = 0.015$ was determined by comparison of theoretical predictions with wave observations made at two off-shore stations at Panama City, Florida (Hasselmann and Collins, 1967). The value is consistent with other experimental data for periodic waves (cf. Jonsson, 1965), but is probably too large for the mean-current case. However, the same value of c_f was taken in both cases for the sake of comparison.

It appears that wave damping by bottom friction can be quite important in shallow seas and continental margins. We mention that although the computations were based on the rather crude friction law (5.5.2), this was not essential for the analysis. The same method can be applied for a more sophisticated friction law.

5.6 Comparison with observations

The direct method of investigating interaction processes experimentally is by cross-spectral or cross-bispectral analysis of the interacting fields. Unfortunately, measurements of this type are difficult to make, and one is limited largely to indirect evidence from wave observations.* However, bispectral analysis was used by Hasselmann et al. (1963) to measure second-order wave interactions. In this case, the measurements involved only the wave field.

(Footnote)

The propagation of ocean swell over long distances may be expected to depend more strongly on interactions within the ocean than wave-air interactions, and should therefore shed some light on the processes discussed in this chapter. We may include here also the wave-wave interactions discussed in section 3.6.

Snodgrass et al. (1966) have measured swell attenuation in the Pacific. Waves radiated from storms South of New Zealand were recorded at six stations spaced at approximately equal distances along a 12,000 km = 110° great circle between New Zealand and Alaska. Twelve major storms were identified during the ten-week experiment. Only low-frequency storm waves ($\sigma/2\pi <$ 0.1 cycles per second) could be detected above the local-sea background. (An increase in wind speed adds additional low-frequency waves to the "fully developed" spectrum, but does not appreciable affect the spectrum at intermediate and high frequencies, cf. equation (2.3.3)).

A significant attenuation was observed only within the first two or three thousand kilometers from the storm center. Over the remaining distance, the waves propagated virtually undamped.

The computed attenuation due to wave-wave scattering was found to be negligible for frequencies below 0.1 cycles per second at distances greater than a few thousand kilometers from the storm center. We have seen that the parametric damping due to small-scale turbulence is also small. The observations show further that wave-turbulence scattering is unimportant in most of the ocean. Scattering should have been noticable, besides by wave attenuation, by the late arrival of scattered energy, which was not detected.

The station spacing was inadequate for accurate measurement of the wave attenuation in the near zone. However, the general features of the observed decay were consistent with the computed energy transfer due to wave-wave scattering. Figure 13 shows a typical example of the spectra observed close to the storm.

The spectrum in the generating region was not measured, but could be estimated from the winds reported in the generating region (by means of the Pierson-Moskowitz formula. The spectra are corrected for distortion due to dispersion. The lower panels show the computed energy transfer due to wave-wave scattering. The small positive energy transfer at the peak appears to be typical of a peak close to a low-frequency cut-off (Hasselmann, 1963 b). The energy lost at intermediate frequencies is transfered to higher frequencies, not shown in the figures.

The travel time for 80 millicycle-per-second waves from the storm to the first station, Cape Palliser, New Zealand, was approximately 10^5 secs (1 day); from Cape Palliser to the second station, Tutuila, the travel time was approximately 2.10^5 secs. Bearing in mind that the transfer rates in each figure refer to the initial spectrum, the wave-wave scattering accounts quite well for the observed changes.

Beyond Tutuila, the spectral densities were reduced so far by dispersion and scattering that the computed scattering became negligible (except for angular beam broadening, which has no direct effect on the one-dimensional frequency spectrum). The observed attenuation beyond Tutuila was also negligible.

Wave-breaking or scattering by turbulence can not be excluded in the near zone by the data. However, the order-of-magnitude agreement with the computed transfer rates due to wave-wave scattering demonstrate that wave-wave scattering is at least an important term in the net energy balance of the wave field.

6. Conclusions

We have discussed the coupling between ocean waves and random fields in the ocean and atmosphere from the viewpoint of a general interaction formalism. The theory is complete, in the sense that we have been able to treat all lowest-order processes. However, it applies only to interactions which are weak and expansible.

The validity of the expansion procedure must be investigated for each process. A rigorous convergence proof was not attempted*, but it can generally be verified that the expansions are consistent in the sense that the expansion parameters are small and the lowest-order interacting fields may be regarded as statistically independent. The convergence question is not associated with finite-order interaction theory as such. It arises already in the linear represensation of 'free' wave fields. The interaction analysis is neither more nor less rigorous than the linear theory (excluding, of course, the problem of statistical closure). Interactions with atmospheric turbulence are an important case in which this was not demonstrated, although the assumptions appear plausible and are valid for sufficiently small wave heights. The question can be resolved by trial computations or measurements.

(Footnote)

Wave breaking and turbulent bottom friction are examples of non-expansible process. However, in both cases the interactions are weak in the mean. This property proved sufficient to determine the damping due to a non-analytic turbulent bottom stress.

The analysis for expansible interactions is basically straight forward, but can become involved algebraically. Interaction diagrams are useful in describing the structure of the expansion independent of algebraic details. The net energy transfer is the result of many interaction combinations, which may be classed into scattering and

parametric processes. Transfer diagrams afford a concise notation for distinguishing between the various processes. Even where the transfer functions are not known in detail, the general structure of the transfer expressions summarized by the transfer diagrams can be helpful in understanding the overall energy balance of the wave field.

Numerical estimates exists at present for only a few processes: the wave-generation processes of Phillips and Miles, wave-wave scattering, and parametric damping by turbulence. We have not attempted to estimate rather complicated transfer expressions by order-of-magnitude dimensional considerations. However, computations based on simplified boundary-layer models should be feasible. A more fundamental problem is estimating the energy loss due to white-capping, at present the one basically undetermined process in the radiation balance equation.

Only very few measurements bearing on the wave energy balance have been made, but these have proved extremely fruitful. Further experiments of this kind would be very desirable. Laboratory (and, if possible, field) studies of the interaction mechanisms by cross correlation techniques would also be invaluable in assessing the relative significance of the various processes.

Acknowledgments

This article is based largely on work done while the author was at the Institute of Geophysics and Planetary Physics at the University of California, San Diego. The author is grateful for many stimulating discussions during this time with Drs. Munk, Cox, Miles, Gilbert, Backus and many others. The work was supported in part by the National Science Foundation under grant GP 2414. The work reported in the second part of section 5.5 was supported by the National Engineering Science Company.

Appendix Coupling coefficients

($\partial \equiv \partial/\partial z$; ∂', ∂'' denote differentiations with respect to z of the component of wave-number $\underset{\sim}{k}'$ and $\underset{\sim}{k}''$, respectively. Hence $\partial \equiv \partial' + \partial''$).

$$A^{(1)} = \begin{cases} \dfrac{k'k_j}{k^2}\partial\partial'' - \dfrac{(k'_\ell k''_\ell k_j + k'_\ell k_\ell k'_j)\partial\partial'}{k^2 k'} + k'k'_j & (j = 1,2) \\ \dfrac{ik'_\ell k_\ell}{k'k^2}\partial\partial'\partial + i\dfrac{k'_\ell k''_\ell}{k'}\partial' - ik'\partial & (j = 3) \end{cases}$$

$$A^{(2)} = \begin{cases} \dfrac{\eta'_\ell k''_\ell}{k^2}(k_j + k'_j)\partial & (j = 1,2) \\ -i\eta'_\ell k''_\ell\left(\dfrac{\partial\partial'}{k^2} + 1\right) & (j = 3) \end{cases}$$

$$A^{(3)} = \begin{cases} \dfrac{k'_\ell k''_\ell}{kk'}\eta_j\partial' - \dfrac{k'\eta_j}{k}\partial'' + \dfrac{k'_\ell \eta_\ell k'_j}{kk'}\partial' & (j = 1,2) \\ -i\dfrac{k'_\ell \eta_\ell}{kk'}\partial\partial' & (j = 3) \end{cases}$$

$$A^{(4)} = \begin{cases} -\dfrac{\eta'_\ell k''_\ell \eta_j}{k} - \dfrac{\eta'_\ell \eta_\ell k'_j}{k} & (j = 1,2) \\ \dfrac{i\eta'_\ell \eta_\ell}{k}\partial' & (j = 3) \end{cases}$$

$$B^{(1)} = \frac{1}{\sqrt{2sg}} \begin{cases} \frac{is'k'_j}{2k'} & (j = 1,2) \\ 0 & (j = 3) \end{cases}$$

$$C^{(1)} = \begin{cases} \frac{\rho a}{k^2}\left(k_j \frac{k'_\ell k''_\ell}{k'} \partial' + \frac{k'_j k'_\ell k_\ell}{k'} \partial' - k'k_j \partial''\right) & (j = 1,2) \\ 0 & (j = 3) \end{cases}$$

$$C^{(2)} = \begin{cases} -\frac{\rho a}{k^2}\left(k'_j \eta'_\ell k_\ell + k''_\ell \eta'_\ell k_j\right) & (j = 1,2) \\ 0 & (j = 3) \end{cases}$$

$$T^{(1)}(z') = \frac{is'}{\sqrt{2sg}} \frac{\partial}{\partial z}\left\{G^{\omega}_{\underset{\sim}{k}}(z,z') w^{s'\sigma'}_{\underset{\sim}{k}}(z')\right\}_{z=0} \left\{A^{(1)} - \frac{A^{(2)} \frac{d\hat{u}'}{dz}}{(\bar{u}' - s'\sigma'/k')}\right\}$$

$$+ \delta(z')\left\{\frac{is'}{\sqrt{2sg}}\left[C^{(1)}\left(\bar{u}' - \frac{s'\sigma'}{k'}\right) - C^{(2)} \frac{d\hat{u}'}{dz}\right]\right.$$

$$\left. + \rho a B^{(1)}\left[\frac{dw^{\omega}_{\underset{\sim}{k}}}{dz'} - \frac{d\bar{u}}{dz'}\right]\right\}$$

where $\bar{U}' = \frac{\underset{\sim}{U}.\underset{\sim}{k}'}{k'}$, $\hat{U}' = \underset{\sim}{U}.\underset{\sim}{\eta}'$ and all terms are taken at z', unless otherwise indicated. The arguments of the coefficients $A^{(1)}$, $A^{(2)}$, $B^{(1)}$, $C^{(1)}$ and $C^{(2)}$ are the same as in the expressions given above.

$$T^{(2)}(z,z') = \left\{ \frac{\partial}{\partial z} G^{\omega}_{\underset{\sim}{k}}(z,z'') \right\}_{z=0} \left\{ \alpha_{jl}\, G^{\omega^\circ}_{\underset{\sim}{k}^\circ}(z'',z') + \beta_{jl}\, \delta(z')\, w^{\omega^\circ}_{\underset{\sim}{k}^\circ}(z'') \right.$$
$$\left. + \gamma_{jl}\, \delta(z'-z'')\, w^{\omega^\circ}_{\underset{\sim}{k}^\circ}(z'') + \varepsilon_{jl}\, \delta(z')\, \delta(z'') \right\}$$

where

$$\alpha_{jl} = \frac{is' \rho_a (\bar{u} - \omega/k)}{\sqrt{2gg}} \left\{ A_l^{(1)} - \lambda^\circ A_l^{(2)} \right\} \left\{ A_j^{(1)} - \lambda' A_j^{(2)} \right\}$$

$$\beta_{jl} = \frac{\rho_a (\bar{u} - \omega/k)}{(\bar{u}^\circ - \omega^\circ/k^\circ)} \left\{ A_l^{(1)} - \lambda^\circ A_l^{(2)} \right\} B_j^{(1)}$$

$$\gamma_{jl} = \frac{is'}{\sqrt{2gg}} \frac{\rho_a (\bar{u} - \omega/k)}{(\bar{u}^\circ - \omega^\circ/k^\circ)} A_l^{(2)} \left\{ A_j^{(3)} - \lambda' A_j^{(4)} \right\}$$

$$\varepsilon_{jl} = \left\{ C_l^{(1)} - \lambda^\circ C_l^{(2)} \right\} B_j^{(1)} + \frac{is'}{\sqrt{2gg}} C_l^{(2)} \left\{ A_j^{(3)} - \lambda' A_j^{(4)} \right\}$$

with $\underset{\sim}{k}^\circ = \underset{\sim}{k}' + \underset{\sim}{k}''$

$$\lambda^\circ = \frac{d\hat{u}^\circ}{dz} \Big/ (\bar{u}^\circ - \omega^\circ/k^\circ)$$

$$\lambda' = \frac{d}{dz}\hat{u}' \Big/ (\bar{u}' - \omega'/k')$$

The arguments of the coefficients $A_j^{(1)}$, $A_j^{(2)}$, ... are the same as in the previous expressions. The wave-numbers $\underset{\sim}{k}'$ and $\underset{\sim}{k}''$ in the coefficients $A_1^{(1)}$, $A_1^{(2)}$, ... are replaced by $\underset{\sim}{k}^\circ$ and $\underset{\sim}{k}'''$, respectively, and j is replaced by 1.

References

Backus, G.E. (1962) Deep Sea Res. 9, 185-197.

Baer, L. (1962) Lockhead Missile and Space Co., Rep.-8o1296.

Barnett, T.P. (1966) Ph.D. thesis, Univ. Cal., San Diego.

Batchelor, G.K. (1963) The Theory of Homogeneous turbulence. Camb. Univ. Press.

Benjamin, B.T. (1959) Journ. Fluid Mech. 6, 161-205.

Bretschneider, C.L. (1959) Beach Erosion Board Tech.Mem. No.118

Bretschneider, C.L. & R.O. Reid (1954) Beach Erosion Board Tech.Mem. No.45.

Burling, R.W. (1959) Dtsch.Hydrogr.Z. 12, 45-117.

Chandrasekhar, S. (1959) Radiative Transfer, Dover Publ.

Darbyshire, J. (1955) Proc.Roy.Soc.A., 230, 560-569.

Darbyshire, J. (1959) Dtsch.Hydrogr.Z. 12, 1-13, 196-203.

Dorrestein, R. (1960) Journ.Geophys.Res. 65, 637-642.

Eckart, C. (1953) Journ.Appl.Phys. 24, 1485-1494.

Fons, C. (1966) Cahiers Oceanogr. 18, 16-33.

Gelci, R., H. Cazalé & J. Vassal (1956) Bull.d'Inform.du Comité Central d'Oceanogr. et d'Etude des Cotes, 8.

Gelci, R. & H. Cazalé (1962) Journ.Mech.Phys. de l'Atmosph., 2 Ser., 4, 15-41.

Grant, H.L., Stewart, R.W. & Moilliet, A. (1962) Journ.Fluid Mech. 12, 241-263.

Groves, G.W. & Melcer, J. (1961) Geofis.Intern. 1, 77-93.

Hasselmann, K. (1960) Schiffstechnik 1, 191-195.

Hasselmann, K. (1962) Journ. Fluid Mech. 12, 481-500.

Hasselmann, K. (1963a) Journ. Fluid Mech. 15, 273-281.

Hasselmann, K. (1963b) Journ. Fluid Mech. 15, 385-398.

Hasselmann, K. (1966) Rev. Geophys. 4, 1-32.

Hasselmann, K. (1967a) Proc.Roy.Soc.A. (in the press).

Hasselmann, K. (1967b) (in preparation).

Hasselmann, K., Munk, W.H. & MacDonald, G.J.F. (1963) Ch. 8, Time Ser. Anal., Ed.M.Rosenblatt John Wiley & Sons, Inc.

Hasselmann, K. & Collins, J.I. (1967) (in preparation).

Inoue, T. (1966) Tech.Rep. 66-6, NYU.

Iwagaki, Y., Tsuchiya, Y. & Sakai, M. (1965) Bull.Disaster Prevention Res.Inst., Kyoto Univ., 14, 45-46.

Jeffreys, H. (1925) Proc.Roy.Soc.A., 107, 189-206.

Jeffreys, H. (1926) Proc.Roy.Soc.A., 110, 241-247.

Jonsson, I.G. (1965) Tech.Univ.Denm., Progr.Rep. No. 10.

Kinsman, B. (1965) Wind waves. Prentice-Hall, Inc.

Kourganoff, V. (1963) Basic methods in transfer problems, Dover Publ.

Lighthill, M.J. (1962) Journ. Fluid Mech. 14, 385-398.

Lighthill, M.J. (1963) AIAA Journ. 1, 1507.

Lock, R.C. (1954) Proc.Camb.Phil.Soc. 50, 105-124.

Longuet-Higgins, M.S. (1957) Proc.Camb.Phil.Soc. 53, 226-229.

Longuet-Higgins, M.S., Cartwright, D.E. & N.D. Smith (1963) in Maryland, Prentice-Hall.

Ocean wave spectra,

Miles, J.W. (1957) Journ. Fluid Mech. 3, 185-204.

Miles, J.W. (1959) Journ. Fluid Mech. 6, 568-582.

Munk, W.H. & MacDonald, G.J.F. (1960) The rotation of the earth. Camb. Univ. Press.

Neumann, G. (1953) Beach Erosion Board, Tech. Mem. No. 43.

Peierls, R.E. (1929) Ann.d.Phys. 3, 1055.

Peierls, R.E. (1955) Quantum theory of solids, Oxford, Clarendon Press.

Phillips, O.M. (1957) Journ. Fluid Mech. 2, 417-445.

Phillips, O.M. (1958) Journ. Fluid Mech. 4, 426-434.

Phillips, O.M. (1959) Journ. Fluid Mech. 5, 177-192.

Phillips, O.M. (1960) Journ. Fluid Mech. 9, 193-217.

Phillips, O.M. (1966) The dynamics of the upper ocean. Camb. Univ. Press.

Pierson, W.J., Neumann, G. & James, R.W. (1955) U.S. Navy Hydrogr. Off., Publ. 603.

Pierson, W.J. & Moskowitz, L. (1964) Journ. Geophys. Res. 69, 5181-5190.

Pierson, W.J., Tick, L.J. & Baer, L. (1966) 6th Naval Hydrodyn. Symp., Washington (in the press)

Priestley, J.T. (1965) Nat.Bur.Stand. Rep. 8942.

Prigogine, I. (1962) Non-equilibrium statistical mechanics. Interscience Publ.

Putnam, J.A. & Johnson, J.W. (1949) Trans.Am.Geophys.Union 30, 67-74.

Roll, H.U. & Fischer, G. (1956) Dtsch.Hydrogr.Z. 9, 9-14.

Savage, R.P. (1953) Beach Erosion Board, Tech. Mem. No. 31.

Shemdin, O.H. & Hsu, E.Y. (1966) Dept.Civil Engin, Stanford Univ., Tech.Rep.No. 66.

Snodgrass, F.E., Groves, G.W., Hasselmann, K., Miller, G.R., Munk, W.H. & Powers, W.H. (1966) Phil.Trans.Roy.Soc.A. 259, 431-497.

Snyder, R.L. & Cox, C.S. (1966) Journ. Marine Res. 24, 141-178.

Suthons, C.T. (1945) Naval Met. Branch - Hydrogr. Depart. Mem. No. 135/45.

Svedrup, H.U. & Munk, W.H. (1947) U.S. Navy Hydrogr. Off. Pub. No.601.

Wuest, W. (1949) Zeitschr.Angew.Math.Mech. 29, 239-252.

Zagustin, K., Hsu, E.Y., Street, R.L. & Perry, B. (1966) Dept.Civil Engin., Stanford Univ., Tech. Rep. No. 60.

Figure captions — Hasselmann

Fig. 1 Interaction diagrams corresponding to the linear transfer expressions (3.4.2) (diagrams (i)) and (3.4.3) (diagrams (ii))

Fig. 2 Interaction diagrams corresponding to the source function (3.4.7). Diagrams (i), (ii) and (iii) correspond to the transfer functions $T^{\nu}_{\nu_1\nu_2\to\nu}$, $T^{\nu}_{\nu\bar{\nu}_1\to\nu_2}$ and $T^{\nu}_{\nu\bar{\nu}_2\to\nu_1}$, respectively.

Fig. 3 Interaction diagrams corresponding to the source function (3.4.19). Diagrams (i) yield the first term of the transfer function $T^{\nu}_{\nu\mu}$, equation (3.4.23). Diagrams (ii) correspond to the second of the four terms in the parentheses $\{.....\}$. The remaining terms in the parentheses are obtained by interchanging components and anti-components.

Fig. 4 Transfer diagrams corresponding to the transfer expressions: (i) S^{ν}_{ν}, equation (3.4.2); (ii) $S^{\vec{\nu}}_{(\mu\vec{\nu})}$, equation (3.4.3); (iii), (iv), (v) $S^{\vec{\nu}}_{(\nu_1\nu_2\vec{\nu})}$, equation (3.4.7); (vi) $S^{\nu}_{\nu\nu_1}$, equation (3.4.13). Diagrams (ii) - (v) represent scattering diagrams, (i) and (vi) parametric diagrams. Diagrams (iii), (iv) and (v) belong to a diagram set.

Fig. 5 Interaction (Feynman) diagrams for conservative gravity-wave interactions. The energy transfer is given by equation (3.6.5). The corresponding transfer diagrams are of the same form as diagram (iii).

Fig. 6 Lowest-order transfer diagrams for wave-atmosphere and wave-ocean interactions. Diagrams (i), (ii) and (v) represent parametric processes, diagrams (iii) and (iv) scattering processes.

Wave-atmosphere interactions (i) : linear interactions with the ocean boundary-layer flow according to Miles, (ii) : non-linear interaction with mean boundary-layer flow, (iii) : Eckart-Phillips wave generation by turbulence. The process can be represented by three diagrams in terms of the turbulent velocity components t or an equivalent linear diagram $p^t \rightarrow g$, where p^t is the turbulence pressure at the surface. (iv), (v) : wave-turbulence interactions.

Wave-ocean interactions (i) : linear interaction with mean current. The energy transfer vanishes in the weak-interaction approximation. (ii) : non-linear interactions with mean currents, (iii) : generation of waves by turbulence, (iv) : scattering of waves by turbulence, (v) : parametric damping of waves by turbulence ("eddy viscosity").

Fig. 7 Spectral distribution of surface pressure for wave-atmosphere interactions (schematic). Shading represents distribution of the three-dimensional spectral density $F_p(\underset{\sim}{k},\omega)$ in the $k_1-\omega$ plane.

Fig. 8 The growth parameter β as function of wind speed U.

J : Jeffreys (1925), MI : Miles, BF : best-fit experimentally; T : an empirical relation $\beta = \frac{\varrho_a}{\varrho}(\underset{\sim}{k},\underset{\sim}{U}-\sigma)$ suggested by Snyder and Cox (1966); The data points are divided into short runs + and long runs □ . (From Snyder and Cox, 1966).

Fig. 9 Non-linear interaction diagram for parametric damping of waves by mean currents.

Fig. 10 Interaction diagrams for parametric damping of waves by turbulence ("eddy viscosity").

Fig. 11 Wave damping due to a turbulent bottom friction $\underset{\sim}{\tau} = -\varrho c_f \underset{\sim}{u}|\underset{\sim}{u}|$, with $c_f = 0.015$. The initial distribution corresponds to a 40-knot Pierson-Moskowitz spectrum with a $\cos^4\varphi$ spreading factor. The water depth is 100 m. (From Hasselmann and Collins, 1967).

Fig. 12 Wave damping due to turbulent bottom friction. The same case as in fig. 11, with a superimposed bottom current of 0.7 m/sec at 45° to the initial mean wave direction. (From Hasselmann and Collins, 1967).

Fig. 13 Wave spectra (upper panels) and the computed energy transfer due to wave-wave scattering (lower panels) in the near zone of a storm. Full and dashed curves in the lower right panel correspond to a $\cos^4\varphi$ and 30° step-function spreading factor, respectively. (From Snodgrass et al, 1966).

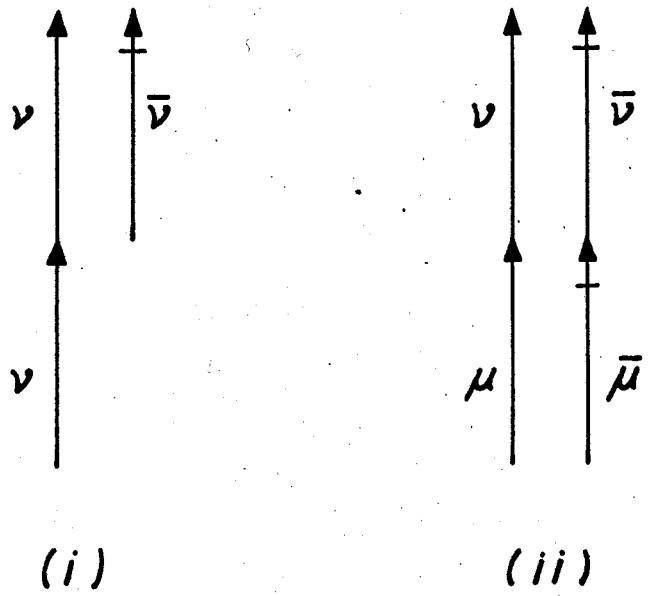

Fig. 1

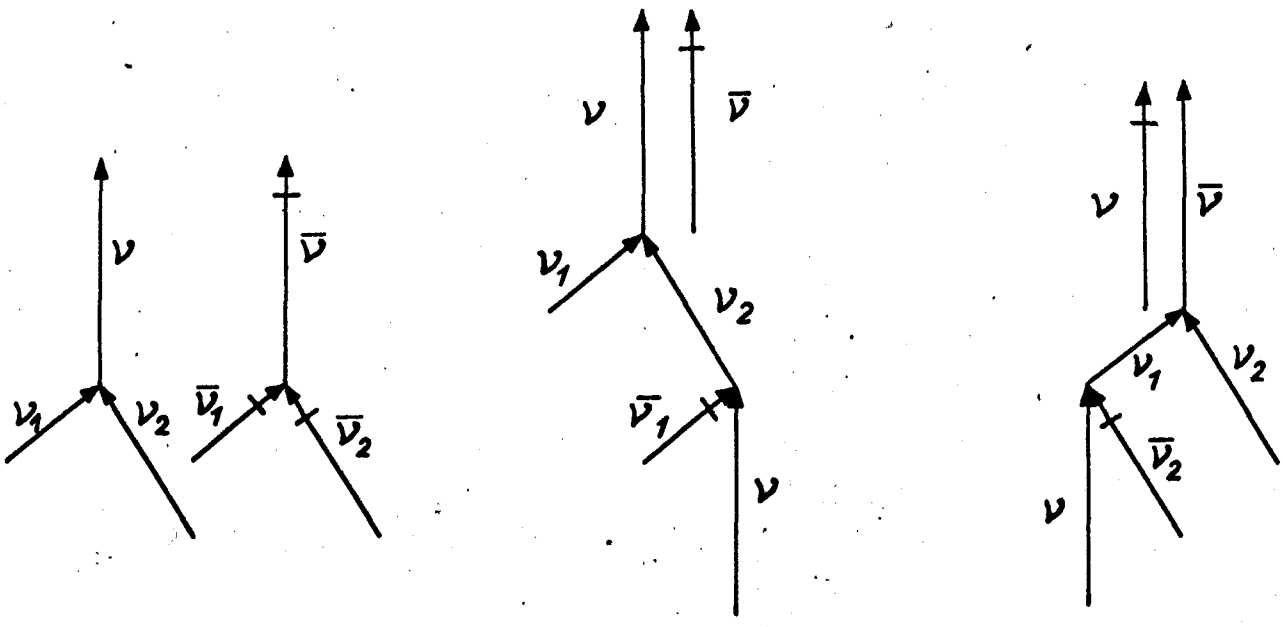

(i) (ii) (iii)

Fig. 2

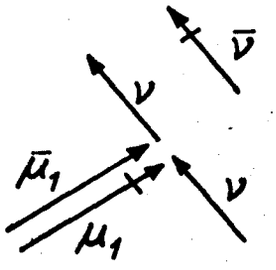

(i)

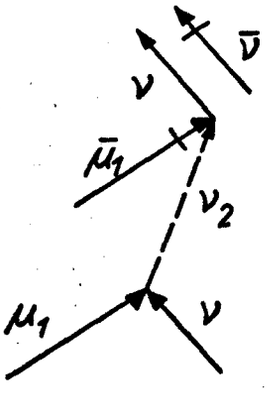

(ii)

Fig. 3

(i)

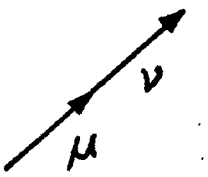

(ii)

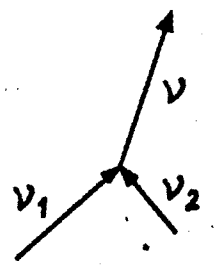

(iii)

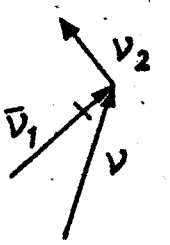

(iv)

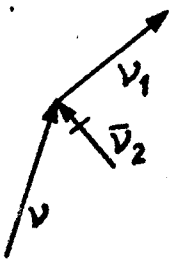

(v)

(vi)

Fig. 4

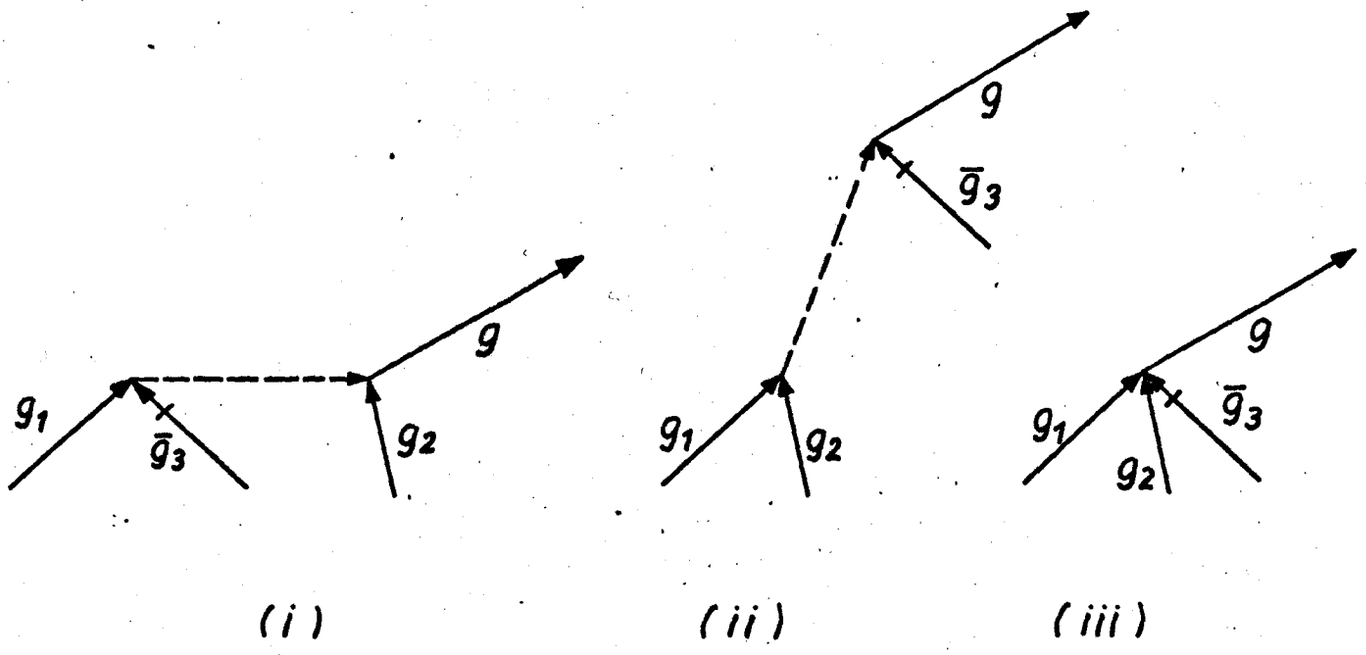

Fig. 5

(i)

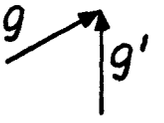

(ii)

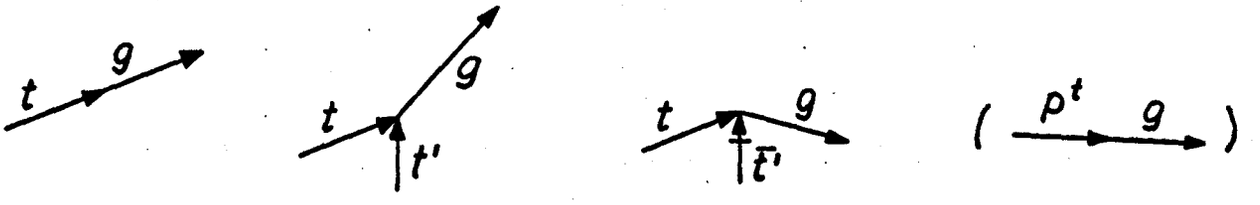

(iii)

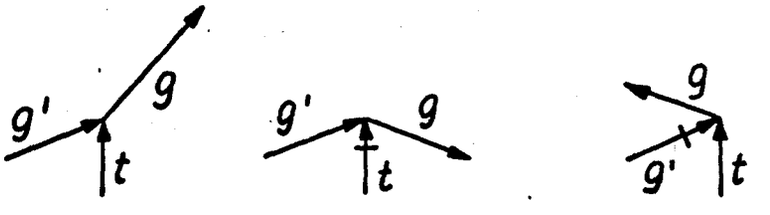

(iv)

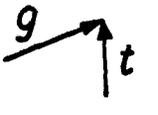

(v)

Fig. 6

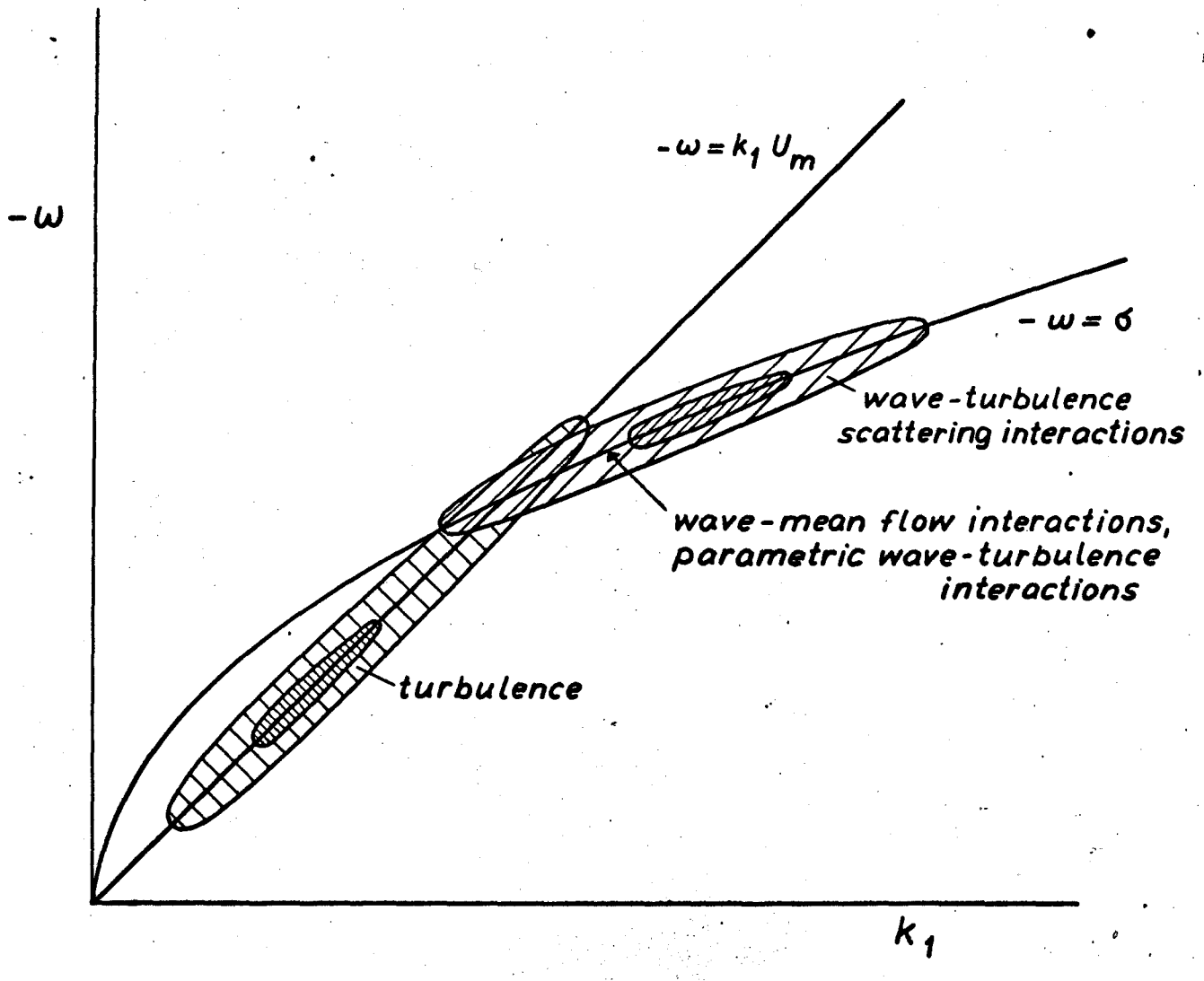
$-\omega = k_1 U_m$
$-\omega$
$-\omega = \sigma$
wave-turbulence
scattering interactions
wave-mean flow interactions,
parametric wave-turbulence
interactions
turbulence
k_1

Fig. 7

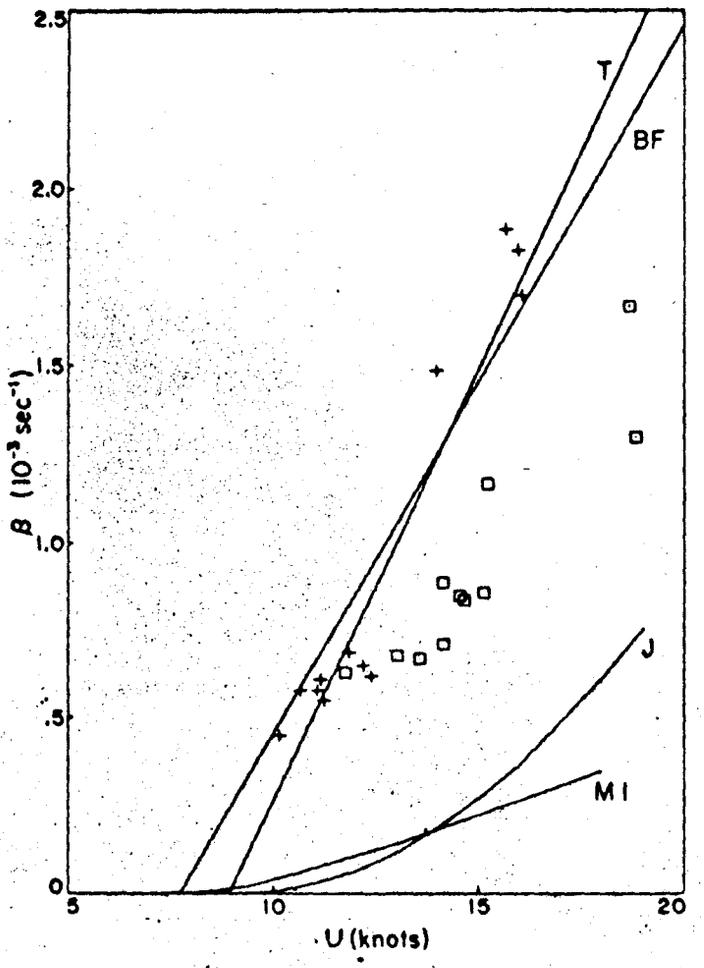

Fig. 8

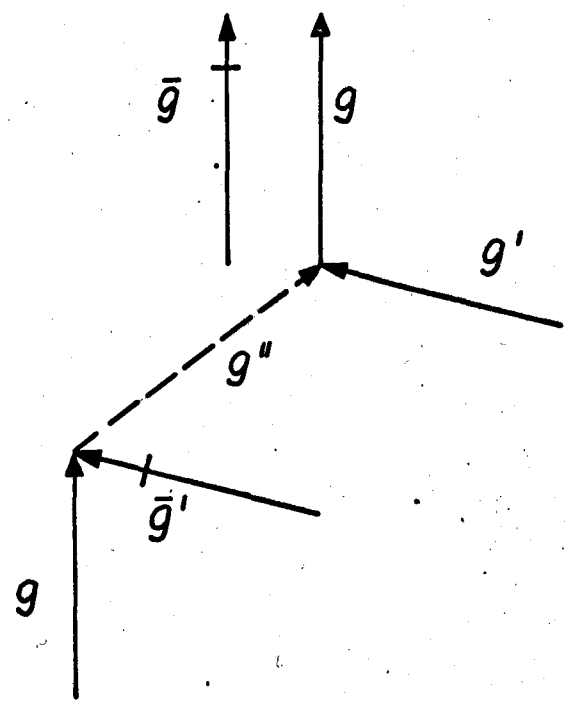

Fig. 9

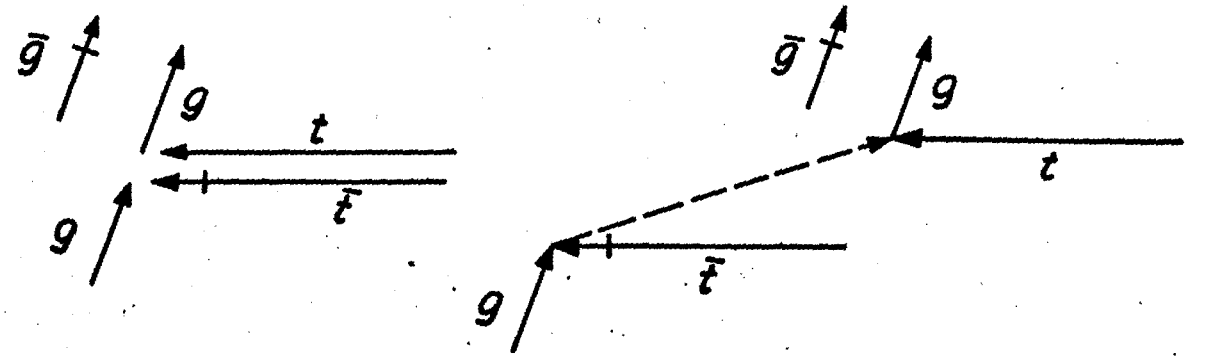

Fig. 10

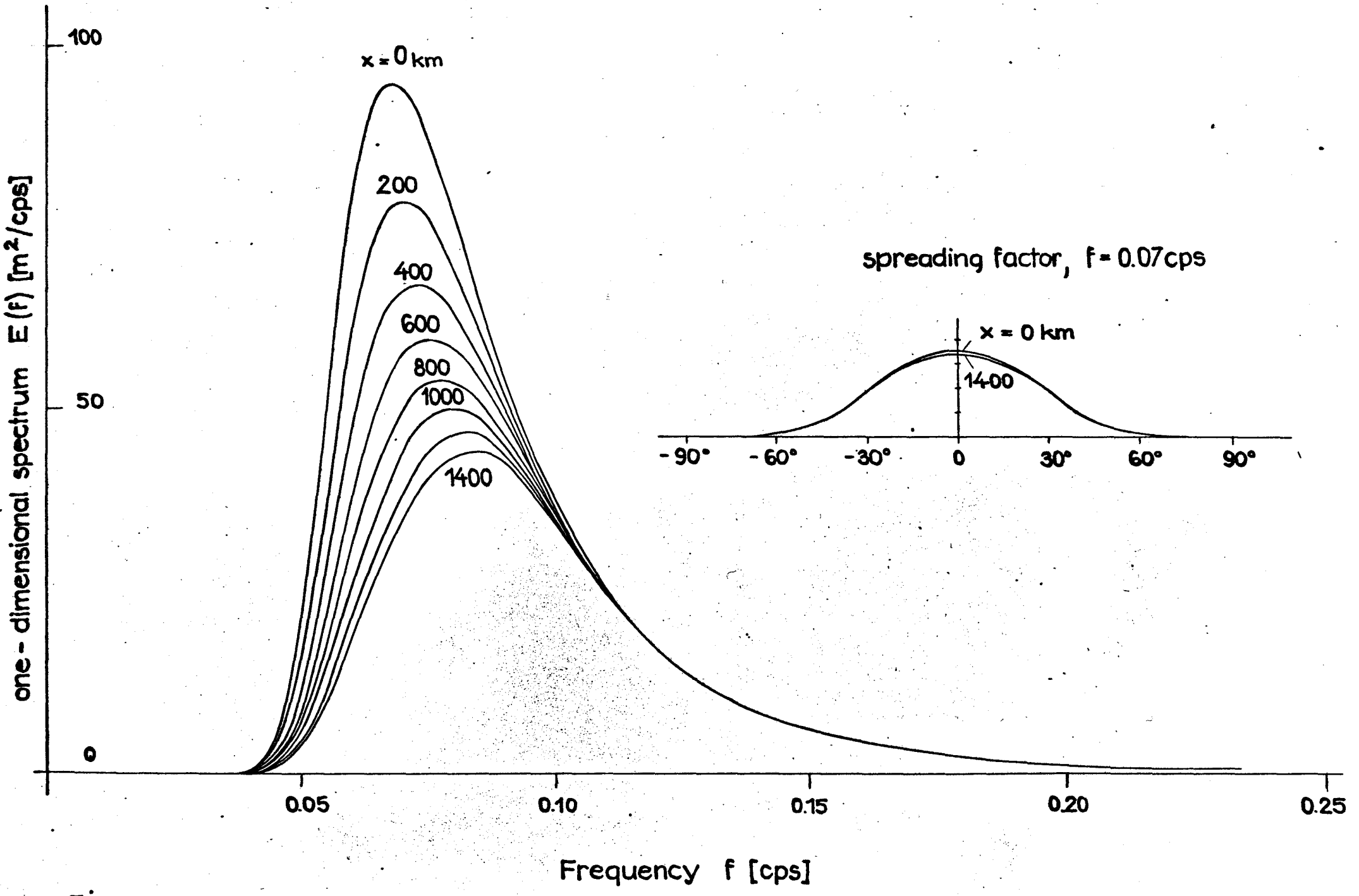
100
50
0
x = 0 km
200
400
600
800
1000
1400
one - dimensional spectrum E(f) [m²/cps]
0.05
0.10
0.15
0.20
0.25
Frequency f [cps]
spreading factor, f = 0.07cps
x = 0 km
1400
-90°
-60°
-30°
0
30°
60°
90°

Fig. 11

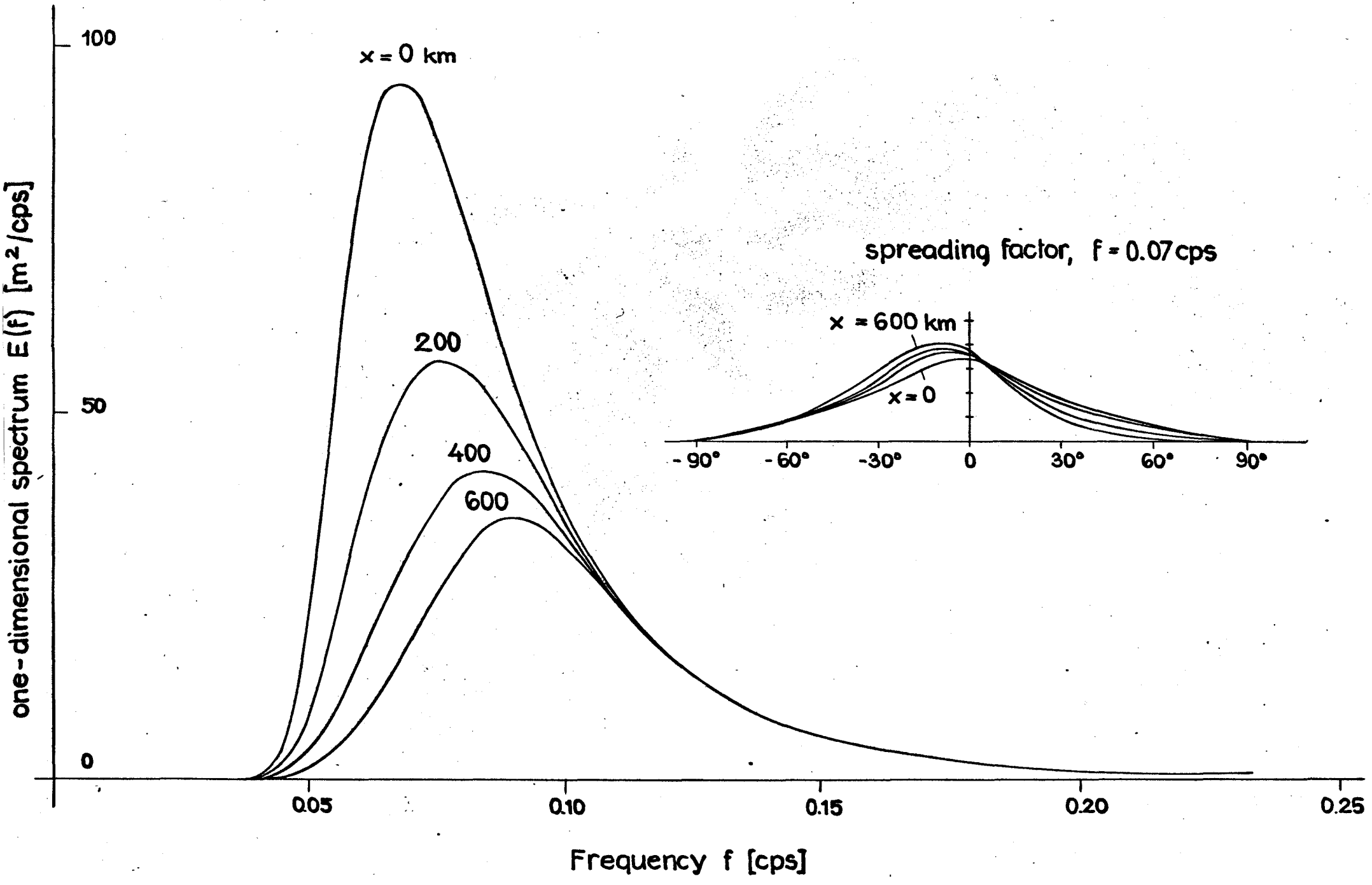
100
50
0
x = 0 km
200
400
600
one-dimensional spectrum E(f) [m²/cps]
0.05
0.10
0.15
0.20
0.25
Frequency f [cps]
spreading factor, f = 0.07 cps
x = 600 km
x = 0
- 90°
- 60°
-30°
0
30°
60°
90°

Fig. 13

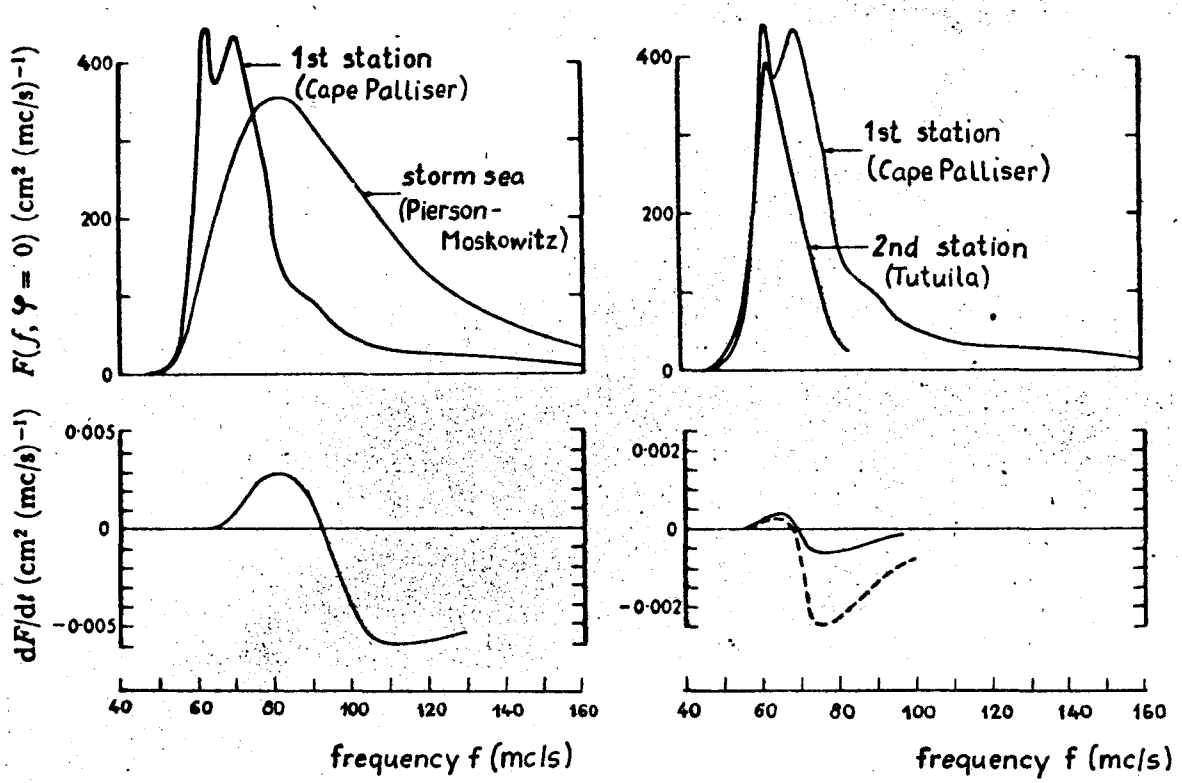
1st station
(Cape Palliser)
storm sea
(Pierson-
Moskowitz)
1st station
(Cape Palliser)
2nd station
(Tutuila)
F(f, Ψ = 0) (cm² (mc/s)⁻¹)
dF/df (cm² (mc/s)⁻¹)
400
200
0
0·005
0
-0·005
0·002
0
-0·002
40
60
80
100
120
140
160
frequency f (mc/s)
frequency f (mc/s)